

**GENERATING THE SPINDLE ASSEMBLY CHECKPOINT  
SIGNAL AT THE KINETOCHORE**

APPROVED BY SUPERVISORY COMMITTEE

Mentor: Hongtao Yu, Ph.D. \_\_\_\_\_

Committee Chairperson: Michael A. White, Ph.D. \_\_\_\_\_

Committee member: Elliott M. Ross, Ph.D. \_\_\_\_\_

Committee member: Xiaodong Wang, Ph.D. \_\_\_\_\_

## **Dedication**

To my parents Parma Nand and Veena Mishra

**GENERATING THE SPINDLE ASSEMBLY CHECKPOINT SIGNAL AT THE  
KINETOCHORE**

by

Rajnish Bharadwaj

DISSERTATION

Presented to the Faculty of the Graduate School of Biomedical Sciences the University of

Texas Southwestern Medical Center at Dallas

In Partial fulfillment of the Requirements

For the Degree of

DOCTOR OF PHILOSOPHY

The University of Texas Southwestern Medical Center at Dallas

Dallas, Texas

August, 2004

## ACKNOWLEDGEMENTS

First of all, I would like to thank my mentor Hongtao who taught me everything from how to run a column to how to write the materials and methods section of a paper scientifically. He created a great set up for good research, both in terms of resources and training. I am extremely indebted to my committee members- Elliott Ross, Xiaodong Wang and Michael White for their affection, support and invaluable advices on my thesis work and how to do science in general. Their intellectual brilliance was always a source of inspiration.

I was fortunate to have such great lab mates. I am thankful to Josh for all the great music and stimulating conversations, to Bing for all the wisdom shared, to Wei and Ting Ting for helping me out with the Spc25 and Cyclin A projects, to Xhanyun for all the scientific help and to Christian, Guohong, Jungseog, Dilhan, Ryan and Maojong for making the graduate school years fun. I am grateful to Melissa, Bing, Sara and Pam who kept the lab running smoothly and often had to bear with my bad habit of ordering stuff at the last moment.

And most of all, I am thankful to my parents for all the 46 chromosomes.



Copyright  
by  
Rajnish Bharadwaj 2004  
All Rights Reserved

GENERATING THE SPINDLE ASSEMBLY CHECKPOINT SIGNAL AT THE  
KINETOCHORE

Publication No. \_\_\_\_\_

Rajnish Bharadwaj, Ph.D.

The University of Texas Southwestern Medical Center at Dallas, 2004

Supervising Professor: Hongtao Yu, Ph.D.

ABSTRACT

To avoid missegregation of chromosomes during mitosis cells employ a surveillance mechanism termed Spindle assembly checkpoint that senses the lack of tension/attachment on the kinetochores and consequently blocks anaphase onset by inhibiting an E3 ubiquitin ligase called anaphase-promoting complex. The roles of two kinases- BubR1 and Mps1, implicated in spindle assembly checkpoint were investigated. A checkpoint complex containing BubR1 and Bub3 has been purified from mitotic human cells. BubR1 directly interacts with Cdc20 and inhibits the activity of APC in vitro, much more efficiently than Mad2. Surprisingly, the kinase activity of BubR1 or

association with Bub3 is not required for the inhibition of APC<sup>Cdc20</sup>. Furthermore, BubR1 restores the mitotic arrest in Cdc20-overexpressing cells treated with nocodazole. Mps1 is a dual specificity kinase that localizes to kinetochores in mitosis. Depletion of Mps1 by RNAi leads to the abrogation of spindle assembly checkpoint.

The kinetochore proteins involved in the recruitment of checkpoint proteins and the generation of wait-anaphase signal have not been identified. Kinetochores also provide the attachment sites for spindle microtubules and are required for the alignment of chromosomes at the metaphase plate (chromosome congression). Components of the conserved Ndc80 complex have been implicated in both these function. To better understand the function of the Ndc80 complex, we have identified two novel subunits of the human Ndc80 complex, termed human Spc25 (hSpc25) and human Spc24 (hSpc24), using an immuno-affinity approach. Human Spc25 interacts with Hec1 (human Ndc80) throughout the cell cycle and localizes to kinetochores during mitosis. RNAi-mediated depletion of hSpc25 in HeLa cells causes aberrant mitosis followed by cell death, a phenotype similar to that of cells depleted for Hec1. Loss of hSpc25 also causes multiple spindle aberrations, including elongated, multipolar, and fractured spindles. In the absence of hSpc25, Mad1 and Hec1 fail to localize to kinetochores during mitosis whereas the kinetochore localization of Bub1 and BubR1 is largely unaffected. Interestingly, the kinetochore localization of Mad1 in cells with a compromised Ndc80 function is restored upon microtubule depolymerization. Thus, hSpc25 is an essential kinetochore component that plays a significant role in proper execution of mitotic events.

<b>Acknowledgements.....</b>	<b>iv</b>
<b>Abstract.....</b>	<b>vi</b>
<b>Table of contents.....</b>	<b>viii</b>
<b>Prior Publications.....</b>	<b>xii</b>
<b>List of figures .....</b>	<b>xiii</b>
<b>List of Abbreviations.....</b>	<b>xv</b>
<b>CHAPTER ONE: Introduction.....</b>	<b>1</b>
Chromosome segregation and the spindle checkpoint.....	1
Molecular components of the spindle checkpoint.....	2
Direct inhibition of APC/C by the mitotic checkpoint complex.....	6
<i>Function of Mad2.....</i>	<i>6</i>
<i>Function of BubR1/Mad3.....</i>	<i>7</i>
<i>The mitotic checkpoint complex (MCC).....</i>	<i>9</i>
Generating the mitotic checkpoint complex.....	12
<i>Role of Mad1.....</i>	<i>12</i>
<i>Role of upstream checkpoint kinases.....</i>	<i>14</i>
<i>Role of Cdc20 phosphorylation.....</i>	<i>15</i>
The sensing mechanism of the spindle checkpoint.....	16
<i>Attachment versus tension.....</i>	<i>16</i>
<i>Distinctive checkpoint responses to different defects.....</i>	<i>18</i>
<i>Molecular sensors of the spindle checkpoint.....</i>	<i>19</i>
Recruitment of checkpoint proteins to the kinetochores.....	22
<i>Recruitment of Bub1 in yeast.....</i>	<i>22</i>
<i>Recruitment of mad1.....</i>	<i>24</i>
Silencing the spindle checkpoint.....	25
<i>Dynein-mediated depletion of checkpoint proteins from kinetochores.....</i>	<i>26</i>
<i>Cmt2-binding and phosphorylation of Mad2.....</i>	<i>27</i>
Defective spindle checkpoint and aneuploidy.....	28
Conclusion.....	30
References.....	31

<b>CHAPTER TWO: Mad2-Independent Inhibition of APC<sup>Cdc20</sup> by the Mitotic Checkpoint Protein BubR1.....</b>	<b>39</b>
Introduction.....	39
Experimental Procedures.....	43
<i>Antibody production, Immunoprecipitation and Immunoblotting.....</i>	<i>43</i>
<i>Purification of the BubR1-Bub3 complex.....</i>	<i>43</i>
<i>Protein expression in SF9 cells and purification.....</i>	<i>44</i>
<i>Cyclin Degradation and H1 kinase assay.....</i>	<i>44</i>
<i>Ubiquitination assay.....</i>	<i>45</i>
<i>Binding assay .....</i>	<i>46</i>
Results.....	47
<i>Purification of a mitotic checkpoint complex.....</i>	<i>47</i>
<i>BubR1 inhibits APC in reconstituted ubiquitination assays and in xenopus extracts.....</i>	<i>49</i>
<i>The kinase activity of BubR1 is not essential for inhibition of APC.....</i>	<i>53</i>
<i>Binding between BubR1 and Cdc20 requires the intact Cdc20.....</i>	<i>55</i>
<i>BubR1 counteracts the effects of Cdc20 overexpression in living cells.....</i>	<i>58</i>
Discussion.....	60
<i>BubR1 as the mammalian homolog of yeast Mad3.....</i>	<i>60</i>
<i>Sequestration of Cdc20 by BubR1.....</i>	<i>62</i>
References .....	64
<b>CHAPTER THREE: Role of Mps1 and Mad2B in Spindle Assembly Checkpoint</b>	
Introduction.....	71
Experimental procedures.....	75
<i>Expression and purification of Mad2B and Mps1.....</i>	<i>75</i>
<i>Antibody preparation and immunoblotting.....</i>	<i>75</i>
<i>Tissue culture and transfection.....</i>	<i>76</i>
<i>Immunofluorescence.....</i>	<i>76</i>
<i>APC ubiquitination assay.....</i>	<i>77</i>
<i>In vitro kinase assay.....</i>	<i>77</i>
Results.....	79

<i>Mps1 localizes to kinetochores and centrosomes in mitosis</i> .....	79
<i>Depletion of Mps1 results in the abrogation of spindle assembly checkpoint</i> ..	79
<i>Mps1 is phosphorylated in mitosis</i> .....	81
<i>Elucidating the biochemical function of Mps1</i> .....	81
<i>Mad2B can inhibit APC in vitro</i> .....	85
<i>Overexpression of Mad2B does not cause a mitotic arrest</i> .....	85
Discussion.....	88
<i>The role of Mad2B in cell cycle regulation</i> .....	88
<i>Mps1 is a spindle assembly checkpoint gene</i> .....	88
References.....	90
<b>CHAPTER FOUR: Identification of Two Novel Components of the Human Ndc80</b>	
<b>Kinetochores Complex</b> .....	<b>92</b>
Introduction.....	92
Experimental procedures.....	96
<i>Expression and purification of recombinant Hec1 proteins and antibody</i> <i>production</i> .....	96
<i>Immunopurification of the human Ndc80 complex</i> .....	96
<i>Cloning expression and purification of recombinant hSpc25 and antibody</i> <i>production</i> .....	97
<i>Tissue culture and transfection</i> .....	98
<i>Immunoprecipitation, immunoblotting and protein binding assays</i> .....	99
<i>Immunofluorescence</i> .....	99
<i>Cold-sensitive or calcium-sensitive microtubule staining</i> .....	100
<i>Cell synchronization experiments</i> .....	101
Results.....	102
<i>Identification of human Spc25 by immunoprecipitation of Ndc80 complex</i> ....	102
<i>Human Spc25 binds to Hec1 in vitro and interacts with Hec1 throughout the cell</i> <i>cycle in vivo</i> .....	104
<i>Human Spc25 localizes to kinetochores during mitosis</i> .....	106
<i>Human Spc25 is required for proper progression through mitosis</i> .....	106

<i>Mitotic arrest in hSpc25-depleted cells depends upon a functional spindle checkpoint.....</i>	108
<i>Inactivation of hNdc80 complex causes apoptosis after a transient mitotic Arrest.....</i>	112
<i>Inactivation of hSpc25 leads to multiple spindle abnormalities.....</i>	115
<i>hSpc25 deficient kinetochores retain the ability to form microtubule attachments.....</i>	117
<i>Depletion of hSpc25 leads to the loss of kinetochore localization of Mad1 in a microtubule-dependent manner.....</i>	117
Discussion.....	121
<i>Roles of the Ndc80 complex in chromosome congression and spindle Morphology.....</i>	121
<i>Loss of Ndc80 function and apoptosis.....</i>	123
<i>Role of Ndc80 in the spindle checkpoint.....</i>	123
References.....	127
<b>CHAPTER FIVE: Conclusions and future directions.....</b>	<b>129</b>

## Prior Publications

1. Bharadwaj R, Qi W, Yu H. (2003). Identification of two novel components of the human Ndc80 kinetochore complex. *J Biol Chem.* *Dec 29* [Epub ahead of print]
2. Bharadwaj R and Yu H. (2004). The Spindle Checkpoint, Aneuploidy and Cancer. *Oncogene.* *23*, 2016-2027.
3. Tang Z, Bharadwaj R, Li B, Yu H. (2001). Mad2-Independent inhibition of APC<sup>Cdc20</sup> by the mitotic checkpoint protein BubR1. *Dev Cell.* *1*, 227-237.
4. Tang Z, Li B, Bharadwaj R, Zhu H, Ozkan E, Hakala K, Deisenhofer J, Yu H. (2001). APC2 Cullin protein and APC11 RING protein comprise the minimal ubiquitin ligase module of the anaphase-promoting complex. *Mol Biol Cell.* *12*, 3839-51.



## LIST OF FIGURES

### CHAPTER ONE

Figure 1. Molecular mechanism of chromosome segregation.....	3
Figure 2. Domain structures and functions of a subset of the human spindle checkpoint proteins.....	5
Figure 3. Two distinct, yet non-exclusive models for the generation of the APC-inhibitory spindle checkpoint signal.....	11

### CHAPTER TWO

Figure 1. Purification of a mitotic BubR1 complex.....	48
Figure 2. BubR1 inhibits the activity of APC <sup>Cdc20</sup> .....	50
Figure 3. BubR1 inhibits the activity of human APC <sup>Cdc20</sup> and blocks the activation of APC in <i>Xenopus</i> egg extracts.....	52
Figure 4. The kinase activity of bubr1 is not required for inhibition of APC <sup>Cdc20</sup> .....	54
Figure 5. Binding of Cdc20 to BubR1 and Mad2.....	56
Figure 7. BubR1 inhibits APC <sup>Cdc20</sup> in HeLa cells.....	59

### CHAPTER THREE

Figure 1. Mps1 localizes to kinetochores and centrosomes in mitosis.....	80
Figure 2. Mps1 is phosphorylated in mitosis and is required for mitotic arrest in the presence of nocodazole.....	82
Figure 3. FACS analysis of mock and Mps1 RNAi treated cells with or without nocodazole treatment.....	83
Figure 4. Mps1 does not phosphorylate Cdc20, Cdh1, Bub1, BubR1 or Bub3 and does not inhibit APC.....	84
Figure 5. Mad2B can inhibit APC activity in vitro.....	86
Figure 6. Mad2B overexpression does not lead to mitotic arrest.....	87

### CHAPTER FOUR

Figure 1. Identification of hSpC25.....	103
Figure 2. Binding between hSpC25 and Hec1.....	105
Figure 3. Kinetochores localization of hSpC25 during mitosis.....	107
Figure 4. Phenotypes of HeLa cells depleted for hSpC25.....	109

Figure 5. Cells depleted of hSp25 arrest in mitosis with low levels of Cyclin A and high levels of Cyclin B1 and securin.....	111
Figure 6. Hec1 RNAi cells undergo a transient mitotic arrest followed by apoptosis.....	113
Figure 7. Aberrant DNA and spindle morphology of mitotic hSp25 RNAi cells.....	117
Figure 8. Human Sp25 is required for the kinetochore localization of Mad1 and Hec1 during mitosis.....	118
Figure 9. Kinetochore localization of Mad1 is restored in Hec1-depleted cells upon microtubule depolymerization.....	120

## **LIST OF ABBREVIATIONS**

APC/C- Anaphase-promoting Complex or cyclosome

RNAi- RNA interference

hSp25- human SPC25

CENP- Centromere protein

GST- Glutathione S- transferase

PBS- Phosphate Buffered Saline

si RNA- Small interfering RNA

PI- Propidium Iodide

FACS- Fluorescence-activated cell sorting

HA- Hemagglutinin

hNuf2- human Nuf2

PIPES- 1,4-piperazinediethanesulfonic acid

DAPI- 4',6-diamidino-2-phenylindole

PARP1-poly(ADP-ribose) polymerase-1

# **CHAPTER ONE**

## **INTRODUCTION**

Chromosomal instability (CIN) leading to an aberrant chromosome number (aneuploidy) is a hallmark of cancers (1). The mechanism and molecular determinants of CIN are not clearly understood (1). However, there is a growing body of evidence to suggest that defects in the spindle checkpoint, a surveillance mechanism crucial for the proper segregation of chromosomes during every cell division, might promote aneuploidy and tumorigenesis (2). Mutations in certain genes involved in the spindle checkpoint have been identified in a variety of human cancers (3). Though these mutations have not been found very frequently and a causal connection between these mutations and CIN has not been established unequivocally, the understanding of the spindle checkpoint might provide valuable insights into CIN and facilitate the design of novel therapeutic approaches to treat cancer.

### **Chromosome segregation and the spindle checkpoint**

The alignment of chromosomes on the cell equator during mitosis is achieved by a stochastic process in which kinetochores of the chromosomes are captured by randomly elongating and contracting microtubules emanating from the two spindle poles (4). Once the two kinetochores of a sister-chromatid pair attach to microtubules from the opposite poles, they congress to the center of the cells (4). Due to the inherent randomness of this

process, it is crucial that chromosome segregation ensues only when all the chromosomes have congressed to the metaphase plate to ensure the even partition of the genetic material into the two daughter nuclei (4,5). This is accomplished by a surveillance mechanism known as the spindle checkpoint, which senses the lack of attachment and/or tension at kinetochores and in response inhibits chromosome segregation (6-8). Through detailed analysis of the timing of various mitotic events in PtK cells by live cell imaging, Rieder *et al.* showed that a single unattached kinetochore can delay the segregation of the already aligned chromosomes (9). The time lag between nuclear envelope breakdown and anaphase onset varies from cell to cell and is highly dependent upon how long the last chromosome takes to congress to the metaphase plate (9). Anaphase occurs approximately twenty minutes after the alignment of the last chromosome in PtK cells. More interestingly, laser ablation of the last unattached kinetochore allows mitosis to proceed in the absence of microtubule attachment, suggesting that an inhibitory checkpoint signal is produced by this kinetochore to block chromosome segregation (9).

## **Molecular components of the spindle checkpoint**

Prior to anaphase, sister-chromatids are kept together by a proteinaceous bridge formed by a multiprotein complex termed cohesin (5,10) (Fig. 1). Anaphase is triggered by the proteolysis of one of the cohesin subunits, Scc1, by a protease called separase (5,10). Separase is normally kept inactive by an associated inhibitor termed securin (5,10,11). After the proper attachment of all sister-chromatids to the mitotic spindle, the spindle checkpoint is satisfied. Securin is then ubiquitinated by the anaphase-promoting complex or cyclosome (APC/C), a multi-subunit E3 ubiquitin ligase (6,12-14). The destruction of

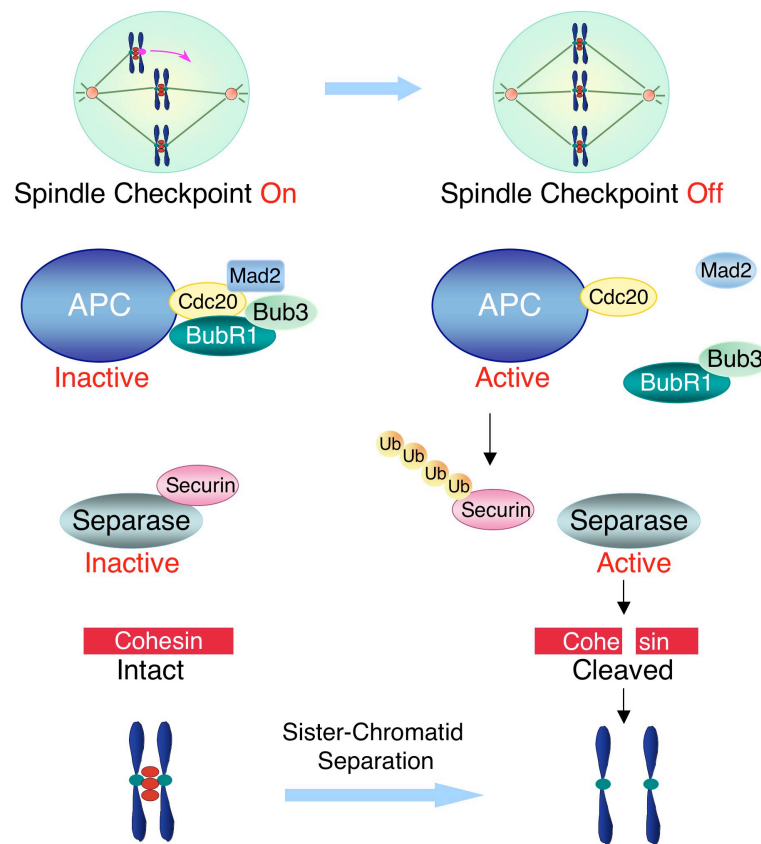


**Figure 1** Molecular mechanism of chromosome segregation. At the metaphase-anaphase transition, APC/C<sup>Cdc20</sup> ubiquitinates securin. Degradation of securin activates separase. Separase then cleaves the Scc1 subunit of cohesion, allowing chromosome segregation. In response to sister-chromatid not properly attached to the mitotic spindle, the spindle checkpoint promotes the assembly of checkpoint protein complexes that inhibit the activity of APC/C, leading to the stabilization of securin, preservation of sister-chromatid cohesion, and a delay in the onset of anaphase.

ubiquitinated securin by the proteasome then leads to separase activation, Scc1 cleavage, loss of chromosome cohesion, and anaphase onset (5,10).

Ubiquitination of securin by APC/C requires the binding of the WD40-repeat-containing Cdc20 protein, which recruits substrates to APC/C (13-17). It turns out that the spindle checkpoint interferes with the productive interaction between APC/C and Cdc20 (6). Thus, the complex between APC/C and Cdc20 (APC/C<sup>Cdc20</sup>) is the most downstream target of the spindle checkpoint (6,18). Unattached kinetochores emit a diffusible signal that inhibits the cytoplasmic pool of APC/C<sup>Cdc20</sup>, thus preventing the separation of already aligned chromosomes (4,6,19). Though the exact nature of this diffusible signal and the mechanism of its generation are not clear, great progress has recently been made toward the understanding of the identities and interactions of some of the proteins involved in this process.

The well-characterized components of the spindle checkpoint include Mad1, Mad2, Mad3 (BubR1), Bub1, Bub3, and Mps1 (Fig. 2) (4,6). In this list, we have not included other kinetochore proteins that might be responsible for the assembly of a functional kinetochore and therefore for the recruitment of the above mentioned checkpoint proteins (4) (also see below). The Mad (mitotic arrest deficient) and Bub (budding uninhibited by benzimidazole) proteins were identified by yeast mutagenesis screens for mutants unable to survive a temporary exposure to microtubule toxins nocodazole or benzimidazole (20,21). Mps1 was identified initially as a centrosomal protein required for the assembly of bipolar spindles, but it was later shown to play a role in the spindle checkpoint as well (22). Homologs for these proteins were subsequently identified in higher organisms including mammals (6). Functional disruption of these

proteins in mammalian cells through dominant negative mutants, antibody injection, or RNA interference (RNAi) results in the abrogation of the spindle checkpoint, leading to chromosome mis-segregation, aneuploidy and a failure to arrest in mitosis in the presence of microtubule poisons, such as nocodazole and taxol (6,23-27). These findings confirm that the mammalian checkpoint proteins identified through sequence homology are indeed functional homologs of their yeast counterparts (6).

Checkpoint Proteins	Domain Structures	Functions
Mad1	1 718 Coiled Coil	Binds to Mad2 and recruits it to kinetochores; Essential for generation of Mad2-Cdc20 complex; Forms a complex with Bub1-Bub3 in mitosis.
Mad2	1 205 HORMA	Binds to Cdc20 and inhibits APC/C <sup>Cdc20</sup> ; Binds to Mad1.
Bub1	1 GLEBS 1085 TPR Kinase	Binds to Bub3 constitutively; Forms a complex with Mad1 and Bub3 in mitosis; Phosphorylates Mad1 in vitro.
BubR1 (Mad3)	1 GLEBS 1050 TPR Kinase	Binds to Bub3 constitutively; Activated by CENP-E Inhibits APC/C <sup>Cdc20</sup> in a Mad2-independent manner Forms a complex with Cdc20, Bub3, and Mad2
Bub3	1 328 WD40	Binds to BubR1 and Bub1.
Cdc20	1 499 WD40	Recruits substrates to APC/C; Molecular target of the spindle checkpoint; Forms a complex with Mad2, BubR1, and Bub3.

**Figure 2.** Domain structures and functions of a subset of the human spindle checkpoint proteins. The numbers indicate the number of amino acids present in each of the proteins. TPR stands for Tetratrico Peptide Repeat; HORMA is a domain found in Hop1, Rev7, and Mad2; and GLEBS is a motif that binds to Bub3 and Rae1.



## **Direct inhibition of APC/C by the mitotic checkpoint complex**

How does the spindle checkpoint block the activity of APC/C<sup>Cdc20</sup>? A decade of genetic and biochemical studies have indicated that the most downstream event in checkpoint signaling is the inhibition of Cdc20, which is believed to be the substrate recognition subunit of APC/C. Inhibition of Cdc20 is accomplished by the mitotic checkpoint complex (MCC) that is composed of Mad2, BubR1, Bub3, and Cdc20 (6,28-30). We will briefly review the evidence supporting this conclusion.

### *Function of Mad2*

The function of Mad2 was elucidated first. Overexpression of Mad2 causes a mitotic arrest in yeast and mammalian cells, presumably through inhibition of APC/C<sup>Cdc20</sup> (31-33). Initial insights into the function of Mad2 came from findings in both budding and fission yeast that Mad2 binds directly to Cdc20 (31,32). Mutations in Cdc20 that renders it unable to bind Mad2 allow cells to undergo mitosis even in the presence of Mad2 overexpression (32). Mad2, Cdc20, and APC/C were then shown to form a ternary complex in mammalian cells (18,34). Further insights into Mad2 function came from in vitro biochemical assays demonstrating that bacterially purified recombinant Mad2 inhibits the ubiquitin ligase activity of APC/C immunopurified from *Xenopus* egg extracts (18,35). The Mad2-binding motif of Cdc20 was then narrowed down to a stretch of 12 amino acids in the N-terminal region of Cdc20 (27). As expected, introduction of a peptide containing this motif into cells leads to the inactivation of the spindle checkpoint (27,36). Structure of Mad2 in complex with a peptide closely resembling this motif has revealed that Mad2 undergoes major conformational changes on binding to this peptide

(27,37). There might be a major kinetic barrier between these two Mad2 conformations and spontaneous transition between these two Mad2 states might be extremely slow *in vivo* (27,37). Furthermore, it must be pointed out here that the binding affinity between Mad2 and the full length Cdc20 is lower than that of the aforementioned Mad2-binding peptide of Cdc20 or the N-terminal fragment of Cdc20 lacking the WD40 repeats (28,36). Therefore, it is very likely that additional mechanisms, probably involving the unattached kinetochores and other checkpoint proteins, exist to facilitate the binding between Mad2 and Cdc20 *in vivo*. In this vein, Mad2 localizes to unattached kinetochores in prometaphase (38,39). Fluorescence recovery after photobleaching (FRAP) experiment reveals that Mad2 association with the unattached kinetochores is highly dynamic with a half-life of approximately 20 seconds (40). This is consistent with the notion that unattached kinetochores might serve as a catalytic device to transform inactive Mad2 molecules into an active form that can bind to Cdc20 and inhibit the activity of APC/C (6,19,41).

#### *Function of BubR1/Mad3*

Recently, BubR1 has emerged as another key player in APC/C inhibition as it directly inhibits APC/C<sup>Cdc20</sup> in a Mad2-independent manner (28). BubR1 is the mammalian homolog of yeast Mad3 (42). Both BubR1 and Mad3 contain the so-called GLEBS motif that mediates their binding to Bub3 (43). Binding between BubR1/Mad3 and Bub3 is constitutive, and is required for the localization of BubR1 to kinetochores during mitosis (42). BubR1 can directly bind to Cdc20 *in vitro* and *in vivo* (28,44). Recombinant BubR1 protein purified from insect cells inhibits the activity of APC/C in ubiquitination

assays more effectively than does recombinant Mad2 (28). Bub3 binding to BubR1 does not contribute significantly to the ability of BubR1 to inhibit APC/C (28). A significant difference between BubR1 and its yeast homolog Mad3 is that BubR1 possesses a kinase domain, which is absent in Mad3. Surprisingly, the kinase domain of BubR1 is not required for its inhibition of APC/C (28).

Recently, the kinase activity of BubR1 has been shown to be essential for checkpoint functions other than APC/C inhibition (45). BubR1 binds to the mitotic motor protein CENP-E, which is required for the maintenance of stable kinetochore-microtubule interactions and for proper checkpoint signaling (46). Using purified BubR1 and CENP-E proteins *in vitro*, Mao *et al.* have shown that the kinase activity of BubR1 toward itself or a non-specific substrate, histone H1, can be stimulated by its binding to CENP-E (45). Immunodepletion of CENP-E from or addition of a CENP-E inactivating antibody to nocodazole treated *Xenopus* egg extracts supplemented with sperm nuclei abolishes the kinase activity of endogenous BubR1 (45). However, there has been some controversy about the actual significance of the BubR1 kinase activity in *Xenopus* egg extracts. It has been reported earlier that BubR1 immunodepletion abolishes the spindle checkpoint which can be restored by the addition of either wild-type or kinase dead recombinant BubR1 proteins to these lysates (47). In contrast, Mao *et al.* found that the kinase dead BubR1 protein cannot effectively restore checkpoint function in BubR1-immunodepleted extract (45). In a set of elegant experiments, Mao *et al.* were able to resolve the apparent discrepancy between the two results (45). They showed that addition of the wild-type BubR1 protein to 10% of its endogenous level does not restore the spindle checkpoint, but further addition of the kinase-dead mutant of BubR1 can

restore the checkpoint (45). Therefore, it is quite possible that, in the earlier experiments, the immunodepletion of BubR1 might not have been complete, and a small amount of persisting BubR1 could have aided the exogenously added kinase-dead BubR1 protein to restore the checkpoint (47). Thus, BubR1 appears to have two roles in the spindle checkpoint: a stoichiometric role involving direct physical association with Cdc20 and a yet unidentified catalytic role requiring only a small portion of the endogenous pool of BubR1. Because the kinase activity of BubR1 is required for the recruitment of CENP-E and Mad2 to the kinetochore in *Xenopus* egg extracts, it is likely that the catalytic function of BubR1 is important for an upstream event of spindle checkpoint signaling (45). A definitive answer to this question requires the identification of key substrates of the CENP-E activated BubR1.

#### *The mitotic checkpoint complex (MCC)*

Though Mad2 and BubR1 can independently inhibit APC/C activity in vitro, there must be synergism between these two proteins in vivo because both of them are indispensable for a functional checkpoint. Consistent with this notion, Fang *et al.* have shown that Mad2 and BubR1 can synergistically inhibit APC/C in vitro (30). In addition, a complex of BubR1–Bub3–Mad2–Cdc20 exists in mammalian cells and in *Xenopus* egg extracts, and has been referred to as mitotic checkpoint complex (MCC) (29,47). A Mad3–Bub3–Mad2–Cdc20 complex has also been demonstrated to exist in both budding and fission yeast (48,49). MCC partially purified from HeLa cells inhibits the activity of APC/C in ubiquitination assays much more effectively than does recombinant Mad2 (29). It is also possible that Cdc20 in the MCC complex has a higher affinity for APC/C than

free Cdc20 or Mad2 bound Cdc20. This might alleviate the requirement of the checkpoint to inhibit the entire cytosolic pool of Cdc20, and can explain the observation that there exists a pool of free Cdc20 not bound to either Mad2 or BubR1 in nocodazole arrested cells.

There is a controversy as to whether the MCC is generated specifically in mitosis or throughout the cell cycle. Several groups have reported that MCC or its sub-complexes (Mad2-Cdc20 and BubR1-Bub3-Cdc20) only form in checkpoint-active mammalian cells or *Xenopus* egg extracts (18,28,30,47). The amount of MCC is negligible in *Xenopus* egg extracts lacking an active checkpoint or thymidine-arrested HeLa cells, due to the lack of Mad2-Cdc20 and BubR1-Cdc20 interactions (18,28,30,47). From these studies, it has been postulated that an active spindle checkpoint stimulates the formation of MCC, which then binds to APC/C in a stoichiometric fashion to inhibit APC/C (6) (Fig. 3). Because all four components of MCC have been found to localize to unattached kinetochores in a dynamic fashion (40,50), it is likely that the unattached kinetochores might be involved in the generation of MCC. In a different model, it has been argued that MCC exists throughout the cell cycle, but fails to bind to APC/C in the absence of checkpoint signaling (29,51). Upon checkpoint activation, APC/C itself is modified, which then leads to efficient MCC binding and prolonged inhibition of APC/C (29,51) (Fig. 3). Consistent with the second model, Sudakin *et al.* have detected MCC in the interphase mammalian cells (29,51). Furthermore, the MCC complex can be immunoprecipitated from yeast cells arrested in S-phase with hydroxyurea (52). In addition, this complex can be generated in Ndc10 mutants lacking a functional kinetochore, suggesting that the kinetochore might not be

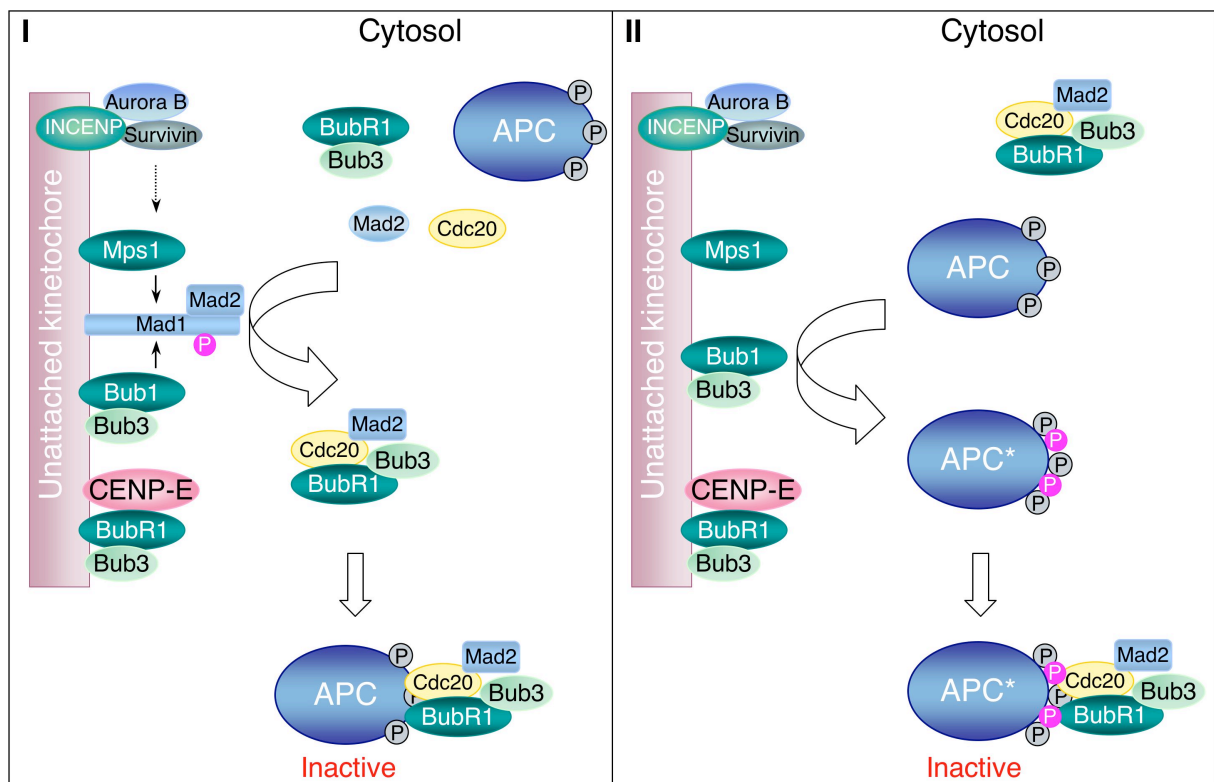


**Figure 3.** Two distinct, yet non-exclusive, models for the generation of the APC-inhibitory spindle checkpoint signal. In model I, the unattached kinetochore serves as a template catalyzing the formation of the BubR1-Bub3-Mad2-Cdc20 (MCC) complex, which then diffuses away from the kinetochore to inhibit the APC. In model II, modification of the APC by the unattached kinetochore promotes its association with the MCC, leading to the inhibition of APC.

absolutely necessary for the formation of MCC (52). Additional studies are obviously needed to resolve these differences. However, we would like to suggest a simple explanation for these discrepancies. It is conceivable that a basal level of MCC can be generated without the assistance of kinetochores at all cell cycle stages, but the level of MCC increases remarkably in mitotic cells that possess an active checkpoint. It is also

possible that, in addition to stimulating the formation of MCC, an active spindle checkpoint also modifies the APC/C that further bolsters its interaction with MCC.

Does Mad2 have any APC-inhibitory activity in vivo in the absence of Mad3? Some key insights into this issue come from unpublished data from Spencer and colleagues (MS Lee and FA Spencer, personal communication). They performed a yeast screen to identify genes that are synthetic lethal with Mad1, Mad2, or Mad3. An identical set of genes were found to be synthetic lethal with either Mad1 or Mad2. However, several deletion mutants were identified that can survive in the absence of Mad3, but not in the absence of Mad2. This indicates that Mad2 can perform functions that do not absolutely require Mad3/BubR1. Of course, these functions could be checkpoint related or unrelated. As we do not have conclusive evidence for a non-checkpoint role for Mad2, we tend to believe that Mad2 by itself might have a residual ability to inhibit APC in vivo. Further studies are needed to resolve this issue.

## **Generating the mitotic checkpoint complex**

### *Role of Mad1*

Elegant studies in several experimental organisms have established a complicated set of protein-protein interactions among various checkpoint components. The kinetochore localization of Mad2 and its binding to Cdc20 require the function of Mad1, but not Bub1, Bub3, or BubR1(Mad3) (48). Mad1 is constitutively bound to Mad2 through its C-terminus domain whereas its N-terminal coiled-coiled domain is required for its kinetochore localization (27,53). A Mad1 mutant containing the Mad2-binding site but lacking the N-terminal coiled-coiled domain disrupts the checkpoint in a dominant

negative fashion (27,54). Surprisingly however, Mad2 overexpression can cause metaphase arrest even in the absence of Mad1, suggesting that, at higher concentrations, Mad2 can function without the assistance of Mad1 (27,49). Mad2 binds to Mad1 through a motif that is highly similar to the Mad2-binding motif of Cdc20 (27). Both solution and crystal structures of Mad2 in association with this motif have been solved (27,55). Mad1 binding to Mad2 induces the same conformational changes in Mad2 as does the Cdc20 peptide (27,55). Thus, Cdc20 and Mad1 binding to Mad2 are mutually exclusive. In vitro, Mad1 can prevent Mad2 from inhibiting APC/C<sup>Cdc20</sup> and Mad1 overexpression in HeLa cells abolishes the spindle checkpoint (27). Paradoxically, Mad1 participates in both the activation and inhibition of Mad2 (27). The ratio of Mad1:Mad2 is thus crucial for proper checkpoint signaling.

The exact mechanism by which Mad1 facilitates the Mad2-Cdc20 interaction is not clear. However, we have previously postulated that Mad1 facilitates the binding of Mad2 to Cdc20 by catalyzing the formation of a Mad2 conformer that is more compatible for Cdc20 binding (6,27). For this mechanism to be correct, the interaction between Mad1 and Mad2 has to be dynamic, i.e. Mad2 has to turn over quickly on Mad1. Because the Mad1-Mad2 interaction is constitutive throughout the cell cycle, the checkpoint may enhance the rate of Mad2 turnover on Mad1 by accelerating its release from Mad1, instead of the steady state levels of the Mad1-Mad2 complex. We do not understand yet whether and how this is accomplished when the checkpoint is activated during mitosis. However, it is tempting to speculate that, upon recruitment to kinetochores, Mad2 might dissociate from Mad1 with the assistance of other kinetochore proteins, and the Mad2 molecules thus released might exist in a conformational state



capable of Cdc20 binding. It is not known whether the formation of Mad2-Cdc20 complex occurs at the kinetochores or the active Mad2 species generated at kinetochores diffuse into the cytoplasm to bind to Cdc20.

#### *Role of upstream checkpoint kinases*

Consistent with the possibility that the Mad1-Mad2 interaction is regulated by the checkpoint, Mad1 is a substrate of the upstream checkpoint kinases such as Mps1 and Bub1 (56,57). Mps1 is a protein kinase required for the spindle checkpoint. Immunodepletion of Mps1 from checkpoint-active *Xenopus* egg extracts or its disruption in mammalian cells with kinase dead mutants or RNAi causes disruption of the spindle checkpoint (25,26). In Mps1 RNAi cells, Mad1 and Mad2 are no longer present at the unattached kinetochores (26). Mps1 overexpression causes a mitotic arrest in yeast that is dependent on the presence of other checkpoint genes including Bub1, Bub3, Mad1, Mad2 and Mad3 (56). In yeast, activation of the checkpoint either by nocodazole treatment or by overexpression of Mps1 leads to hyperphosphorylation of Mad1 and the formation of a Mad1-Bub1-Bub3 complex (56,58). Moreover, hyperphosphorylation of Mad1 depends on Mps1 *in vivo* and Mad1 can be directly phosphorylated by Mps1 *in vitro* (56). These data suggest that phosphorylation of Mad1 by Mps1 may play role in regulating the dynamics of the Mad1-Mad2 interaction and consequently the assembly of the MCC.

Bub1 is another checkpoint kinase that might be involved in regulating the Mad1-Mad2 interaction. Similar to BubR1, Bub1 contains a GLEBS motif and is constitutively bound to Bub3 (43). Bub1 localizes to the kinetochores in prometaphase and its

kinetochore localization persists at a lower level even in anaphase cells (59). In budding yeast, the N-terminus domain of Bub1 is sufficient for its kinetochore localization and checkpoint function (60). The kinase domain of Bub1 has been found to be dispensable for its checkpoint function (60). Instead, it is required for proper chromosome segregation (60). However, the kinase activity of Bub1 has recently been shown to be essential for the spindle checkpoint in fission yeast (61). Obviously, this discrepancy needs to be resolved with additional studies. Nevertheless, Bub1-Bub3 forms a complex with Mad1 in mitosis (58). Coupled with the fact that human Bub1 phosphorylates human Mad1 in vitro (57), it is conceivable that phosphorylation of Mad1 by Bub1 may be required for the dissociation of Mad2 from Mad1 and the subsequent formation of the Mad2-Cdc20-containing complex.

#### *Role of Cdc20 phosphorylation*

In addition to the conformational activation of Mad2, modification of Cdc20 may also be required for the efficient formation of MCC. Recently, MAPK phosphorylation of Cdc20 in the Mad2 binding domain has been shown to be required for Mad2 and BubR1 binding to Cdc20 in *Xenopus* egg extract (62). Addition of Cdc20 mutant proteins lacking these phosphorylation sites to *Xenopus* egg extracts immunodepleted of endogenous Cdc20 does not restore spindle checkpoint, presumably due to a defect in the formation of the MCC (62). Further studies are needed to check whether this phenomenon is conserved in mammalian somatic cell cycles.

## The sensing mechanism of the spindle checkpoint

### *Attachment versus tension*

There has been an ongoing debate on the exact nature of the mitotic defects that are sensed by the spindle checkpoint. There are two main models: 1) the most upstream sensor of the spindle checkpoint monitors the occupancy status of microtubule binding sites on the kinetochore; or 2) it senses the tension across the sister-chromatid pair generated by the attachment of kinetochore microtubules emanating from the opposite poles of the mitotic spindle. Multiple attempts have been made in different organisms to uncouple microtubule attachment at the kinetochores from the subsequent development of tension across the kinetochores. Treatment of mammalian cells with microtubule toxins, such as taxol, vinblastine or noscapine at low concentrations or, in the case of PtK cells, exposure to hypothermia, alters microtubule dynamics in such a way that kinetochore microtubule attachment remains largely unaffected, but the tension across the paired kinetochores is absent (63-67). These cells show a prolonged mitotic arrest under these conditions, suggesting that microtubule attachment per se might not be sufficient to silence the checkpoint. Moreover, in cells with monastrol, an inhibitor of the mitotic motor Eg5, some of the syntelically attached chromosomes still show Mad2 staining, indicative of an active spindle checkpoint (68). This is consistent with the notion that microtubule attachment alone is not sufficient for satisfying the checkpoint. Further support for this notion comes from studies on budding yeast cells lacking Cdc6, a protein essential for the initiation of DNA replication (69). The  $\Delta CDC6$  yeast cells do not arrest in S-phase because the replication intermediates that are sensed by the replication checkpoints are missing in these cells (69). However, they arrest in mitosis in a spindle

checkpoint dependent manner. The kinetochores in these cells are attached to microtubules as indicated by their proximity to spindle poles and an equal segregation frequency to the mother and daughter cells (69). Obviously, these kinetochores do not experience any tension because they are unpaired. This suggests that microtubule attachment at kinetochores alone may not be sufficient to satisfy the spindle checkpoint, which also senses the lack of tension across the kinetochores (69).

On the other hand, other experiments suggest that attachment by itself is sufficient to silence the spindle checkpoint. For example, laser ablation of the last unattached kinetochore allows cells to undergo mitosis (9). In this situation, the undamaged kinetochore that pairs with the laser ablated one is attached to microtubules, and should not experience any tension. Yet the cells escape mitosis, suggesting that lack of tension at this kinetochore is apparently unable to maintain the checkpoint signal (9). Studies in maize cells paint a more complicated picture (70). In this organism, the spindle might monitor microtubule attachment in mitosis, but tension in meiosis (70). Furthermore, the interpretation of studies that implicate the lack of tension as a mechanism of checkpoint activation is complicated by the interdependence between tension and microtubule attachment at the kinetochores. It is well accepted that tension promotes the stabilization of kinetochore microtubule attachment (71). A formal argument can be made that, although kinetochore attachments appear to be grossly normal under all these conditions, the attachment is not stable and some of the microtubule binding sites may become unoccupied at a given time. It is the transient lack of attachment that then triggers the checkpoint. It is almost technically impossible to rule out this possibility and

thus definitively answer the question of whether the checkpoint senses attachment versus tension.

*Distinctive checkpoint responses to different defects?*

Nevertheless, studies toward resolving this issue have provided significant insights into the functions of several checkpoint proteins in response to different spindle defects. For example, both Mad2 and BubR1 are required for the maintenance of mitotic arrest in response to taxol, vinblastine or hypothermic treatment (66). Microinjection of antibodies against either of these proteins causes premature escape from mitosis under these conditions (66). Mad2 is absent from the tension-free attached kinetochores in all the above-mentioned situations, indicating that kinetochore localization of Mad2 responds primarily to attachment, and not tension (63). In insect spermatocytes, if attachment of one kinetochore of a sister-chromatid pair is repeatedly disrupted by microneedle manipulation, Mad2 persists on the unattached kinetochore, but not on the attached one, despite the fact that both kinetochores in this case lack tension (71). It is intriguing that, though Mad2 is undetectable at the kinetochores, the spindle checkpoint is still active and the cytoplasmic pool of Mad2 appears to be essential for its maintenance. Thus, it is gradually being recognized that Mad2 localization to kinetochores is not always essential for an active checkpoint. Similar observation has been made in mammalian cells depleted for the kinetochore protein Hec1 using RNAi (see below) (72). In these Hec1 RNAi cells, Mad2 is absent from the kinetochores, but the cells are still arrested in mitosis and this arrest depends upon the presence of Mad2 (72). How can these Mad2 depleted kinetochores maintain an active spindle checkpoint? Again, it is

possible that a residual amount of Mad2 undetectable by the currently available techniques is present on the kinetochores and is responsible for the observed checkpoint activation. But a somewhat convoluted but more provocative explanation might be that there are two pathways for the formation of Mad2-containing APC/C inhibitors. An intact unattached kinetochore with high concentrations of Mad2 is required for an initial nucleation of the Mad2-containing inhibitors. A subsequent process that involves the Mad2-lacking kinetochores then maintains the existing pool of these Mad2-containing inhibitors, which might be sufficient for the maintenance of the already activated checkpoint. For example, the Mad2-lacking kinetochores might maintain the pre-existing inhibitory complex by inhibiting the putative activities that might disrupt the MCC. Another possibility is that BubR1 might be performing some functions on its own in these cells for which kinetochore bound Mad2 is not required. Consistent with BubR1 playing a compensatory role, in taxol-arrested cells, the BubR1 levels on the kinetochores are higher than normal cells while the kinetochore concentrations of Mad2 are lower (64).

#### *Molecular sensors of the spindle checkpoint*

Regardless of the nature of the defects that the spindle checkpoint responds to, recent studies on the chromosome passenger proteins, including Aurora B, INCENP, and Survivin, have begun to shed light on the molecular mechanisms by which the spindle checkpoint senses these defects (73,74). Aurora B, INCENP, and Survivin physically interact and form a complex, which localizes to the kinetochores in prometaphase, to the cell equator during metaphase, and to the midbody during cytokinesis (73,75,76). Functional disruption of these proteins in several model organisms have revealed their

involvement in multiple mitotic events, including chromosome congression, chromosome segregation, the spindle checkpoint, and cytokinesis (76-80). These proteins are also required to establish bipolar attachment of chromosomes, probably by destabilizing kinetochore microtubule attachments that lack tension (81,82). As mentioned above, Cdc6 budding yeast mutants enter mitosis without a prior round of replication and arrest in mitosis in a Mad2-dependent manner (69). Cdc6 mutants can attach the kinetochores to microtubules originating from either of the spindle poles at equal frequency whereas double mutants lacking both Cdc6 and Ipl1 (Aurora B in *S. cerevisiae*) segregate all their chromosomes to the mother cell (81). This indicates that Ipl1 promotes biorientation by destabilizing monotelic or syntelic kinetochore microtubule attachments that lack tension (81). It was later shown Ipl1-mediated phosphorylation of Dam1, a component of the DASH complex, is required for the establishment of bi-orientation (83,84). More interestingly, the Ipl1 mutants are not only defective in establishing chromosome biorientation, but also in spindle checkpoint signaling (82). Despite problems in establishing bi-orientation, the Cdc6 and Ipl1 double mutants can escape mitosis, indicative of a defective spindle checkpoint. Surprisingly, these cells can arrest in the presence of nocodazole, which depolymerizes microtubules and leaves all kinetochores unattached. This suggests that Ipl1 might be selectively required for checkpoint activation responding to the absence of tension (82).

Inhibition of Aurora B by various means in different systems has subsequently confirmed the findings made in budding yeast. Recently, two small molecule inhibitors of Aurora B, hesperadin and ZM447439, have been developed (79,85). Treatment with these inhibitors or Aurora B RNAi allows the cells to escape mitosis in the presence of

Taxol, but not in the presence of nocodazole (77,79,85). Similar findings have been observed in cells depleted for Survivin using RNAi (80). There are two possible explanations for this. In the first scenario, the spindle checkpoint might have two arms: one responds to attachment that is independent of Aurora B, and the other monitors tension for which Aurora B is essential. The tension sensing machinery might be dysfunctional in the absence of Aurora B. In nocodazole-treated cells, the lack of attachment might be sensed by the Aurora B-independent pathway, leading to mitotic arrest. In the Taxol-treated cells, the kinetochores remain attached to microtubules and the “attachment-sensing arm” of the checkpoint is satisfied. Aurora B thus becomes indispensable for maintaining the mitotic arrest in these cells. In a second scenario, the spindle checkpoint can only detect lack of microtubule occupancy at the kinetochores. Aurora B is required for destabilizing kinetochore microtubule attachments in the absence of tension to generate transiently unattached kinetochores. In Taxol-treated cells, Aurora B continuously keeps on severing kinetochore-microtubule connections, and the resulting transiently unattached kinetochores activate the checkpoint. In the absence of Aurora B, all the kinetochores are attached to microtubules despite a lack of tension and thus the checkpoint is silenced. Though it is unclear how the Aurora B-INCENP-Survivin complex senses spindle defects and promotes bi-orientation, it has become increasingly clear that this complex is a crucial part of defect sensing mechanism of the spindle checkpoint.

How does the Aurora B complex communicate with the other downstream checkpoint components is a subject of active investigation. Recent studies have provided some tantalizing clues. For example, RNAi-mediated depletion of Aurora B or Survivin



in mammalian cells diminishes the kinetochore localization of BubR1 (80). Moreover, BubR1 is normally hyperphosphorylated in checkpoint-active cells. This hyperphosphorylation of BubR1 is absent in Aurora B-depleted cells (85). Thus, it is possible that Aurora B directly phosphorylates BubR1. Mps1 might be another downstream target of Aurora B, as Ipl1 is required for the mitotic arrest exerted by overexpression of Mps1 in yeast (82). Coupled with the fact that certain Mps1 mutations are synthetic lethal with certain Dam1 mutations (86), it is very likely that Mps1 and Ipl1 are involved in some common functions.

## **Recruitment of checkpoint proteins to the kinetochores**

### *Recruitment of Bub1 in yeast*

What is the mechanism by which the checkpoint proteins are recruited to the kinetochores? Recent studies have begun to shed light on this baffling question in the spindle checkpoint field. Recently, the yeast Skp1 protein has been identified as a Bub1-binding protein in a yeast two-hybrid screen (87). The physical interaction between the two proteins is direct, as demonstrated by in vitro binding assays using recombinant proteins (87). Furthermore, Skp1 was shown to be required for the recruitment of Bub1 to kinetochores in yeast (87). Skp1 is an essential component of the CBF3 complex that is absolutely required for the assembly of a functional kinetochore. CBF3 mutants do not arrest in mitosis despite their inability to segregate their chromosomes, because they are essentially kinetochore-null and thus cannot recruit any of the checkpoint proteins (87). Therefore, the Skp1 mutations can perturb the checkpoint either due to a generalized defect in the assembly of the functional kinetochore or specifically due to a lack of

interaction with Bub1. To distinguish between these two possibilities, Kitagawa *et al.* identified a Skp1 mutant that is still proficient in kinetochore assembly but does not interact with Bub1 (87). This mutant does not show any significant chromosome missegregation phenotype, which is a hallmark of kinetochore dysfunction, but are checkpoint deficient under specific circumstances. Furthermore, this mutant can efficiently arrest in mitosis under circumstances where kinetochore microtubule attachment is disrupted, e.g. in the presence of nocodazole. However, these cells cannot arrest in situations where kinetochore microtubule attachment is normal and there is only a lack of tension at the kinetochores. The authors further tested the effect of this mutation in the presence of three other mutations: Ctf8, Scc1 and Cdc6 (87). In Ctf8 and Scc1 mutants, the kinetochores can still attach to microtubules. But the tension at kinetochores is diminished because the linkage between sister-chromatids is compromised. Similarly, in Cdc6 mutants, as mentioned before, the kinetochores are unpaired and consequently lack tension though these kinetochores are capable of microtubule attachment. The Skp1 mutant cells fail to arrest in mitosis in all three situations. The inability of Skp1 mutants to arrest in these situations further bolsters the idea that the set of proteins required to sense the absence of attachment might be different from that involved in sensing tension. Unfortunately, mammalian Skp1 has not been shown to be involved in kinetochore function (88,89). Whether Skp1 plays a role in recruiting Bub1 to kinetochores in mammalian cells needs remains to be determined.

*Recruitment of Mad1*

Progress has also been made toward the mechanism by which Mad1 is recruited to kinetochores in prometaphase. Martin-Lluesma *et al.* have recently shown that human Hec1 interacts with human Mad1 in a yeast two-hybrid screen (72). Mad1 no longer localizes to kinetochores in mitotic cells that are depleted for Hec1 RNAi (72). However, no direct interactions between Hec1 and Mad1 have been detected either in vivo or in vitro, suggesting that the interaction between Hec1 and Mad1 observed in the yeast two-hybrid assay might be bridged through other components (72). Hec1 is the mammalian homolog of the budding yeast Ndc80, which forms a complex with Nuf2, Spc25, and Spc24 (90). The Ndc80 complex in yeast is a key kinetochore component and is required for proper chromosome segregation (90). Mutants singly disrupted for Ndc80 and Nuf2 arrest in mitosis, indicating that the checkpoint is active in either cases. However, simultaneous disruption of both genes leads to an inactivation of the checkpoint, allowing the double mutant cells to escape mitosis without proper chromosome segregation. Similarly, Spc24 and Spc25 mutants are checkpoint defective, suggesting a role for the Ndc80 complex in the establishment of the spindle checkpoint in yeast. A similar Ndc80 complex has been characterized and shown to perform functions ranging from kinetochore assembly, chromosome congression, and the spindle checkpoint in *Xenopus* (91). The Ndc80 complex must also exist in mammalian cells, as cells depleted for Nuf2 using RNAi show similar phenotypes as the cells depleted for Hec1 (92,93). It is possible that the mammalian homologs of Spc24 and Spc25 are responsible for bridging the interactions between Hec1 and Mad1. Consistent with this notion, yeast Spc25 and Mad1 proteins have been shown to interact in a yeast two-hybrid screen (94).

Unfortunately, the mammalian homologs of Spc25 and Spc24 cannot be identified through sequence similarity alone. It will be interesting to identify these missing components of the vertebrate Ndc80 complex and to test whether the intact Ndc80 complex is responsible for recruiting Mad1 to the kinetochores in mitosis.

Inactivation of other kinetochore components also impairs the kinetochore localization of checkpoint proteins. For example, RNAi-mediated depletion of CENP-I, a mammalian kinetochore protein homologous to the *S. pombe* Mis6 protein, causes a transient mitotic delay that is dependent upon Mad2 (95). The kinetochore localization of Mad1 and Mad2 is also compromised in cells received CENP-I RNAi (95). In a very recent report, the Ran GTPase has been shown to be involved in the recruitment of the kinetochore proteins in *Xenopus* extracts (96). Addition of high levels of RCC1, an exchange factor for Ran, or depletion of Ran GAP1 perturbs the spindle checkpoint *Xenopus* extract supplemented with sperm nuclei and nocodazole. In this case, the checkpoint defect might be a consequence of diminished levels of Mad2, Bub1, and CENP-E proteins. Thus, Ran might regulate the loading of checkpoint proteins onto the kinetochores. However, instead of specific functions in recruiting certain checkpoint proteins, CENP-I and Ran might be generally required for the intactness of mature mitotic kinetochores. Disruption of their functions might cause pleiotropic defects at the kinetochores that in turn leads to the loss of kinetochore localization of various checkpoint proteins.

## **Silencing the spindle checkpoint**

*Dynein-mediated depletion of checkpoint proteins from kinetochores*

We also have some clues about the mechanisms leading to the silencing of the checkpoint after all the chromosomes are properly aligned. Studies in *Drosophila* neuroblasts and mammalian PtK cells have implicated the minus end directed motor, dynein, in the process of checkpoint inactivation (97,98). In particular, dynein-mediated transport of the checkpoint proteins from the kinetochores to the spindle poles might be required for shutting off the checkpoint. First, Wojcik *et al.* showed that dynamitin, a subunit of the dynactin complex, accumulates at the unaligned kinetochores in prometaphase in *Drosophila* cells and migrates to the poles once the chromosomes align on the metaphase plate (97). The dynactin complex is physically associated with dynein and is thought to recruit and bind cargo proteins to dynein. Thus, the localization pattern of dynactin might also reflect the localization pattern of functional dynein, which is certainly consistent with it playing a role in transporting certain checkpoint proteins from the kinetochores to the spindle poles. They further showed that a cargo of the dynein/dynactin complex is the kinetochore protein, Rough Deal (Rod), which has been implicated in the spindle checkpoint and exhibits similar cellular localization pattern as observed for dynactin (97). Rod was initially identified in *Drosophila* and its functional homologs were later found in mammalian cells (99,100). In *Drosophila*, the redistribution of Rod to the spindle poles following chromosome alignment is blocked in a specific hypomorphic dynein mutant (97). In contrast to the wild-type cells, high levels of Rod can be observed on the kinetochores even in metaphase in these mutants. These cells exhibit a metaphase block that is dependent upon an active spindle checkpoint,

suggesting that dynein-mediated depletion of Rod at the kinetochores is required for switching off the checkpoint (97).

In a complementary study, Howell *et al.* showed that several checkpoint proteins, including Mad2 and BubR1, are also transported to the spindle poles in a dynein-dependent manner (98). Inhibition of dynein in metaphase cells by microinjection of an anti-dynein antibody or recombinant p50 dynamitin protein leads to metaphase arrest. This arrest is dependent upon the spindle checkpoint because microinjection of anti-Mad2 antibodies allows these cells to escape from this mitotic arrest. Dynein is required for various aspects of mitosis, including chromosome congression and proper spindle formation and positioning. However, chromosome congression occurs normally in cells microinjected with p50 dynamitin in prometaphase. Electron microscopy further revealed that the number of chromosomes attached to each kinetochore in dynamitin injected cells is similar to that of the wild-type cells. Thus, the metaphase arrest and persistence of Mad2 on the kinetochores in these cells with a compromised dynein function is not due to defects in kinetochore microtubule attachment. Instead, it is more likely that these cells are unable to shut off the spindle checkpoint due to a failure to deplete Mad2 and other checkpoint proteins from the kinetochores.

#### *Cmt2-binding and phosphorylation of Mad2*

The dynein-mediated redistribution of kinetochore proteins provides clues as to how the generation of the wait anaphase signal is abolished in metaphase, but does not explain how the already existing APC/C inhibitory complexes in the cytosol are dismantled. The MCC might dissociate spontaneously or there might exist active mechanisms to break it

up. A newly identified protein, Cmt2, has been implicated in the disassembly of the Mad2-containing checkpoint complexes (101). Cmt2 was identified as a Mad2-binding protein in a yeast-two-hybrid assay and was subsequently shown to interact with Mad2 *in vivo* (101). The timing of Cmt2 binding to Mad2 coincides with the dissociation of Mad2 and Cdc20. Overexpression of Cmt2 disrupts the checkpoint and allows cells to escape mitosis in the presence of nocodazole. Depletion of Cmt2 by antisense oligonucleotides results in a transient delay in metaphase followed by cell death. These findings suggest that Cmt2 counteracts the function of Mad2 and might be required to silence the checkpoint (101). Another mechanism of turning off Mad2-dependent checkpoint signaling involves phosphorylation of Mad2. Wassmann *et al.* showed that Mad2 is phosphorylated at multiple sites in its C-terminal region *in vivo* (102). Phosphorylation of Mad2 increased as cells exit from a nocodazole-mediated mitotic arrest. Moreover, Mad2 mutants mimicking the phosphorylated form of Mad2 were not only unable to bind to Cdc20, but also inhibited the spindle checkpoint signaling in a dominant negative manner (102). These results suggested that phosphorylation of Mad2 inhibits its function and might be an important mechanism for checkpoint inactivation.

## **Defective spindle checkpoint and aneuploidy**

Genetic instability has long been thought to be a primary contributor to tumorigenesis. It can occur in two forms: microsatellite instability (MIN) characterized by a high mutational load and chromosome instability (CIN) resulting in aberrant chromosome numbers or aneuploidy. Defects in DNA damage repair pathways have been implicated in MIN whereas the mechanisms behind CIN remain poorly understood. The well-

established role of the spindle checkpoint in proper chromosome segregation prompted the speculation that its dysfunction might be responsible for CIN. Cahill *et al.* demonstrated that a large number of CIN colorectal cancer cell lines are defective in the spindle checkpoint (3). In some of these cell lines, one of the Bub1 alleles was mutated. These mutated Bub1 alleles inhibit the function of the intact copy of the Bub1 gene in a dominant negative fashion, as their introduction into otherwise checkpoint proficient MIN cell lines resulted in a loss of spindle checkpoint function. Mutations in checkpoint genes have subsequently been shown in many CIN cancer cell lines in numerous studies (103,104). However, a large number of aneuploid cell lines do not appear to harbor mutations in the known spindle checkpoint genes. It is possible that the spindle checkpoint defects in these cell lines might result from altered expression levels of the known checkpoint genes or mutations of as yet unidentified checkpoint genes.

Paradoxically, a complete inactivation of certain checkpoint genes in higher organisms results in early embryonic lethality. For example, Mad2 null mouse causes embryonic lethality and the Mad2 null embryos show high levels of chromosome missegregation and apoptosis (105). Deletion of Bub1 in *Drosophila* is also embryonic lethal (106). It is unclear whether the spindle checkpoint is essential for early development of multicellular organisms or whether Mad2, Bub1, and other checkpoint genes have yet unidentified essential non-checkpoint functions. Nevertheless, Mad2 haploinsufficiency is compatible with viability (107). The level of Mad2 in these cells is approximately 70% of that of the wild-type, suggesting partial compensation of protein levels by the remaining allele (107). The reduced Mad2 levels in Mad2<sup>+/-</sup> cells results in spindle checkpoint deficiency. These mice display a high incidence of lung tumors after



long latencies (107). Thus, relatively minor alterations in the levels of spindle checkpoint proteins can promote tumorigenesis. Instead of a complete inactivation, partial disruption of the spindle checkpoint is more likely to be observed in cancers, because too frequent loss or gain of chromosomes might compromise cell viability.

## **Conclusion**

In summary, there is tantalizing evidence supporting the notion that a defective spindle checkpoint contributes to chromosome instability in human cancers. Furthermore, antimotitic anti-cancer drugs, such as Taxol and vinblastine, kill cancer cells through exploiting defects in their spindle checkpoint. A better understanding of the mechanism of this checkpoint, in particular how the checkpoint proteins collaborate to inhibit the ubiquitin ligase activity of APC/C, will eventually lead to new strategies to combat cancer.

## REFERENCES

1. Jallepalli, P. V., and Lengauer, C. (2001) *Nat. Rev. Cancer* **1**, 109-117
2. Wassmann, K., and Benezra, R. (2001) *Curr. Opin. Genet. Dev.* **11**, 83-90
3. Cahill, D. P., Lengauer, C., Yu, J., Riggins, G. J., Willson, J. K., Markowitz, S. D., Kinzler, K. W., and Vogelstein, B. (1998) *Nature* **392**, 300-303
4. Cleveland, D. W., Mao, Y., and Sullivan, K. F. (2003) *Cell* **112**, 407-421
5. Nasmyth, K. (2002) *Science* **297**, 559-565
6. Yu, H. (2002) *Curr. Opin. Cell Biol.* **14**, 706-714
7. Millband, D. N., Campbell, L., and Hardwick, K. G. (2002) *Trends Cell Biol.* **12**, 205-209
8. Musacchio, A., and Hardwick, K. G. (2002) *Nat. Rev. Mol. Cell Biol.* **3**, 731-741
9. Rieder, C. L., Cole, R. W., Khodjakov, A., and Sluder, G. (1995) *J. Cell Biol.* **130**, 941-948
10. Nasmyth, K., Peters, J. M., and Uhlmann, F. (2000) *Science* **288**, 1379-1385
11. Zou, H., McGarry, T. J., Bernal, T., and Kirschner, M. W. (1999) *Science* **285**, 418-422
12. Yu, H., Peters, J. M., King, R. W., Page, A. M., Hieter, P., and Kirschner, M. W. (1998) *Science* **279**, 1219-1222
13. Peters, J. M. (2002) *Mol. Cell* **9**, 931-943
14. Harper, J. W., Burton, J. L., and Solomon, M. J. (2002) *Genes Dev.* **16**, 2179-2206
15. Fang, G., Yu, H., and Kirschner, M. W. (1998) *Mol. Cell* **2**, 163-171

16. Pflieger, C. M., Lee, E., and Kirschner, M. W. (2001) *Genes Dev.* **15**, 2396-2407
17. Hilioti, Z., Chung, Y. S., Mochizuki, Y., Hardy, C. F., and Cohen-Fix, O. (2001) *Curr. Biol.* **11**, 1347-1352
18. Fang, G., Yu, H., and Kirschner, M. W. (1998) *Genes Dev.* **12**, 1871-1883
19. Shah, J. V., and Cleveland, D. W. (2000) *Cell* **103**, 997-1000
20. Li, R., and Murray, A. W. (1991) *Cell* **66**, 519-531
21. Hoyt, M. A., Totis, L., and Roberts, B. T. (1991) *Cell* **66**, 507-517
22. Winey, M., and Huneycutt, B. J. (2002) *Oncogene* **21**, 6161-6169
23. Taylor, S. S., and McKeon, F. (1997) *Cell* **89**, 727-735
24. Gorbsky, G. J., Chen, R. H., and Murray, A. W. (1998) *J. Cell Biol.* **141**, 1193-1205
25. Abrieu, A., Magnaghi-Jaulin, L., Kahana, J. A., Peter, M., Castro, A., Vigneron, S., Lorca, T., Cleveland, D. W., and Labbe, J. C. (2001) *Cell* **106**, 83-93
26. Stucke, V. M., Sillje, H. H., Arnaud, L., and Nigg, E. A. (2002) *EMBO J.* **21**, 1723-1732
27. Luo, X., Tang, Z., Rizo, J., and Yu, H. (2002) *Mol. Cell* **9**, 59-71
28. Tang, Z., Bharadwaj, R., Li, B., and Yu, H. (2001) *Dev. Cell* **1**, 227-237
29. Sudakin, V., Chan, G. K., and Yen, T. J. (2001) *J. Cell Biol.* **154**, 925-936
30. Fang, G. (2002) *Mol. Biol. Cell* **13**, 755-766
31. Hwang, L. H., Lau, L. F., Smith, D. L., Mistrot, C. A., Hardwick, K. G., Hwang, E. S., Amon, A., and Murray, A. W. (1998) *Science* **279**, 1041-1044
32. Kim, S. H., Lin, D. P., Matsumoto, S., Kitazono, A., and Matsumoto, T. (1998) *Science* **279**, 1045-1047

33. Fang, G., Yu, H., and Kirschner, M. W. (1999) *Philos. Trans. R. Soc. Lond. B Biol. Sci.* **354**, 1583-1590
34. Wassmann, K., and Benezra, R. (1998) *Proc. Natl. Acad. Sci. U. S. A.* **95**, 11193-11198
35. Li, Y., Gorbea, C., Mahaffey, D., Rechsteiner, M., and Benezra, R. (1997) *Proc. Natl. Acad. Sci. U. S. A.* **94**, 12431-12436
36. Zhang, Y., and Lees, E. (2001) *Mol. Cell Biol.* **21**, 5190-5199
37. Luo, X., Fang, G., Coldiron, M., Lin, Y., Yu, H., Kirschner, M. W., and Wagner, G. (2000) *Nat. Struct. Biol.* **7**, 224-229
38. Chen, R. H., Waters, J. C., Salmon, E. D., and Murray, A. W. (1996) *Science* **274**, 242-246
39. Li, Y., and Benezra, R. (1996) *Science* **274**, 246-248
40. Howell, B. J., Hoffman, D. B., Fang, G., Murray, A. W., and Salmon, E. D. (2000) *J. Cell Biol.* **150**, 1233-1250
41. Gorbsky, G. J. (2001) *Curr. Biol.* **11**, R1001-1004
42. Taylor, S. S., Ha, E., and McKeon, F. (1998) *J. Cell Biol.* **142**, 1-11
43. Wang, X., Babu, J. R., Harden, J. M., Jablonski, S. A., Gazi, M. H., Lingle, W. L., de Groen, P. C., Yen, T. J., and van Deursen, J. M. (2001) *J. Biol. Chem.* **276**, 26559-26567
44. Wu, H., Lan, Z., Li, W., Wu, S., Weinstein, J., Sakamoto, K. M., and Dai, W. (2000) *Oncogene* **19**, 4557-4562
45. Mao, Y., Abrieu, A., and Cleveland, D. W. (2003) *Cell* **114**, 87-98

46. Abrieu, A., Kahana, J. A., Wood, K. W., and Cleveland, D. W. (2000) *Cell* **102**, 817-826
47. Chen, R. H. (2002) *J. Cell Biol.* **158**, 487-496
48. Hardwick, K. G., Johnston, R. C., Smith, D. L., and Murray, A. W. (2000) *J. Cell Biol.* **148**, 871-882
49. Millband, D. N., and Hardwick, K. G. (2002) *Mol. Cell Biol.* **22**, 2728-2742
50. Kallio, M. J., Beardmore, V. A., Weinstein, J., and Gorbsky, G. J. (2002) *J. Cell Biol.* **158**, 841-847
51. Hoyt, M. A. (2001) *J. Cell Biol.* **154**, 909-911
52. Fraschini, R., Beretta, A., Sironi, L., Musacchio, A., Lucchini, G., and Piatti, S. (2001) *EMBO J.* **20**, 6648-6659
53. Chen, R. H., Shevchenko, A., Mann, M., and Murray, A. W. (1998) *J. Cell Biol.* **143**, 283-295
54. Chung, E., and Chen, R. H. (2002) *Mol. Biol. Cell* **13**, 1501-1511
55. Sironi, L., Mapelli, M., Knapp, S., Antoni, A. D., Jeang, K. T., and Musacchio, A. (2002) *EMBO J.* **21**, 2496-2506
56. Hardwick, K. G., Weiss, E., Luca, F. C., Winey, M., and Murray, A. W. (1996) *Science* **273**, 953-956
57. Seeley, T. W., Wang, L., and Zhen, J. Y. (1999) *Biochem. Biophys. Res. Commun.* **257**, 589-595
58. Brady, D. M., and Hardwick, K. G. (2000) *Curr. Biol.* **10**, 675-678
59. Jablonski, S. A., Chan, G. K., Cooke, C. A., Earnshaw, W. C., and Yen, T. J. (1998) *Chromosoma* **107**, 386-396

60. Warren, C. D., Brady, D. M., Johnston, R. C., Hanna, J. S., Hardwick, K. G., and Spencer, F. A. (2002) *Mol. Biol. Cell* **13**, 3029-3041
61. Yamaguchi, S., Decottignies, A., and Nurse, P. (2003) *EMBO J.* **22**, 1075-1087
62. Chung, E., and Chen, R. H. (2003) *Nat. Cell Biol.* **5**, 748-753
63. Waters, J. C., Chen, R. H., Murray, A. W., and Salmon, E. D. (1998) *J. Cell Biol.* **141**, 1181-1191
64. Hoffman, D. B., Pearson, C. G., Yen, T. J., Howell, B. J., and Salmon, E. D. (2001) *Mol. Biol. Cell* **12**, 1995-2009
65. Zhou, J., Panda, D., Landen, J. W., Wilson, L., and Joshi, H. C. (2002) *J. Biol. Chem.* **277**, 17200-17208
66. Shannon, K. B., Canman, J. C., and Salmon, E. D. (2002) *Mol. Biol. Cell* **13**, 3706-3719
67. Skoufias, D. A., Andreassen, P. R., Lacroix, F. B., Wilson, L., and Margolis, R. L. (2001) *Proc. Natl. Acad. Sci. U. S. A.* **98**, 4492-4497
68. Kapoor, T. M., Mayer, T. U., Coughlin, M. L., and Mitchison, T. J. (2000) *J. Cell Biol.* **150**, 975-988
69. Stern, B. M., and Murray, A. W. (2001) *Curr. Biol.* **11**, 1462-1467
70. Yu, H. G., Muszynski, M. G., and Kelly Dawe, R. (1999) *J. Cell Biol.* **145**, 425-435
71. Nicklas, R. B., Waters, J. C., Salmon, E. D., and Ward, S. C. (2001) *J. Cell Sci.* **114**, 4173-4183
72. Martin-Lluesma, S., Stucke, V. M., and Nigg, E. A. (2002) *Science* **297**, 2267-2270

73. Tanaka, T. U. (2002) *Curr. Opin. Cell Biol.* **14**, 365-371
74. Stern, B. M. (2002) *Curr. Biol.* **12**, R316-318
75. Bolton, M. A., Lan, W., Powers, S. E., McClelland, M. L., Kuang, J., and Stukenberg, P. T. (2002) *Mol. Biol. Cell* **13**, 3064-3077
76. Murata-Hori, M., Tatsuka, M., and Wang, Y. L. (2002) *Mol. Biol. Cell* **13**, 1099-1108
77. Kallio, M. J., McClelland, M. L., Stukenberg, P. T., and Gorbsky, G. J. (2002) *Curr. Biol.* **12**, 900-905
78. Murata-Hori, M., and Wang, Y. (2002) *Curr. Biol.* **12**, 894-899
79. Hauf, S., Cole, R. W., LaTerra, S., Zimmer, C., Schnapp, G., Walter, R., Heckel, A., van Meel, J., Rieder, C. L., and Peters, J. M. (2003) *J. Cell Biol.* **161**, 281-294
80. Lens, S. M., Wolthuis, R. M., Klompmaker, R., Kauw, J., Agami, R., Brummelkamp, T., Kops, G., and Medema, R. H. (2003) *EMBO J.* **22**, 2934-2947
81. Tanaka, T. U., Rachidi, N., Janke, C., Pereira, G., Galova, M., Schiebel, E., Stark, M. J., and Nasmyth, K. (2002) *Cell* **108**, 317-329
82. Biggins, S., and Murray, A. W. (2001) *Genes Dev.* **15**, 3118-3129
83. Li, Y., Bachant, J., Alcasabas, A. A., Wang, Y., Qin, J., and Elledge, S. J. (2002) *Genes Dev.* **16**, 183-197
84. Kang, J., Cheeseman, I. M., Kallstrom, G., Velmurugan, S., Barnes, G., and Chan, C. S. (2001) *J. Cell Biol.* **155**, 763-774
85. Ditchfield, C., Johnson, V. L., Tighe, A., Ellston, R., Haworth, C., Johnson, T., Mortlock, A., Keen, N., and Taylor, S. S. (2003) *J. Cell Biol.* **161**, 267-280

86. Jones, M. H., Bachant, J. B., Castillo, A. R., Giddings, T. H., Jr., and Winey, M. (1999) *Mol. Biol. Cell* **10**, 2377-2391
87. Kitagawa, K., Abdulle, R., Bansal, P. K., Cagney, G., Fields, S., and Hieter, P. (2003) *Mol. Cell* **11**, 1201-1213
88. Freed, E., Lacey, K. R., Huie, P., Lyapina, S. A., Deshaies, R. J., Stearns, T., and Jackson, P. K. (1999) *Genes Dev.* **13**, 2242-2257
89. Gstaiger, M., Marti, A., and Krek, W. (1999) *Exp. Cell Res.* **247**, 554-562
90. Wigge, P. A., and Kilmartin, J. V. (2001) *J. Cell Biol.* **152**, 349-360
91. McClelland, M. L., Gardner, R. D., Kallio, M. J., Daum, J. R., Gorbsky, G. J., Burke, D. J., and Stukenberg, P. T. (2003) *Genes Dev.* **17**, 101-114
92. Hori, T., Haraguchi, T., Hiraoka, Y., Kimura, H., and Fukagawa, T. (2003) *J. Cell Sci.* **116**, 3347-3362
93. DeLuca, J. G., Moree, B., Hickey, J. M., Kilmartin, J. V., and Salmon, E. D. (2002) *J. Cell Biol.* **159**, 549-555
94. Newman, J. R., Wolf, E., and Kim, P. S. (2000) *Proc. Natl. Acad. Sci. U. S. A.* **97**, 13203-13208
95. Liu, S. T., Hittle, J. C., Jablonski, S. A., Campbell, M. S., Yoda, K., and Yen, T. J. (2003) *Nat. Cell Biol.* **5**, 341-345
96. Arnaoutov, A., and Dasso, M. (2003) *Dev. Cell* **5**, 99-111
97. Wojcik, E., Basto, R., Serr, M., Scaerou, F., Karess, R., and Hays, T. (2001) *Nat. Cell Biol.* **3**, 1001-1007
98. Howell, B. J., McEwen, B. F., Canman, J. C., Hoffman, D. B., Farrar, E. M., Rieder, C. L., and Salmon, E. D. (2001) *J. Cell Biol.* **155**, 1159-1172



- 99. Basto, R., Gomes, R., and Karess, R. E. (2000) *Nat. Cell Biol.* **2**, 939-943
- 100. Chan, G. K., Jablonski, S. A., Starr, D. A., Goldberg, M. L., and Yen, T. J. (2000) *Nat. Cell Biol.* **2**, 944-947
- 101. Habu, T., Kim, S. H., Weinstein, J., and Matsumoto, T. (2002) *EMBO J.* **21**, 6419-6428
- 102. Wassmann, K., Liberal, V., and Benezra, R. (2003) *EMBO J.* **22**, 797-806
- 103. Ru, H. Y., Chen, R. L., Lu, W. C., and Chen, J. H. (2002) *Oncogene* **21**, 4673-4679
- 104. Ohshima, K., Haraoka, S., Yoshioka, S., Hamasaki, M., Fujiki, T., Suzumiya, J., Kawasaki, C., Kanda, M., and Kikuchi, M. (2000) *Cancer Lett.* **158**, 141-150
- 105. Dobles, M., Liberal, V., Scott, M. L., Benezra, R., and Sorger, P. K. (2000) *Cell* **101**, 635-645
- 106. Basu, J., Bousbaa, H., Logarinho, E., Li, Z., Williams, B. C., Lopes, C., Sunkel, C. E., and Goldberg, M. L. (1999) *J. Cell Biol.* **146**, 13-28
- 107. Michel, L. S., Liberal, V., Chatterjee, A., Kirchwegger, R., Pasche, B., Gerald, W., Dobles, M., Sorger, P. K., Murty, V. V., and Benezra, R. (2001) *Nature* **409**, 355-359

## **CHAPTER TWO**

# **Mad2- Independent Inhibition of APC<sup>Cdc20</sup> by the Mitotic Checkpoint Protein BubR1**

### **Introduction**

During the cell division cycle, cells first replicate their DNA and then package the DNA into sister-chromatids, which are held together by the cohesin protein complex (Nasmyth et al., 2000). After all sister-chromatids have achieved bipolar attachment to the mitotic spindle, a ubiquitin ligase called the anaphase-promoting complex or cyclosome (APC) tags the securin protein with poly-ubiquitin chains (King et al., 1996; Zachariae and Nasmyth, 1999). Degradation of the ubiquitinated securin by the proteasome in turn activates the proteolytic activity of the separase (Uhlmann et al., 2000). Proteolytic cleavage of a cohesin protein by the separase destroys the cohesion between the sister-chromatids and triggers the onset of anaphase (Uhlmann et al., 2000). To ensure the high-fidelity transmission of the genetic material, the timing of sister-chromatid separation is closely monitored by the spindle assembly or mitotic checkpoint (Straight and Murray, 1997; Burke, 2000). This checkpoint senses the existence of kinetochores not yet occupied by microtubules (Gorbsky and Ricketts, 1993; Li and Nicklas, 1995; Nicklas et al., 1995). A single unattached kinetochore within a cell is sufficient to trigger this checkpoint, resulting in the inhibition of APC, stabilization of securin, and delay of the onset of anaphase (Nicklas, 1997).

The molecular mechanism of the mitotic checkpoint has recently begun to unravel. Several molecular components of this pathway were initially identified in budding yeast, including Mad1, Mad2, Mad3, Bub1, Bub2, Bub3, and Mps1 (Hoyt et al., 1991; Li and Murray, 1991; Roberts et al., 1994; Hardwick et al., 1996). Homologs of most of these proteins were then found in other organisms including vertebrates (Chen et al., 1996; Li and Benezra, 1996; Taylor and McKeon, 1997; Chen et al., 1998; Jin et al., 1998; Taylor et al., 1998). Interestingly, the vertebrate homologs of Mad1, Mad2, Bub1, and Bub3 were shown to localize to kinetochores during mitosis (Chen et al., 1996; Li and Benezra, 1996; Taylor and McKeon, 1997; Chen et al., 1998; Taylor et al., 1998; Martinez-Exposito et al., 1999). In addition, a mammalian protein kinase called BubR1 that shares homology with both the yeast Mad3 and Bub1 proteins, was also found at the kinetochores in mitosis (Chan et al., 1998; Jablonski et al., 1998; Taylor et al., 1998; Chan et al., 1999). Subsequent genetic and biochemical studies showed that, with the exception of Bub2, all these molecules are involved in delaying the onset of anaphase in the presence of spindle damage and may partially account for the proper timing of chromosome segregation during normal mitosis (Taylor and McKeon, 1997; Fraschini et al., 1999; Li, 1999; Bardin et al., 2000; Bloecher et al., 2000; Gardner and Burke, 2000; Pereira et al., 2000). Bub1 and BubR1 are protein kinases and both interact with Bub3 (Taylor et al., 1998). Mad1 is a coiled-coil protein and forms a tight complex with Mad2 throughout the cell cycle (Hardwick and Murray, 1995; Chen et al., 1998; Chen et al., 1999). The biochemical function of Mad2 is relatively well understood. Several lines of evidence have established that Mad2 binds directly to Cdc20, an activator of APC, thereby inhibiting the activity of APC (Li et al., 1997; Fang et al., 1998a; Fang et al., 1998b; Hwang et al., 1998; Kim et al., 1998; Dobles et al., 2000). In contrast, the exact biochemical functions of Bub1, BubR1, Bub3, and Mad1 are

not clear. Because these proteins localize to kinetochores in mitosis and because several of them interact physically, it has been postulated that these checkpoint proteins may function as multi-protein complexes (Chan et al., 1999; Brady and Hardwick, 2000; Hardwick et al., 2000).

Elegant experiments on mammalian cells have revealed two extraordinary features of the mitotic checkpoint. First, as a single unattached kinetochore can delay the onset of sister-chromatid separation, it must generate an inhibitory signal to block the activity of APC (Rieder et al., 1995). Moreover, this signal needs to be distributed throughout the cell to account for the inhibition of APC that is not associated with the unattached kinetochore (Shah and Cleveland, 2000). Although the nature of this diffusive inhibitory signal has not been established, it is likely to involve the Mad2 protein due to its direct role in the inhibition of APC<sup>Cdc20</sup>. Second, one of the traits of the unattached kinetochores that the checkpoint senses may be the lack of tension exerted by microtubules (Li and Nicklas, 1995). This notion is further strengthened by the recent finding that the kinesin-like motor CENP-E is an essential component of the mitotic checkpoint in mammalian cells and in *Xenopus* extracts (Abrieu et al., 2000; Yao et al., 2000). CENP-E interacts directly with BubR1 in mitosis and this interaction may be a part of the force-sensing mechanism (Chan et al., 1999; Yao et al., 2000). However, it is unclear how an imbalance of force can be translated into an activity that inhibits APC.

To gain insights into the roles of the checkpoint proteins in transducing the inhibitory kinetochore signal, we purified a 500 kD BubR1 complex from mitotic HeLa cell lysate using a combination of conventional and immuno-affinity chromatography. Mass spectrometric analysis revealed that this complex consisted of BubR1 and Bub3 at 1:1 molar ratio and Cdc20 was present at a sub-stoichiometric level. This was consistent with the recent finding of Wu et al. that BubR1 associated with Cdc20 in nocodazole-arrested cells (Wu et al., 2000). Purified

recombinant BubR1 inhibited the activity of APC<sup>Cdc20</sup> in ubiquitination assays at a much lower concentration ( $K_i=40$  nM) as compared to Mad2 ( $K_i=2$   $\mu$ M). BubR1 also blocked the mitotic activation of APC in *Xenopus* extracts. Surprisingly, the kinase activity of BubR1 was not required for its ability to inhibit APC. Both BubR1 and Mad2 inhibited APC through blocking the binding of Cdc20 to APC. Furthermore, a fragment of BubR1 lacking the Bub3-binding domain blocked the ability of exogenous Cdc20 to prevent mitotic arrest in nocodazole-treated HeLa cells. Taken together, our findings suggest that BubR1 sequesters Cdc20 and inhibits APC<sup>Cdc20</sup> in mitosis. Because BubR1 binds to CENP-E directly, the affinity of the BubR1–Cdc20 interaction at the kinetochores may be regulated by microtubule attachment, thus providing a potential link between the molecular sensor of the checkpoint and the inhibition of APC. Zhanyun Tang a postdoctoral fellow in our lab was the primary contributor of the following work.

## **Experimental Procedures**

### **Antibody Production, Immunoprecipitation, and Immunoblotting**

To generate antibodies against Bub1 and BubR1, several fragments, including Bub1N (residues 1-200), BubR1N1 (residues 1-200), and BubR1N2 (residues 201-400), were expressed as GST fusion proteins in bacteria and purified. The proteins were used to immunize rabbits at Zymed Laboratories (San Francisco). The antisera were purified using the appropriate antigens. The production of anti-APC2, anti-APC3 (Cdc27), and anti-Mad2 polyclonal antibodies was reported previously (Fang et al., 1998a; Fang et al., 1998b). A goat polyclonal anti-Cdc20 antibody was purchased from Santa Cruz Biotechnology. The anti-Myc (9E10) monoclonal antibody was purchased from Roche. For immuno-blotting, the antibodies were used at 1:1000 dilution of crude serum or at 1 µg/ml of affinity-purified IgG. For immuno-precipitation, antibodies were coupled to Affi-Prep Protein A beads (Bio-Rad) at a concentration of 1 mg/ml.

### **Purification of the BubR1–Bub3 Complex**

HeLa cells were grown in Dulbecco's modified Eagle's medium (DMEM; Gibco) supplemented with 10% fetal bovine serum. For the purification of the BubR1–Bub3 complex, a total of 40 plates (150mm) of HeLa cells were grown to confluency, treated with 300 nM nocodazole for 18 hrs, and harvested. The cells were lysed with the NP-40 lysis buffer (50 mM Tris-HCl, pH7.7, 150 mM NaCl, 0.5% NP-40, 1 mM DTT, 10% glycerol, 0.5 µM okadaic acid, and 10 µg/ml each of leupeptin, pepstatin, and chymostatin). The lysate was centrifuged at 40,000 rpm for 1 hr. The supernatant was fractionated on a 50 ml resource Q column (Pharmacia). Ammonium sulfate was added to the BubR1-containing fractions to 30% saturation and the resulting precipitates were dissolved and fractionated on a 26 ml Superose 6 column (Pharmacia). The

BubR1-containing fractions were combined and subjected to immunoprecipitation by two different anti-BubR1 antibodies. After extensive washing, the antibody beads were eluted with 100 mM glycine (pH 2.5), concentrated, and analyzed by SDS-PAGE, followed by staining with Coomassie blue (Bio-Rad). The protein bands were excised and subjected to LC/MS/MS analysis.

### **Protein Expression in Sf9 Cells and Purification**

For the production of human Bub1, BubR1, Bub3, Cdc20, and BubR1 mutant proteins, recombinant baculoviruses encoding these proteins fused at the N-termini with a His<sub>6</sub>-tag were constructed using the Bac-to-Bac system (Gibco). Sf9 cells were grown to a density of  $2 \times 10^6$  /ml and infected with the appropriate viruses at a multiplicity of infection (MOI) of 1-5 for 50 hrs. The cells were lysed with a buffer containing 20 mM Tris (pH 7.7), 150 mM NaCl, and 0.1% Triton X-100. The proteins were incubated with Ni<sup>2+</sup>-NTA beads (Qiagen) and eluted with a step gradient of imidazole. When necessary, the proteins were further purified by anion exchange or gel filtration chromatography.

### **Cyclin Degradation and H1 Kinase Assays**

The *Xenopus* egg extracts were prepared as described previously (Murray, 1991). To assay the activation of APC in crude *Xenopus* egg extracts, the BubR1 protein at a final concentration of 1  $\mu$ M or an equal volume of XB buffer (10 mM HEPES, pH 7.7, 100 mM KCl, 0.1 mM CaCl<sub>2</sub>, 1 mM MgCl<sub>2</sub>, 50 mM sucrose) was incubated with the interphase extract for 30 min. The  $\square$ 90-cyclin B1 protein was then added to a final concentration of 5  $\mu$ M. After 90 min at room temperature, 1  $\mu$ l of the extract was removed and incubated for 10 min with 9  $\mu$ l of the H1 kinase

reaction mixture that contained 50  $\mu$ M non-labeled ATP, 60  $\mu$ Ci of  $^{32}$ P-ATP, and 140  $\mu$ g/ml of histone H1 (Bohringer Mannheim) in EB buffer (80 mM  $\beta$ -glycerophosphate, pH7.4, 15 mM  $MgCl_2$ , 10 mM EGTA and 0.1% NP-40). The reactions were quenched with SDS loading buffer, analyzed by SDS-PAGE, and autoradiography. To assay cyclin degradation, the N-terminal fragment of human cyclin B1 (residues 1-102) with a Myc-tag and ubiquitin were added to the extracts at final concentrations of 100 nM and 150  $\mu$ M, respectively. Aliquots of the reaction mixture were quenched by SDS sample buffer at the indicated time, separated by SDS-PAGE, and blotted with anti-Myc.

### **Ubiquitination Assay**

To purify interphase APC, the anti-APC3 (Cdc27) beads were incubated with 10 volumes of interphase *Xenopus* egg extracts for 2 hrs at 4 °C and washed five times with XB containing 500 mM KCl and 0.5% NP-40 and twice with XB. The interphase APC beads were then incubated for 1 hr at room temperature with human Cdc20 protein that had been pre-incubated with BubR1, Mad2, or other checkpoint proteins. After incubation, the APC beads were washed twice with XB, and assayed for cyclin ubiquitination activity. Each ubiquitination assay was performed in a volume of 5  $\mu$ l. The reaction mixture contained an energy-regenerating system, 150  $\mu$ M of bovine ubiquitin, 5  $\mu$ M of the Myc-tagged N-terminal fragment of human cyclin B1, 5  $\mu$ M of human E1, 2  $\mu$ M of UbcH10, and 2  $\mu$ l of the APC beads. The reactions were incubated at room temperature for 1 hr, quenched with SDS sample buffer, and analyzed by SDS-PAGE followed by immunoblotting with anti-Myc.

To isolate human APC, HeLa cells were grown in the presence of 2 mM thymidine (Sigma) for 18 hrs to arrest the cell cycle at the G1/S boundary, washed with PBS, and grown in



fresh medium without thymidine for 8 hrs. Cells were then incubated with 2 mM thymidine for another 18 hours, transferred into fresh medium, and harvested at various timepoints. The cells were lysed with the NP-40 lysis buffer. The cell lysates were then incubated with the anti-APC3 antibody beads for 2 hrs at 4 °C. The beads were then washed, incubated with Cdc20 and other proteins, and assayed for ubiquitination activity as described above.

### **Binding Assay**

The full-length Cdc20 and the N- and C-terminal fragments of Cdc20 were translated in reticulocyte lysate in the presence of <sup>35</sup>S-methionine. Purified His<sub>6</sub>-tagged Mad2 proteins (wild-type, ΔN10, and ΔC10) were bound to Ni<sup>2+</sup>-NTA beads, incubated with the <sup>35</sup>S-labeled Cdc20 protein, and washed three times with TBS containing 0.05% Tween. The proteins retained on beads were analyzed by SDS-PAGE followed by autoradiography. Binding of BubR1 to Cdc20 and Bub3 was assayed similarly.

## Results

### Purification of A Mitotic Checkpoint Complex

Several mitotic checkpoint proteins, including Bub1, BubR1, Bub3, Mad1, Mad2, and Mad3, were reported to form various complexes either in yeast or in mammalian cells (Chan et al., 1999; Brady and Hardwick, 2000; Hardwick et al., 2000). We therefore examined the fractionation profiles of several proteins involved in this pathway on a gel filtration column. Bub1 eluted as part of a 1,000 kD complex in HeLa cells treated with nocodazole, which depolymerized microtubules and activated the spindle assembly checkpoint (Figure 1A). However, the Bub1 complex was also present in cells arrested at the G1/S boundary by thymidine. The fractionation profiles of APC2 and Mad2 in mitotic and G1/S lysates did not vary, either. In contrast, while BubR1 existed as a part of a 500 kD complex in G1/S cell lysate, a significant portion of BubR1 was incorporated into a larger complex (1,500 kD) when checkpoint was activated. Interestingly, the majority of Cdc20 eluted around 250 kD in G1/S lysate. Upon checkpoint activation, Cdc20 formed two additional larger complexes, which appeared to co-elute with the two forms of BubR1 complexes in the same lysate (Figure 1A & 1B).

Because BubR1 and Cdc20 exhibited a similar fractionation profile in mitosis, we decided to purify the 500 kD BubR1 complex from nocodazole-treated HeLa cells. Using a combination of conventional and immuno-affinity chromatography, the BubR1 complex was purified to homogeneity (Figure 1C). Based on Coomassie-staining, only two bands, p150 and p40, appeared to be present at stoichiometric levels (Figure 1D). Identical banding patterns were observed for two different antibodies against BubR1. The p150 and p40 proteins were subjected to tryptic digestion followed by liquid chromatography and tandem mass spectrometry

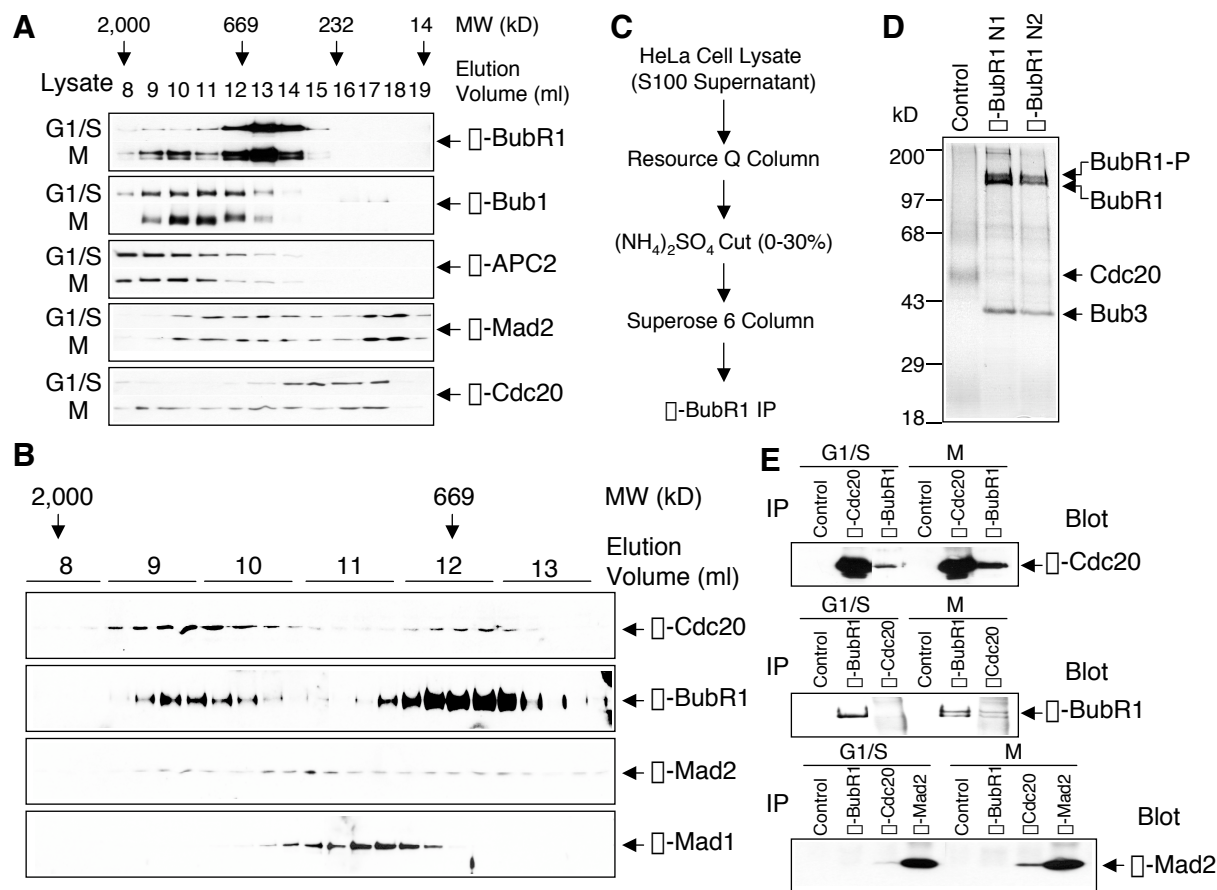


**Figure 1** Purification of a mitotic BubR1 complex. (A) Lysates of HeLa cells arrested at the G1/S boundary by thymidine or in mitosis by nocodazole were fractionated on a Superose 6 gel filtration column and blotted with various antibodies. The elution volume and the native molecular mass standards are indicated. (B) The S100 supernatant of the mitotic HeLa cells was fractionated on a Superose 6 gel filtration column. Fractions of 0.25 ml each were collected, instead of the 1 ml fractions shown in (A). Only the fractions containing the higher molecular weight species of BubR1, Cdc20, Mad1, and Mad2 were separated by SDS-PAGE and blotted with antibodies against Cdc20, BubR1, Mad2, and Mad1. The two peaks of Cdc20 co-eluted with the two peaks of BubR1. Mad2 fractionated more broadly and peaked differently from BubR1. The fractionation profile of Mad2 more closely resembled that of Mad1. (C) Purification scheme of the BubR1 complex. The BubR1-containing fractions were identified by immuno-blotting. (D) The BubR1-containing Superose 6 fractions were combined and immuno-precipitated with two different anti-BubR1 antibodies. The immuno-precipitates were analyzed by SDS-PAGE followed by Coomassie-staining. The bands belonging to BubR1, Bub3, and Cdc20 are labeled. BubR1 migrates as a doublet. The upper band presumably belongs to the phosphorylated form of BubR1. (E) Lysates of HeLa cells arrested at the G1/S boundary by thymidine or in mitosis by nocodazole were immuno-precipitated by anti-BubR1, anti-Cdc20, or anti-Mad2, and blotted with the indicated antibodies.

(LC/MS/MS) analysis and were identified with high confidence as human BubR1 and human Bub3, respectively. A total of 18 peptides spanning 17.7% of the entire length of BubR1 were identified while seven peptides covering 21.6% of the Bub3 sequence were detected. Several additional bands were present at sub-stoichiometric levels. One of these bands migrated with a molecular mass of 55kD belonged to human Cdc20, as mass spectrometric analysis identified a peptide corresponding to residues 84-97 of human Cdc20.

The presence of Cdc20 in the mitotic BubR1–Cdc20 complex was confirmed by immuno-blotting (Figure 1E). In nocodazole-treated cells, Cdc20 was detected in the anti-BubR1 immuno-precipitates, and vice versa. About four-fold less of Cdc20 was present in the BubR1 immuno-precipitates from G1/S cells. The increased association between BubR1 and Cdc20 may be due to the fact that the Cdc20 protein is present at higher levels in mitosis. About four-fold more of Cdc20 appeared to bind to Mad2 in mitosis, as compared to G1/S. However, Mad2 was not detected in the BubR1 immuno-precipitates (Figure 1E).

### **BubR1 Inhibits APC in Reconstituted Ubiquitination Assays and in *Xenopus* Extracts**

We next tested whether the association of BubR1 with Cdc20 affected the activity of APC<sup>Cdc20</sup>. APC with only basal level activity was immuno-purified from interphase *Xenopus* egg extracts and incubated with recombinant human Cdc20 protein purified from Sf9 cells, in the presence of human Bub1, BubR1, Bub3, or oligomeric Mad2 proteins. Purified ubiquitin-activating enzyme (E1), UbcH10, ubiquitin, ATP, and a fragment of human cyclin B1 were also included in the assay. Addition of Cdc20 to interphase APC greatly enhanced its ligase activity toward cyclin B1 whereas Mad2 inhibited the activity of APC<sup>Cdc20</sup> (Figure 2A). Interestingly, BubR1 also blocked the activity of APC<sup>Cdc20</sup>. As controls, Bub1 and Bub3 had no effect on the APC activity.

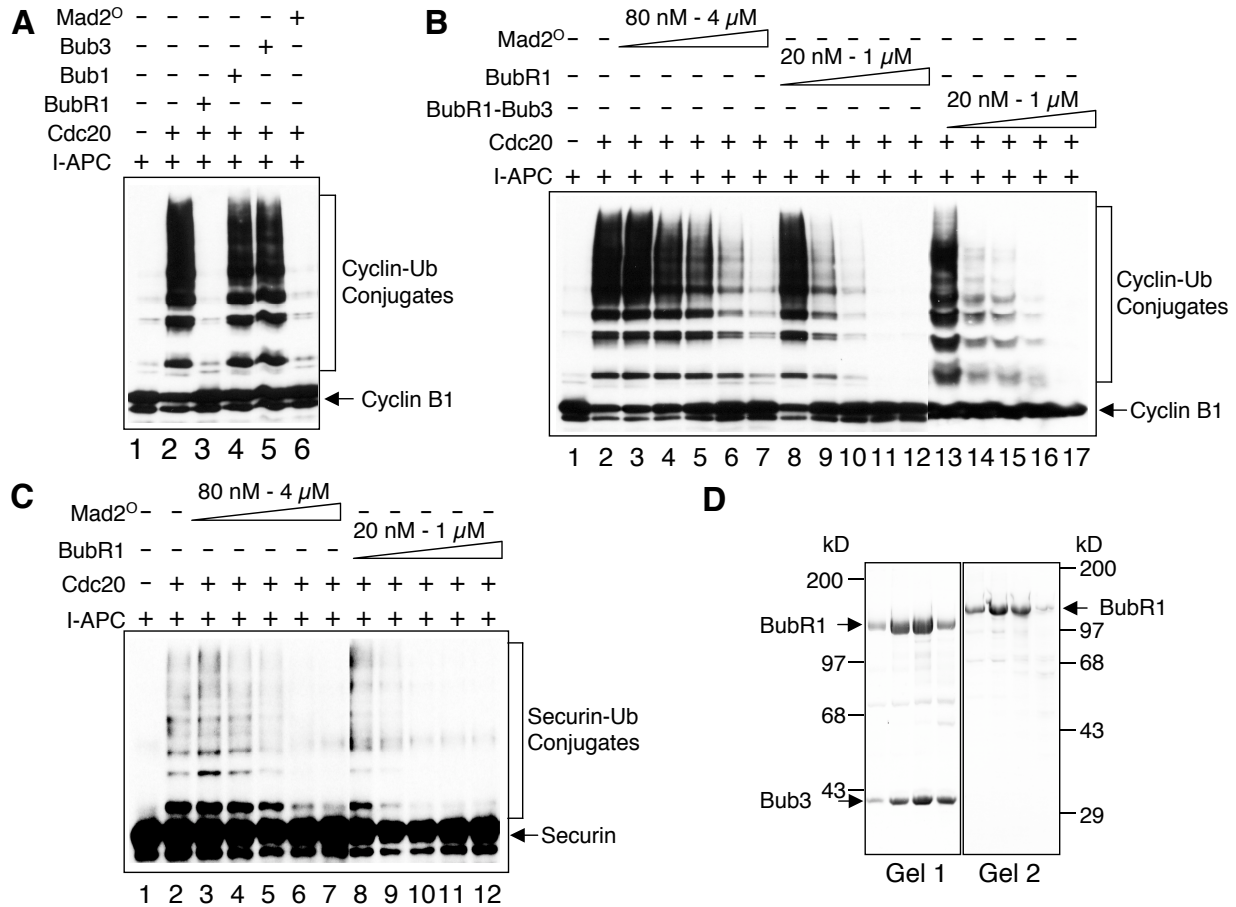


**Figure 2** BubR1 inhibits the activity of APC<sup>Cdc20</sup>. (A) I-APC was isolated from interphase *Xenopus* egg extracts and incubated with recombinant human Cdc20 protein, in the presence of buffer (Lane 2), BubR1 (Lane 3), Bub1 (Lane 4), Bub3 (Lane 5), and oligomeric Mad2 (Lane 6). The ubiquitination activity of APC was assayed with a Myc-tagged N-terminal fragment of human cyclin B1. The reaction mixtures were separated on SDS-PAGE and blotted with the anti-Myc antibody. The positions of the cyclin B1 substrate and the cyclin B1-ubiquitin conjugates are labeled. (B) Dose-response experiments of Mad2, BubR1, and the recombinant BubR1-Bub3 complex. Increasing concentrations of Mad2, BubR1, or the BubR1-Bub3 complex were added, together with Cdc20, to interphase APC (I-APC) from *Xenopus*. The concentration ranges of each of the proteins are indicated. (C) Same as (B) except that human securin was used as the substrate for APC<sup>Cdc20</sup> and that the oligomeric human Mad2 protein was expressed and purified from Sf9 cells. (D) The recombinant BubR1-Bub3 complex and the BubR1 protein produced in Sf9 cells were purified by Ni<sup>2+</sup>-NTA column followed by a Superose 6 gel filtration column. The Superose 6 column fractions containing the BubR1-Bub3 complex (Gel 1) and BubR1 (Gel2) were separated on SDS-PAGE followed by Coomassie-staining. The bands corresponding to BubR1 and Bub3 are labeled.

We next compared the potency of BubR1 and oligomeric Mad2 to inhibit APC<sup>Cdc20</sup>. To our surprise, BubR1 inhibited APC<sup>Cdc20</sup> at a much lower concentration ( $K_i = 40$  nM) than Mad2 ( $K_i = 2$   $\mu$ M), using either cyclin B1 (Figure 2B) or human securin (Figure 2C) as the substrates. Based on quantitative immuno-blotting, we estimated that the total concentrations of BubR1, Mad2, Cdc20, and APC2 in mitotic HeLa cells were around 90 nM, 120 nM, 100 nM, and 80 nM, respectively (see supplemental online data). Therefore, BubR1 can inhibit APC<sup>Cdc20</sup> at the physiological concentration. On the contrary, the concentration of Mad2 in mitotic HeLa cells is well below the  $K_i$  of 2  $\mu$ M, and is thus not sufficient to inhibit APC<sup>Cdc20</sup> in vivo without the intervention from other checkpoint proteins. We then examined whether BubR1 and Mad2 can act synergistically to inhibit APC. BubR1 and Mad2 appeared to inhibit APC in an additive manner at several concentrations (data not shown). Because the majority of BubR1 forms a 1:1 complex with Bub3 in vivo, we co-expressed BubR1 and Bub3 in Sf9 cells and purified the BubR1–Bub3 complex to homogeneity (Figure 2D). Binding of Bub3 to BubR1 did not affect the ability of BubR1 to inhibit APC<sup>Cdc20</sup> as the BubR1–Bub3 complex inhibited APC at similar concentrations (Figure 2B).

BubR1 also inhibited human APC purified from synchronized HeLa cell lysates (Figure 3A). Addition of Cdc20 activated APC in S, G2 and early mitosis (Fang et al., 1998b). When BubR1 protein was added together with Cdc20, it blocked the ability of Cdc20 to stimulate the activities of APC from S, G2, and early mitosis (Figure 3A & 3B). However, BubR1 did not inhibit the activity of APC in late mitosis or G1.

Addition of a non-degradable form of cyclin B,  $\Delta 90$ -cyclin B, is sufficient to drive the interphase *Xenopus* egg extracts into mitosis, leading to the activation of cyclin B/cdc2 and APC. We therefore checked whether BubR1 inhibited the activity of APC in *Xenopus* extracts. When

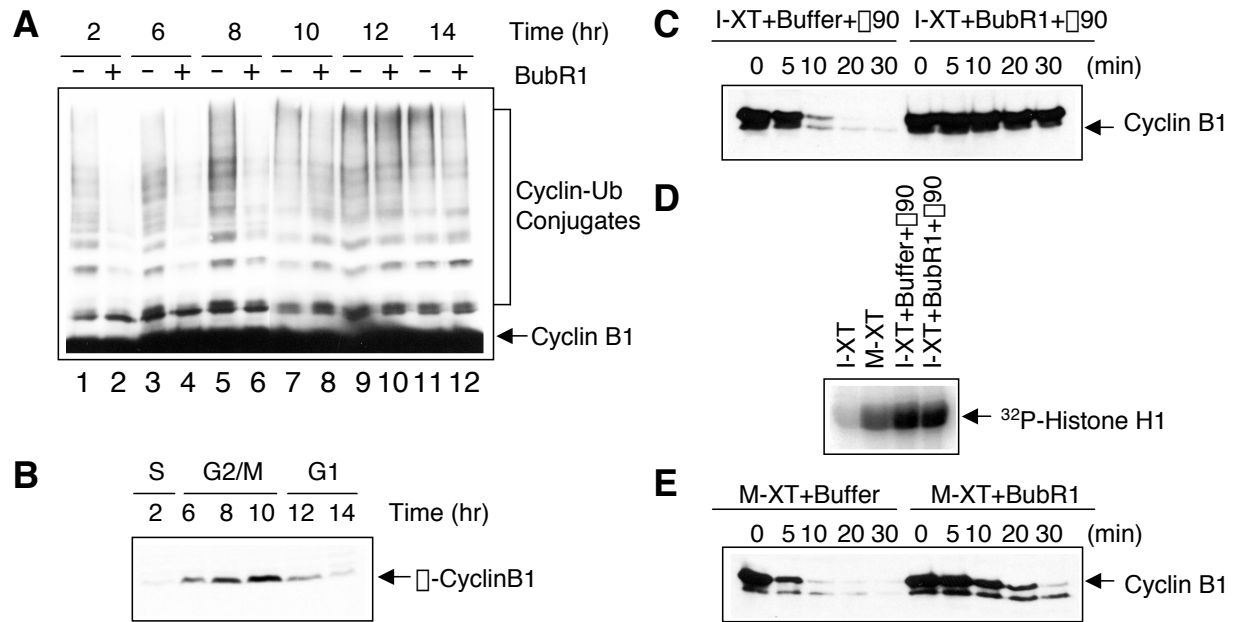


**Figure 3** BubR1 inhibits the activity of human APC<sup>Cdc20</sup> and blocks the activation of APC in *Xenopus* egg extracts. **(A)** HeLa cells were synchronized at the G1/S boundary by a double-thymidine block, released into fresh medium, and harvested at the indicated timepoints after removal of thymidine (2 hr, 6 hr, 8 hr, 10 hr, 12 hr, and 14 hr). APC was isolated from the synchronized HeLa cell lysates, incubated with Cdc20 in the presence (+) and absence (-) of BubR1, and assayed for the ubiquitination activity. **(B)** The same cell lysates used in **(A)** were blotted with anti-cyclin B1 antibody. The cell cycle status of these lysates is labeled above. **(C)** The  $\square$ 90-cyclin B protein was added to the interphase *Xenopus* egg extract, in the presence or absence of BubR1. After 90 min of the addition of  $\square$ 90-cyclin B, the Myc-tagged N-terminal fragment (1-102) of human cyclin B1 was added. Samples were taken at the indicated timepoints and blotted with anti-Myc antibody. **(D)** The same extracts, prior to the addition of the N-terminal cyclin B fragment, were assayed for histone H1 kinase activity. **(E)** Interphase *Xenopus* egg extract was incubated with  $\square$ 90-cyclin B for 90 min. The resulting mitotic extract was assayed for its ability to degrade the N-terminal cyclin B1 fragment in the absence or presence of BubR1.

BubR1 was added to the interphase extracts together with  $\square$ 90-cyclin B, the degradation of an N-terminal fragment of cyclin B1 was effectively blocked (Figure 3C). BubR1 did not block the activation of cyclin B/cdc2 based on the H1 kinase assay (Figure 3D), indicating that BubR1 prevented the activation of APC at a later step. BubR1 also partially inhibited the degradation of cyclin B1 when added to the mitotic extracts (Figure 3E). However, this effect is less profound

than that observed with the interphase extracts, consistent with the fact that the mitotic APC was more resistant to the inhibition of BubR1.

### **The Kinase Activity of BubR1 Is Not Essential for Inhibition of APC**

BubR1 achieved maximal inhibition of APC<sup>Cdc20</sup> at roughly 1:1 molar ratio with Cdc20. Furthermore, BubR1 inhibited APC<sup>Cdc20</sup> in the presence of AMP-PNP (data not shown). Although AMP-PNP can effectively support the ubiquitination reaction, it cannot be used by kinases to phosphorylate substrates. These results suggested that BubR1 did not function catalytically. To confirm this, we constructed a kinase-inactive mutant of BubR1, K795A, which was likely to disrupt its ability to bind ATP. As expected, the K795A mutation abolished the ability of BubR1 to auto-phosphorylate, suggesting that BubR1-K795A might not possess kinase activity (data not shown). To identify the regions within BubR1 responsible for the inhibition, a series of BubR1 truncation mutants were prepared (Figure 4A & 4B). The kinase-inactive BubR1-K795A mutant inhibited APC<sup>Cdc20</sup> with equal efficiency as the wild-type BubR1 protein (Figure 4C). Therefore, the kinase activity of BubR1 was dispensable for the inhibition of APC<sup>Cdc20</sup>. Furthermore, two overlapping fragments of BubR1, BubR1b (residues 526-1050) and BubR1f (residues 1-700), inhibited APC at similar concentrations as the intact BubR1 (Figure 5C). This suggested that the region spanning residues 526-700 might be critical for the inhibitory activity of BubR1. Alternatively, BubR1 might contain multiple Cdc20-binding sites. The latter possibility was more consistent with the fact that the BubR1d fragment containing residues 351-700 had no inhibitory activity toward APC (Figure 4C). Therefore, the APC-inhibitory region of BubR1 cannot be localized to a single small domain. However, a fragment



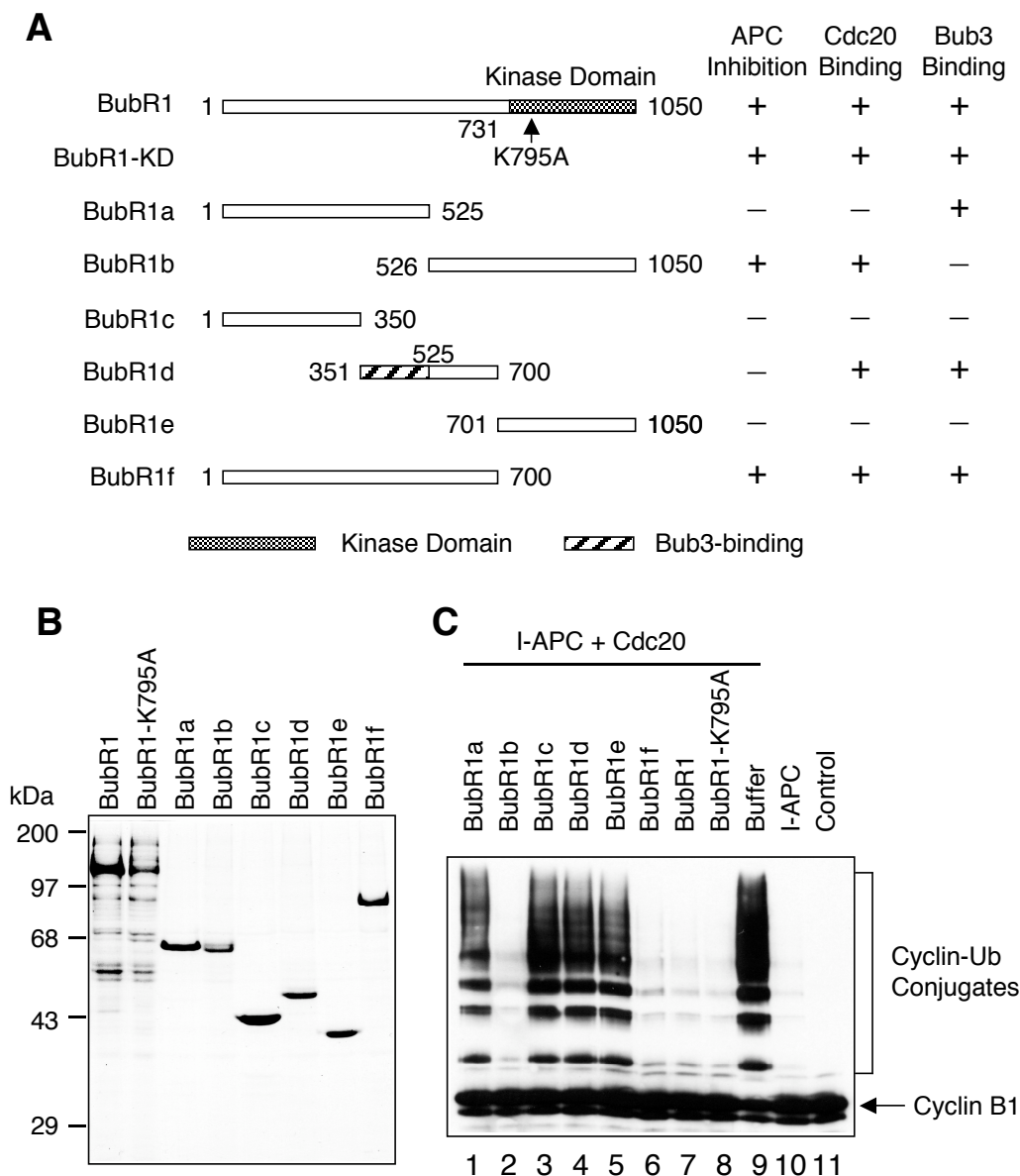


**Figure 4** The kinase activity of BubR1 is not required for inhibition of APC<sup>Cdc20</sup>. **(A)** Schematic drawing of the regions within BubR1 that are essential for inhibiting APC, binding to Cdc20, or binding to Bub3. **(B)** Purified BubR1 and its mutant proteins were analyzed by SDS-PAGE followed by Coomassie-blue staining. The fast-migrating species in the BubR1 and BubR1-K795A lanes belong to degradation products of these two proteins. **(C)** Interphase APC was incubated with Cdc20 in the presence of equal molar amount (100 nM) of various BubR1 mutant proteins and assayed for ubiquitination activity. The control lane (lane 11) did not contain APC.

of BubR1 lacking the entire kinase domain (BubR1f) was sufficient to inhibit APC, further supporting the notion that the kinase activity of BubR1 was not required for APC inhibition.

### **Binding between BubR1 and Cdc20 Requires the Intact Cdc20**

We next examined the binding between Cdc20 and the BubR1 fragments. To qualitatively compare the affinities of the BubR1–Cdc20 and the Mad2–Cdc20 interactions, the binding assay between Mad2 and Cdc20 was also repeated. We had previously shown that Mad2 interacted with a small fragment within the N-terminal region of Cdc20 (Luo et al., 2000). Digestion of *in vitro* translated <sup>35</sup>S-labeled Cdc20 with chymotrypsin resulted in two well-defined fragments of roughly 40 kD and 16 kD in size (Figure 5A). Immunoblotting revealed that the 16 kD fragment contained the N-terminus of Cdc20 while the 40 kDa fragment corresponded to its C-terminal WD40 domain (data not shown). Therefore, Cdc20 indeed behaved like a two-domain protein. Two truncation mutants of Cdc20 corresponding to the N- and C-terminal domains were then constructed (Figure 5B). The wild-type oligomeric Mad2 interacted strongly with the N-terminal domain of Cdc20 as did a monomeric form of a Mad2 mutant (with the N-terminal 10 residues deleted, ΔN10-Mad2). As a control, the Mad2 mutant with its C-terminal 10 residues deleted (ΔC10-Mad2) did not bind to Cdc20. As expected, none of the Mad2 proteins associated with the C-terminal WD40 domain of Cdc20. Unexpectedly, both the monomeric and oligomeric forms of Mad2 interacted only weakly with the intact Cdc20. The weak interactions between Mad2 and the intact Cdc20 was not due to the inability to form the Mad2–Cdc20 complex post-translationally, because only minor portions (about 20%) of Mad2 and Cdc20 were able to form a complex even when both proteins were co-expressed in Sf9 cells (data not shown). Similar

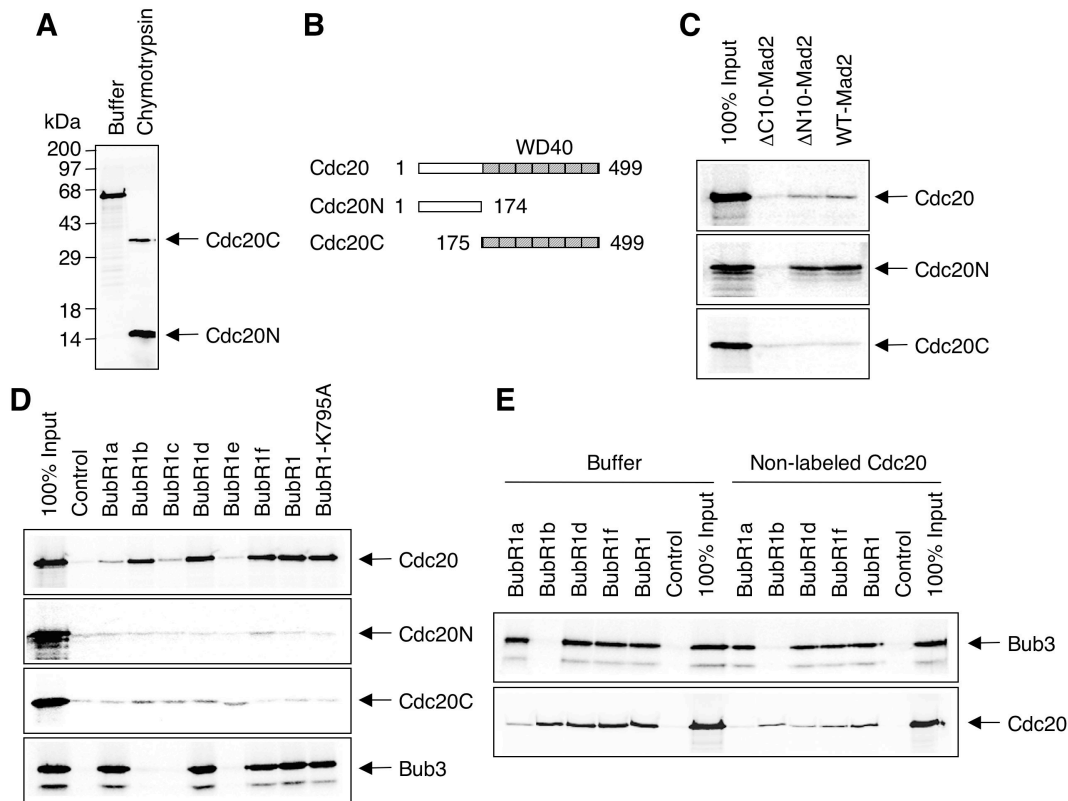


**Figure 5** Binding of Cdc20 to BubR1 and Mad2. (A)  $^{35}\text{S}$ -labeled Cdc20 protein was digested with 10  $\mu\text{g/ml}$  chymotrypsin (Roche) for 10 min at room temperature and separated on SDS-PAGE followed by autoradiography. The bands belonging to the two domains of Cdc20 are labeled. (B) Schematic drawing of the boundaries of the Cdc20 constructs corresponding to the N-terminal and C-terminal domains of Cdc20. (C) The wild-type Mad2 oligomer, the monomeric Mad2 protein with its C-terminal 10 residues deleted ( $\Delta\text{C10-Mad2}$ ), and the monomeric Mad2 protein with its N-terminal 10 residues deleted ( $\Delta\text{N10-Mad2}$ ) were bound to  $\text{Ni}^{2+}$ -NTA beads and incubated with the  $^{35}\text{S}$ -labeled Cdc20, the N-terminal domain of Cdc20 (Cdc20N), or the C-terminal domain of Cdc20 (Cdc20C). After washing, the proteins retained on beads were analyzed by SDS-PAGE followed by autoradiography. (D) Various BubR1 mutant proteins were bound to  $\text{Ni}^{2+}$ -NTA beads and incubated with the  $^{35}\text{S}$ -labeled Cdc20, the N-terminal domain of Cdc20 (Cdc20N), the C-terminal domain of Cdc20 (Cdc20C), or Bub3. The empty  $\text{Ni}^{2+}$ -NTA beads were used as the control. After washing, the proteins retained on beads were analyzed by SDS-PAGE followed by autoradiography. (E) Various BubR1 mutant proteins were bound to  $\text{Ni}^{2+}$ -NTA beads and incubated with the  $^{35}\text{S}$ -labeled Bub3 or Cdc20 in the absence or presence of non-labeled human Cdc20 protein purified from Sf9 cells. After washing, the proteins retained on beads were analyzed by SDS-PAGE followed by autoradiography.

results were also obtained in a yeast two-hybrid assay (data not shown). Therefore, Mad2 cannot form a complex efficiently with the intact Cdc20 in the absence of other checkpoint proteins.

In contrast, BubR1 did not bind to either the N- or C-terminal domains of Cdc20. However, it interacted strongly with the intact Cdc20 (Figure 5D). The two BubR1 fragments that were sufficient to inhibit APC, BubR1b and BubR1f, also associated with Cdc20. Interestingly, although the BubR1d fragment did not inhibit APC, it appeared to be sufficient for binding to Cdc20. There are several plausible explanations for this finding. First, the BubR1d fragment might not interact with Cdc20 as strongly as the intact BubR1 or the other functional BubR1 fragments. The difference in affinity cannot be distinguished by our qualitative binding assays. It is also possible that the BubR1d fragment is not properly folded, which generates a non-native molecular surface that interacts with Cdc20 non-specifically. Finally, there might be a distinction between binding of bubR1 to Cdc20 and the ability of BubR1 to inhibit APC<sup>Cdc20</sup>. BubR1 might inhibit APC<sup>Cdc20</sup> only when an extensive interaction between BubR1 and Cdc20 is established, which involves multiple contacting sites between large segments of the BubR1 and Cdc20 proteins.

We also mapped the region of BubR1 that was responsible for binding to Bub3. As shown in Figure 5D, BubR1a, BubR1d, and BubR1f interacted with Bub3. Therefore, the Bub3-binding region of BubR1 is likely to reside in residues 351-525. This is consistent with earlier findings that residues 392 to 433 of BubR1 are required for binding to Bub3 (Taylor et al., 1998). We tested whether the interactions of Bub3 and Cdc20 with BubR1 were mutually exclusive. Though non-labeled Cdc20 protein produced in Sf9 cells efficiently displaced the binding of <sup>35</sup>S-labeled Cdc20 to BubR1, it did not block the binding of <sup>35</sup>S-labeled Bub3 to BubR1 (Figure 5E). Therefore, both Bub3 and Cdc20 can simultaneously bind to BubR1 to form a ternary complex.

This is consistent with our finding that the BubR1–Bub3 complex inhibited APC<sup>Cdc20</sup> as efficiently as BubR1 alone.

### **BubR1 Counteracts the Effect of Cdc20 Overexpression in Living Cells**

In budding yeast, cells overexpressing Cdc20 do not arrest in mitosis in response to spindle damage, presumably because elevated levels of Cdc20 activate APC and allow cells to bypass the mitotic checkpoint (Hwang et al., 1998; Schott and Hoyt, 1998). Overexpression of Cdc20 in mammalian cells caused a similar phenotype (Figure 6A). HeLa cells were transfected with plasmids encoding Cdc20 and GFP, treated with nocodazole at 300 nM for 24 hrs, and stained with Hoechst 33342. Upon nocodazole treatment, about 80% of cells transfected with GFP alone arrested in mitosis, as judged by cell shape and DNA morphology (Figure 6). Co-transfection of GFP and Cdc20 greatly reduced the mitotic index (18%) of transfected cells in the presence of nocodazole. We next checked whether BubR1 could restore the mitotic arrest of the Cdc20 overexpressing cells. When cells were co-transfected with Cdc20 and the BubR1b fragment, about 80% of cells arrested in mitosis in the presence of nocodazole (Figure 6). As a control, co-transfection of Cdc20 and the BubR1d fragment that cannot inhibit APC did not restore the mitotic arrest (Figure 6B & 6C). Unexpectedly, overexpression of BubR1d alone reduced the mitotic index of transfected cells upon nocodazole treatment. Because BubR1d retained the ability to bind Bub3, this fragment might interfere with the function of Bub3 in a dominant-negative fashion. Consistent with hypothesis, co-transfection of Bub3 with BubR1d restored the mitotic arrest in nocodazole-treated cells (Figure 6B & 6C). Taken together, our data suggest that BubR1 can inhibit APC<sup>Cdc20</sup> in living cells and Bub3 is important for checkpoint signaling.

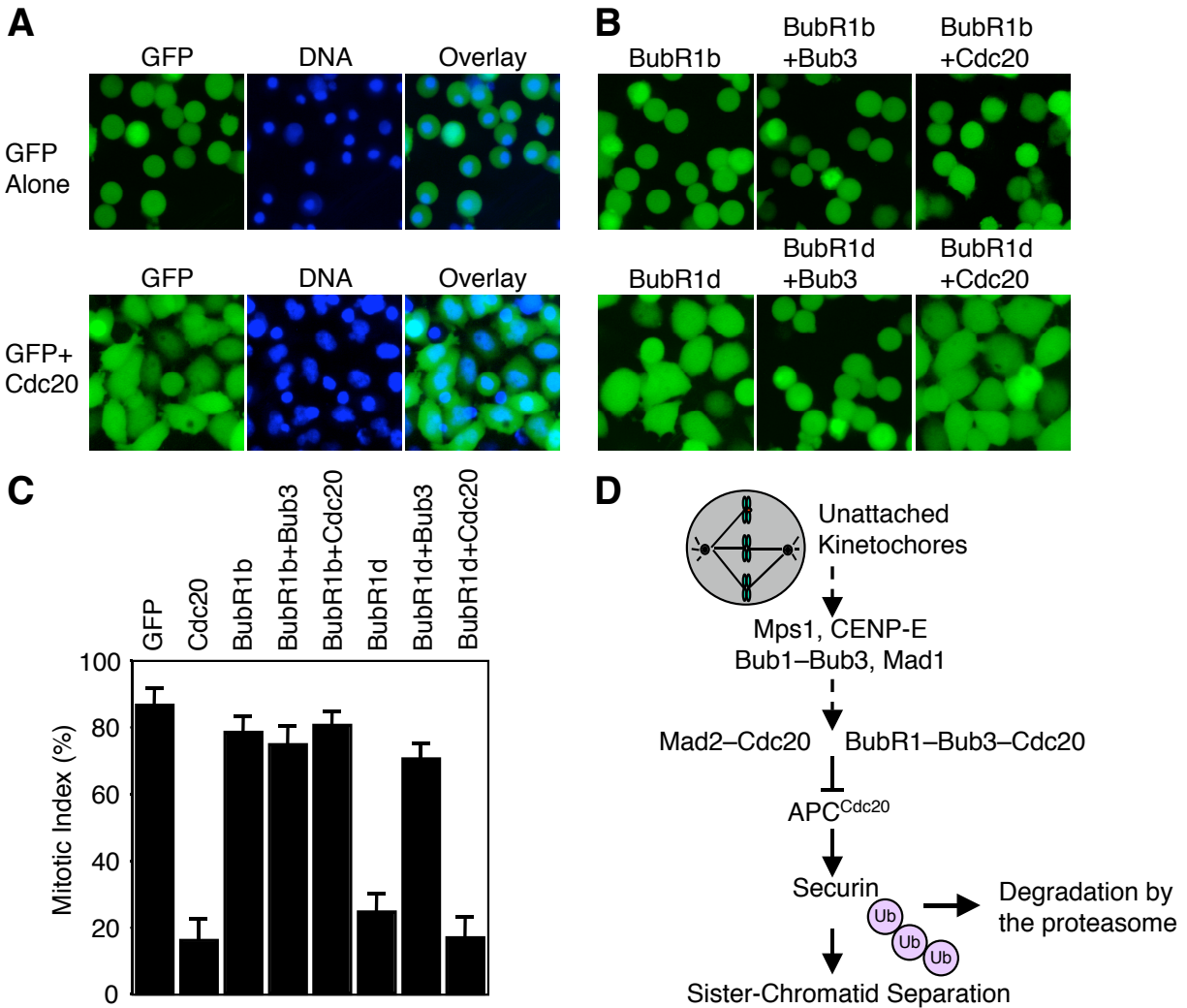


**Figure 6** BubR1 inhibits APC<sup>Cdc20</sup> in HeLa cells. **(A)** HeLa cells were transfected with either pCS2-GFP alone or pCS2-GFP together with pCS2-Cdc20, treated with nocodazole, and stained with Hoechst 33342. GFP is shown in green and DNA staining is shown in blue. **(B)** HeLa cells were transfected with the indicated plasmids together with pCS2-GFP and treated with nocodazole. The transfected cells are shown in green. **(C)** The mitotic index of cells transfected with various plasmids. The results were obtained by counting cells in three separate fields with at least 100 cells each and averaged. **(D)** A model for the spindle assembly checkpoint. See **Discussion** for details.

## Discussion

Tremendous progress has been made in the identification of the molecular components of the spindle assembly checkpoint from various organisms. However, how these proteins interact with each other to generate the checkpoint signal in response to unattached kinetochores remains a mystery (Shah and Cleveland, 2000). The results reported herein establish that the checkpoint kinase BubR1 can directly inhibit APC<sup>Cdc20</sup> independent of Mad2. Moreover, BubR1 is a much more potent inhibitor of APC<sup>Cdc20</sup> as compared to Mad2 in vitro. Therefore, our findings suggest that the BubR1–Bub3 complex may act, in a pathway parallel to Mad2, to inhibit APC<sup>Cdc20</sup> (Figure 7D).

### BubR1 as the Mammalian Homolog of Yeast Mad3

On the basis of sequence analysis alone, it is difficult to determine whether BubR1 is the ortholog of yeast Mad3 (Murray and Marks, 2001). The homology between BubR1 and the yeast Mad3 protein is restricted to the N-terminal 200 residues; this region also shares sequence similarity to the yeast Bub1 protein. In addition, the yeast Mad3 protein lacks a C-terminal kinase domain. Despite the ambiguity in sequence alignment and the difference in domain structure between BubR1 and Mad3, our biochemical results support the notion that BubR1 is the functional homolog of yeast Mad3. In yeast, Mad3 interacts with Cdc20 physically and the Mad3–Cdc20 interaction is critical for checkpoint signaling. This is consistent with the data of Wu et al. and our finding that BubR1 binds directly to Cdc20 (Wu et al., 2000). In addition, BubR1 can inhibit the ability of ectopically expressed Cdc20 to prevent mitotic arrest in the presence of spindle damage. More importantly, the kinase activity of BubR1 is dispensable for the inhibition

of APC<sup>Cdc20</sup> in vitro. Though BubR1 contains a Bub1-like kinase domain at its C-terminus, there is so far no evidence to indicate that the kinase activity of BubR1 is required for its function in the checkpoint pathway. Therefore, in terms of mechanism of action, BubR1 is more closely related to the yeast Mad3 protein than to the yeast Bub1 protein.

In yeast, the N-terminal region (homology region I) of Mad3 is required for its interaction with Cdc20 (Hardwick et al., 2000). Our data suggest that BubR1 might contain multiple Cdc20-binding regions and binding of BubR1 to Cdc20 might involve an extensive interface, involving the entire Cdc20 protein and large segments of BubR1. At present, we do not fully understand the reason for this discrepancy. However, neither the assays of Hardwick et al. (yeast two-hybrid and immuno-precipitation) nor our in vitro binding assays are quantitative (Hardwick et al., 2000). Therefore, it is entirely possible that some of the fragments of Mad3 and BubR1 might have lost certain Cdc20-binding elements and bind to Cdc20 with weaker affinity than their full-length counterparts. In fact, based on a yeast two-hybrid assay, the homology region I alone of Mad3 interacted with Cdc20 significantly weaker than the full-length Mad3 (Hardwick et al., 2000). Consistent with our data, truncation of a small C-terminal region (residues 410-515) of Mad3 significantly weakened the interactions between Mad3 and Cdc20 (Hardwick et al., 2000). Alternatively, this discrepancy might be a consequence of the rather divergent amino acid sequences of the yeast and human proteins. Although the C-terminal WD40 domains of the yeast and human Cdc20 proteins are conserved, there is little sequence homology between the N-terminal domains of these two proteins. Because both the N- and C-terminal domains of human Cdc20 are required for binding to



BubR1, it is possible that BubR1 may use multiple binding determinants to interact with human Cdc20. Due to sequence differences in the Cdc20 proteins, some of these binding elements may not be strictly conserved between yeast and human. This notion is further supported by the fact that, despite the existence of homology region I in human Bub1, no significant interaction was observed between Bub1 and Cdc20 in HeLa cells (Fig. 1A, and data not shown).

### **Sequestration of Cdc20 by BubR1**

Based on the genetic and biochemical studies in yeast and metazoans, it has become increasingly clear that the mitotic checkpoint proteins form a complicated signaling network, instead of a linear pathway (Burke, 2000). In several organisms, numerous complexes of checkpoint proteins, including Mad1–Mad2, Bub1–Bub3, and Mad3/BubR1–Bub3, are detected throughout the cell cycle. Other checkpoint complexes, such as BubR1–Bub3–Cdc20 and Mad2–Cdc20, seem to be enriched in mitotic cells, possibly due to the higher concentrations of Cdc20 in mitosis. Upon checkpoint activation, some of these complexes may interact transiently to produce even larger macromolecular assemblies and such larger complexes may also be important for the inhibition of APC. Therefore, it is critical to dissect the individual contributions of these interactions to checkpoint signaling.

Both Mad2 and BubR1 can interact with Cdc20 and inhibit APC<sup>Cdc20</sup> in vitro. What are the physiological functions of these interactions? One simple model is that Mad2 and BubR1 act in parallel pathways and sequester different pools of Cdc20 to block the activation of APC. Both proteins are required to effectively inhibit APC<sup>Cdc20</sup> in

living cells. Consistent with this sequestration model, both Mad2 and BubR1 are present at relatively high concentrations in cells. The concentrations of Mad2 and BubR1 in HeLa cells are estimated to be 120 nM and 90 nM, respectively, which are comparable to the concentration of Cdc20 (100 nM) in mitotic cells. Furthermore, Mad2 and BubR1 appear to inhibit APC<sup>Cdc20</sup> in an additive fashion in vitro (data not shown). Alternatively, it is possible that, in addition to sequestering Cdc20, binding of BubR1 and Cdc20 helps to recruit Cdc20 to kinetochores at pro-metaphase, facilitating the formation of other inhibitory checkpoint complexes containing Mad2 and Cdc20. Yet another possibility is that BubR1 and Mad2 might respond to distinct forms of spindle damage during mitosis. As recently suggested by Skoufias et al., Mad2 might sense the attachment of microtubules to kinetochores whereas BubR1 might respond to the lack of tension at the kinetochores (Skoufias et al., 2001). The hypothesis that BubR1 is involved in tension sensing is consistent with the fact that BubR1 interacts with the mitotic motor CENP-E during mitosis (Abrieu et al., 2000; Yao et al., 2000). It is conceivable that binding of the BubR1–Bub3 complex to Cdc20 might be regulated by CENP-E in response to tension at the kinetochores.

## References

- Abrieu, A., Kahana, J. A., Wood, K. W., and Cleveland, D. W. (2000). CENP-E as an essential component of the mitotic checkpoint in vitro. *Cell* *102*, 817-826.
- Bardin, A. J., Visintin, R., and Amon, A. (2000). A mechanism for coupling exit from mitosis to partitioning of the nucleus. *Cell* *102*, 21-31.
- Bloecher, A., Venturi, G. M., and Tatchell, K. (2000). Anaphase spindle position is monitored by the BUB2 checkpoint. *Nat. Cell Biol.* *2*, 556-558.
- Brady, D. M., and Hardwick, K. G. (2000). Complex formation between Mad1p, Bub1p and Bub3p is crucial for spindle checkpoint function. *Curr. Biol* *10*, 675-678.
- Burke, D. J. (2000). Complexity in the spindle checkpoint. *Curr. Opin. Genet. Dev.* *10*, 26-31.
- Chan, G. K., Jablonski, S. A., Sudakin, V., Hittle, J. C., and Yen, T. J. (1999). Human BUBR1 is a mitotic checkpoint kinase that monitors CENP-E functions at kinetochores and binds the cyclosome/APC. *J. Cell Biol.* *146*, 941-954.
- Chan, G. K., Schaar, B. T., and Yen, T. J. (1998). Characterization of the kinetochore binding domain of CENP-E reveals interactions with the kinetochore proteins CENP-F and hBUBR1. *J. Cell Biol.* *143*, 49-63.
- Chen, R. H., Brady, D. M., Smith, D., Murray, A. W., and Hardwick, K. G. (1999). The spindle checkpoint of budding yeast depends on a tight complex between the mad1 and mad2 proteins. *Mol. Biol. Cell* *10*, 2607-2618.
- Chen, R. H., Shevchenko, A., Mann, M., and Murray, A. W. (1998). Spindle checkpoint protein Xmad1 recruits Xmad2 to unattached kinetochores. *J. Cell Biol.* *143*, 283-295.

- Chen, R. H., Waters, J. C., Salmon, E. D., and Murray, A. W. (1996). Association of spindle assembly checkpoint component XMad2 with unattached kinetochores. *Science* 274, 242-246.
- Dobles, M., Liberal, V., Scott, M. L., Benezra, R., and Sorger, P. K. (2000). Chromosome missegregation and apoptosis in mice lacking the mitotic checkpoint protein Mad2. *Cell* 101, 635-645.
- Fang, G., Yu, H., and Kirschner, M. W. (1998a). The checkpoint protein MAD2 and the mitotic regulator CDC20 form a ternary complex with the anaphase-promoting complex to control anaphase initiation. *Genes Dev.* 12, 1871-1883.
- Fang, G., Yu, H., and Kirschner, M. W. (1998b). Direct binding of CDC20 protein family members activates the anaphase-promoting complex in mitosis and G1. *Mol. Cell* 2, 163-171.
- Fraschini, R., Formenti, E., Lucchini, G., and Piatti, S. (1999). Budding yeast Bub2 is localized at spindle pole bodies and activates the mitotic checkpoint via a different pathway from Mad2. *J. Cell Biol.* 145, 979-991.
- Gardner, R. D., and Burke, D. J. (2000). The spindle checkpoint: two transitions, two pathways. *Trends Cell Biol.* 10, 154-158.
- Gorbsky, G. J., and Ricketts, W. A. (1993). Differential expression of a phosphoepitope at the kinetochores of moving chromosomes. *J. Cell Biol.* 122, 1311-1321.
- Hardwick, K. G., Johnston, R. C., Smith, D. L., and Murray, A. W. (2000). MAD3 encodes a novel component of the spindle checkpoint which interacts with Bub3p, Cdc20p, and Mad2p. *J. Cell Biol.* 148, 871-882.

- Hardwick, K. G., and Murray, A. W. (1995). Mad1p, a phosphoprotein component of the spindle assembly checkpoint in budding yeast. *J. Cell Biol.* *131*, 709-720.
- Hardwick, K. G., Weiss, E., Luca, F. C., Winey, M., and Murray, A. W. (1996). Activation of the budding yeast spindle assembly checkpoint without mitotic spindle disruption. *Science* *273*, 953-956.
- Howell, B. J., Hoffman, D. B., Fang, G., Murray, A. W., and Salmon, E. D. (2000). Visualization of Mad2 dynamics at kinetochores, along spindle fibers, and at spindle poles in living cells. *J. Cell Biol.* *150*, 1233-1250.
- Hoyt, M. A., Totis, L., and Roberts, B. T. (1991). *S. cerevisiae* genes required for cell cycle arrest in response to loss of microtubule function. *Cell* *66*, 507-517.
- Hwang, L. H., Lau, L. F., Smith, D. L., Mistrot, C. A., Hardwick, K. G., Hwang, E. S., Amon, A., and Murray, A. W. (1998). Budding Yeast Cdc20: A Target of the Spindle Checkpoint. *Science* *279*, 1041-1044.
- Jablonski, S. A., Chan, G. K., Cooke, C. A., Earnshaw, W. C., and Yen, T. J. (1998). The hBUB1 and hBUBR1 kinases sequentially assemble onto kinetochores during prophase with hBUBR1 concentrating at the kinetochore plates in mitosis. *Chromosoma* *107*, 386-396.
- Jin, D.-Y., Spencer, F., and Jeang, K.-T. (1998). Human T cell leukemia virus type 1 oncoprotein Tax targets the human mitotic checkpoint protein MAD1. *Cell* *93*, 81-91.
- Kim, S. H., Lin, D. P., Matsumoto, S., Kitazono, A., and Matsumoto, T. (1998). Fission Yeast Slp1: An Effector of the Mad2-Dependent Spindle Checkpoint. *Science* *279*, 1045-1047.

- King, R. W., Deshaies, R. J., Peters, J.-M., and Kirschner, M. W. (1996). How proteolysis drives the cell cycle. *Science* 274, 1652-1659.
- Kotani, S., Tanaka, H., Yasuda, H., and Todokoro, K. (1999). Regulation of APC activity by phosphorylation and regulatory factors. *J. Cell Biol.* 146, 791-800.
- Kramer, E. R., Scheuringer, N., Podtelejnikov, A. V., Mann, M., and Peters, J. M. (2000). Mitotic regulation of the APC activator proteins CDC20 and CDH1. *Mol. Biol. Cell* 11, 1555-1569.
- Li, R. (1999). Bifurcation of the mitotic checkpoint pathway in budding yeast. *Proc. Natl. Acad. Sci. U.S.A.* 96, 4989-4994.
- Li, R., and Murray, A. W. (1991). Feedback control of mitosis in budding yeast. *Cell* 66, 519-531.
- Li, X., and Nicklas, R. B. (1995). Mitotic forces control a cell-cycle checkpoint. *Nature* 373, 630-632.
- Li, Y., and Benezra, R. (1996). Identification of a human mitotic checkpoint gene: hsMAD2. *Science* 274, 246-248.
- Li, Y., Gorbea, C., Mahaffey, D., Rechsteiner, M., and Benezra, R. (1997). MAD2 associates with the cyclosome/anaphase-promoting complex and inhibits its activity. *Proc. Natl. Acad. Sci. U.S.A.* 94, 12431-12436.
- Luo, X., Fang, G., Coldiron, M., Lin, Y., Yu, H., Kirschner, M. W., and Wagner, G. (2000). Structure of the Mad2 spindle assembly checkpoint protein and its interaction with Cdc20. *Nat. Struct. Biol.* 7, 224-229.

- Martinez-Exposito, M. J., Kaplan, K. B., Copeland, J., and Sorger, P. K. (1999). Retention of the BUB3 checkpoint protein on lagging chromosomes. *Proc. Natl. Acad. Sci. U.S.A.* *96*, 8493-8498.
- Murray, A. W. (1991). Cell cycle extracts. *Meth. Cell Biol.* *36*, 581-605.
- Murray, A. W., and Marks, D. (2001). Can sequencing shed light on cell cycling? *Nature* *409*, 844-846.
- Nasmyth, K., Peters, J. M., and Uhlmann, F. (2000). Splitting the chromosome: cutting the ties that bind sister chromatids. *Science* *288*, 1379-1385.
- Nicklas, R. B. (1997). How cells get the right chromosomes. *Science* *275*, 632-637.
- Nicklas, R. B., Ward, S. C., and Gorbsky, G. J. (1995). Kinetochore chemistry is sensitive to tension and may link mitotic forces to a cell cycle checkpoint. *J. Cell Biol.* *130*, 929-939.
- Pereira, G., Hofken, T., Grindlay, J., Manson, C., and Schiebel, E. (2000). The Bub2p spindle checkpoint links nuclear migration with mitotic exit. *Mol. Cell* *6*, 1-10.
- Peters, J.-M., King, R. W., Höög, C., and Kirschner, M. W. (1996). Identification of BIME as a subunit of the anaphase-promoting complex. *Science* *274*, 1199-1201.
- Rieder, C. L., Cole, R. W., Khodjakov, A., and Sluder, G. (1995). The checkpoint delaying anaphase in response to chromosome monoorientation is mediated by an inhibitory signal produced by unattached kinetochores. *J. Cell Biol.* *130*, 941-948.
- Roberts, B. T., Farr, K. A., and Hoyt, M. A. (1994). The *Saccharomyces cerevisiae* checkpoint gene BUB1 encodes a novel protein kinase. *Mol. Cell Biol.* *14*, 8282-8291.
- Schott, E. J., and Hoyt, M. A. (1998). Dominant alleles of *Saccharomyces cerevisiae* CDC20 reveal its role in promoting anaphase. *Genetics* *148*, 599-610.

Shah, J. V., and Cleveland, D. W. (2000). Waiting for anaphase: Mad2 and the spindle assembly checkpoint. *Cell* 103, 997-1000.

Skoufias, D. A., Andreassen, P. R., Lacroix, F. B., Wilson, L., and Margolis, R. L. (2001). Mammalian mad2 and bub1/bubR1 recognize distinct spindle-attachment and kinetochore-tension checkpoints. *Proc. Natl. Acad. Sci. U.S.A.* 98, 4492-4497.

Straight, A. F., and Murray, A. W. (1997). The spindle assembly checkpoint in budding yeast. *Methods Enzymol.* 283, 425-440.

Taylor, S. S., Ha, E., and McKeon, F. (1998). The human homologue of Bub3 is required for kinetochore localization of Bub1 and a Mad3/Bub1-related protein kinase. *J. Cell Biol.* 142, 1-11.

Taylor, S. S., and McKeon, F. (1997). Kinetochore localization of murine Bub1 is required for normal mitotic timing and checkpoint response to spindle damage. *Cell* 89, 727-735.

Uhlmann, F., Wernic, D., Poupart, M. A., Koonin, E. V., and Nasmyth, K. (2000). Cleavage of cohesin by the CD clan protease separin triggers anaphase in yeast. *Cell* 103, 375-386.

Wu, H., Lan, Z., Li, W., Wu, S., Weinstein, J., Sakamoto, K. M., and Dai, W. (2000). p55CDC/hCDC20 is associated with BUBR1 and may be a downstream target of the spindle checkpoint kinase. *Oncogene* 19, 4557-4562.

Yao, X., Abrieu, A., Zheng, Y., Sullivan, K. F., and Cleveland, D. W. (2000). CENP-E forms a link between attachment of spindle microtubules to kinetochores and the mitotic checkpoint. *Nat. Cell Biol.* 2, 484-491.



Zachariae, W., and Nasmyth, K. (1999). Whose end is destruction: cell division and the anaphase-promoting complex. *Genes Dev.* *13*, 2039-2058.

## **CHAPTER THREE**

### **Role of Mps1 and Mad2B in Spindle Assembly Checkpoint**

#### **INTRODUCTION:**

Mps1 (Monopolar spindle 1) was initially identified in *S. cerevisiae* through a genetic screen for mutants defective in spindle pole body (SPB) duplication (1). As its name suggests, the predominant phenotype in Mps1 mutant cells was the presence of a monopolar spindle due to their inability to duplicate their spindle poles, a process essential for the formation of a bipolar spindle. Other spindle pole duplication mutants like Mps2 or Cdc37 arrest in mitosis with a monopolar spindle due to an active spindle assembly checkpoint. However, Mps1 mutants progressed through mitosis in the presence of monopolar spindles suggesting that apart from SPB duplication, Mps1 might play a role in the spindle checkpoint also (2). Further support for this notion came from the finding that Mps1 overexpression can block cells in mitosis in yeast. Other checkpoint genes like Mad2, Mad1 and Bub1 are essential for this arrest (3). Furthermore, Mad1 was observed to be hyperphosphorylated in Mps1 overexpressing cells. Surprisingly, kinetochores are dispensable for this arrest because a kinetochore null mutant Ndc10-1 can still arrest in mitosis in response to Mps1 overexpression (4). Interestingly, Aurora B, a chromosome passenger protein which is implicated in tension sensing at the kinetochore microtubule attachment, is also required for Mps1 induced mitotic arrest (5). Sequence database searches lead

to the identification of a putative mouse and xenopus Mps1 homolog which shared a high level of sequence similarity with their yeast counterpart in the kinase domain (6), (7). The mouse and human homologs of Mps1 were identified earlier in an expression cloning screen for tyrosine-phosphorylated proteins using an anti-phosphotyrosine antibody and termed TTK and ESK respectively (8), (9). These proteins were shown to be dual specificity kinases, specifically expressed in proliferating tissues. Mps1 homologs are present in a wide range of species including *S. cerevisiae*, *S. pombe*, zebrafish, mouse and human, the sequence similarity between the kinase domains ranging from 33%-90% (10), (11). These proteins have an N-terminal domain of approximately 50 KD, which does not appear to be conserved throughout evolution. Functional characterization of these proteins in different species have confirmed that they are the functional orthologs of each other.

The *S. pombe* Mps1 homolog- Mph1 was identified through a genetic screen and has been implicated in the spindle assembly checkpoint but not centrosomal duplication. Mph1 is essential for the kinetochore recruitment of the spindle checkpoint protein Mad3 (12). The *S. pombe* Mph1 mutation can be complemented by the *S. cerevisiae* Mps1. The first evidence for a conserved role of Mps1 in vertebrates came from independent studies on xenopus and mouse Mps1. Disruption of Mps1 function by either immunodepletion or by addition of anti-Mps1 antibody to Nocodazole treated xenopus-oocyte extracts indicated that Mps1 is essential for both the establishment and maintenance of spindle assembly checkpoint mediated mitotic arrest (6). On the other hand, studies on mouse Mps1 using overexpression of wild type or kinase-dead Mps1 implicated it in centrosome duplication similar to its yeast counterpart. Overexpression of wild type Mps1 results in reduplication of centrosomes during S-phase arrest in mouse NIH 3T3 cells whereas overexpression of kinase-dead Mps1 mutant blocks centrosome duplication (7).

There is some controversy regarding the role of Mps1 in centrosome duplication in vertebrate cells. The centrosome duplication defects could not be reproduced in human cell lines like HeLa or U2OS, suggesting that the role of Mps1 in centrosome duplication might be a cell line specific phenomenon (13). It should be noted that unlike yeast, overexpression of human Mps1 does not cause a mitotic arrest. Recently a temperature sensitive Mps1 mutation was identified in zebrafish in a screen for mutants unable to regenerate their fins. The authors have shown that Mps1 deficient proliferating cells display a high frequency of aneuploidy and inability to arrest in the presence of spindle poisons like Nocodazole (14). With these observations in background, we set out to examine the regulation and function of human Mps1 in HeLa cells. Here we report that human Mps1 localizes to kinetochores, is phosphorylated in mitosis and is essential for a functional spindle checkpoint.

Mad2B was identified on the basis of its sequence similarity with the checkpoint protein Mad2 (15). Mad2B was a previously uncharacterized protein sharing approximately 19% sequence similarity to human Mad2. The sequence similarity between Mad2 and Mad2B prompted us to hypothesize that Mad2B might play some role in cell cycle progression. Searching the yeast genome for putative homologs, revealed two proteins– ScMad2 and ScRev7 sharing 18% and 15% sequence similarity with human Mad2B, respectively. Rev7 mutants in *S. cerevisiae* exhibit a decreased rate of UV induced mutagenesis (16), (17). Biochemical studies have demonstrated that Rev7 protein forms a complex termed polymerase zeta in conjunction with two other proteins, Rev1 and Rev3, both of which show a resistance to error prone mutagenesis, when mutated (18). Rev3 possesses some of the motifs characteristic of DNA polymerases, indicating that it forms the catalytic subunit of polymerase zeta, whereas Rev1 is a deoxycytidyl transferase (19).

Translesion DNA synthesis is a widely conserved DNA damage tolerance mechanism. In response to high levels of DNA damage, cells employ low fidelity polymerase, which can bypass the DNA lesions on the template strand, which the replicative polymerases are unable to pass through. This provides a temporary mechanism to continue DNA replication in the face of massive DNA damage that cannot be rectified immediately. However, the price for this temporary survival advantage has to be paid in the form of a higher mutagenesis rate, as the error prone polymerases often end up introducing nucleotides that are not complementary to the original sequence in the template strand. Cells lacking the polymerase zeta are more sensitive to different DNA damage agents and exhibit a lower rate of DNA damage induced mutagenesis (20). Homologs of Rev1, Rev3 and Rev7 have been identified in vertebrates. Biochemical characterization of these proteins has revealed that they serve similar functions as their yeast counterpart. The yeast rev proteins are not essential for viability but Rev3 null mice are embryonic lethal indicating that translesion DNA synthesis is either indispensable for tackling DNA damage during normal development in higher vertebrates or has assumed other essential functions (21), (22).

## EXPERIMENTAL PROCEDURES:

*Expression and purification of Mad2B-* The coding region of Mps1 and Mad2B was amplified from a human fetal thymus cDNA library (Clontech) using PCR and cloned into pFASTBAC and pET28a vector, respectively. For the production of wild type and kinase-dead human Mps1, recombinant baculoviruses encoding these proteins fused at the N-termini with a His<sub>6</sub>-tag were constructed using the Bac-to-Bac system (Gibco). Sf9 cells were grown to a density of  $2 \times 10^6$ /ml and infected with the appropriate viruses at a multiplicity of infection (MOI) of 1-5 for 50 hrs. For the production of Mad2B pET28a vector harboring the Mad2B coding sequence was transformed into BL21 DE3 bacteria cells. Expression of His-tagged Mad2B was induced by the addition of IPTG (250  $\mu$ M final concentration) to the bacterial culture at an OD<sub>600</sub> of 0.6. The cells were allowed to grow for another 3 hrs at room temperature. The SF9 or bacterial cells were lysed with a buffer containing 20 mM Tris (pH 7.7), 150 mM NaCl, and 0.1% Triton X-100. The proteins were incubated with Ni<sup>2+</sup>-NTA beads (Qiagen) and eluted with a step gradient of imidazole.

*Antibody preparation and immunoblotting-* To generate antibodies against Mps1 a N-terminus fragment encoding the first 300 amino-acid of Mps1 was expressed as GST fusion proteins in bacteria and purified, whereas for anti-Mad2B antibody bacterially purified His-Mad2B was used. These proteins were injected into rabbits for antibody production (Zymed). The antisera were purified using the corresponding antigen coupled to Affi-gel beads (Bio-Rad). For immunoblotting, the affinity-purified  $\alpha$ -Mps1 antibody was used at a final concentration of 1  $\mu$ g/ml. Horseradish Peroxidase conjugated anti-rabbit IgG was used as secondary antibody and

the immunoblots were developed using the ECL reagent as per manufacturer's protocols (Amersham).

*Tissue culture and transfection-* HeLa Tet-on cells (Clontech) were grown to 40-50% confluency and co-transfected with the pCS2-GFP and either pCS2 Mad2B or pCS2-Mad2 plasmids using the Effectene reagent (Qiagen) according to manufacturer's protocol. After 48 hrs of transfection percentage of mitotic cells was counted according to DNA and cell morphology. For RNAi experiments, the siRNA oligonucleotides specific for human Mps1 or Mad2B were chemically synthesized. They contained sequences corresponding to nucleotides 181-203 of the coding region of human Mps1, nucleotides 325-347 of the coding region of Mad2B respectively. The annealing of the siRNAs and subsequent transfection of the RNA duplexes into HeLa cells were performed exactly as described (23). 48 hrs after the first round of RNAi transfection, cells were re-plated to 30% confluency. At 12 hours after re-plating, the cells were transfected again with Mps1 siRNA oligonucleotides. The time points mentioned in the paper for these RNAi experiments were referring to the time after the second round of RNAi transfection. Cells transfected with oligofectamine alone were used as controls. 24 hours after the second round of transfection 100nM Nocodazole was added to cells for 18 hours. To determine the cell cycle status, the transfected cells were fixed with 70% ethanol, stained with propidium iodide (PI), and analyzed by flow cytometry (FACS). The phenotypes of these cells were also analyzed by indirect immunofluorescence.

*Immunofluorescence-* For the immunostaining of endogenous Mps1 HeLa cells were grown to 80% confluency. Cells were washed with PBS and extracted with 0.5% Triton X-100 in PHEM buffer (60 mM PIPES, 25 mM HEPES, 10 mM EGTA and 4mM MgSO<sub>4</sub>) for 5 minutes at 37°C. Cells were then fixed with either freshly prepared 4% paraformaldehyde or ice cold

methanol for 10 minutes, washed three times with 0.2 %Triton X-100 in PBS, and incubated with blocking solution containing 3% BSA in PHEM for 1 hr. Cells were incubated with primary antibodies in 3% BSA in PHEM for 1 hr, washed three times with PBS plus 0.2% Triton X-100, and further incubated with fluorescent secondary antibodies at 1:500 dilution (Molecular Probes). DNA was stained with DAPI. Cells were washed three times with PBS, mounted, and viewed with a 63X objective on a Zeiss Axiovert 200M fluorescence microscope. The images were acquired with a CCD camera using the Intelligent Imaging software and further processed with Adobe Photoshop. Kinetochores were immunostained with CREST serum at 1:1000 dilution (Immunovision).

*APC ubiquitination assay-* To purify interphase APC, the anti-APC3 (Cdc27) beads were incubated with 10 volumes of interphase *Xenopus* egg extracts for 2 hrs at 4 °C and washed five times with XB containing 500 mM KCl and 0.5% NP-40 and twice with XB. The interphase APC beads were then incubated for 1 hr at room temperature with human Cdc20 protein that had been pre-incubated with BubR1, Mad2, or other checkpoint proteins. After incubation, the APC beads were washed twice with XB, and assayed for cyclin ubiquitination activity. Each ubiquitination assay was performed in a volume of 5  $\mu$ l. The reaction mixture contained an energy-regenerating system, 150  $\mu$ M of bovine ubiquitin, 5  $\mu$ M of the Myc-tagged N-terminal fragment of human cyclin B1, 5  $\mu$ M of human E1, 2  $\mu$ M of UbcH10, and 2  $\mu$ l of the APC beads. The reactions were incubated at room temperature for 1 hr, quenched with SDS sample buffer, and analyzed by SDS-PAGE followed by immunoblotting with anti-Myc.

*In vitro kinase assay-* Recombinant Bub1 KD/Bub3, BubR1 KD/Bub3, Cdc20, Cdh1 were purified from SF9 cells as described earlier. The kinase reaction mix contained the above



mentioned proteins as substrates along with either wild type or kinase-dead Mps1, cold ATP, p<sup>32</sup> labeled ATP in 10mM HEPES, pH 7.4. The reaction was allowed to continue for an hour after which it was quenched by adding SDS sample buffer and resolved by SDS PAGE. The samples were analyzed by autoradiography.

## RESULTS:

*Mps1 localizes to kinetochores and centrosome in mitosis-* A rabbit polyclonal antibody was raised against a GST-fusion fragment of Mps1 including amino acid 1-300. After affinity-purification using the corresponding antigen, the antibody detected a protein of approximately 100 KD in HeLa cell lysates on western blotting. The 100 KD band disappeared upon depletion of Mps1 by siRNA treatment, confirming that that this band belonged to the endogenous Mps1 protein. To examine the localization of endogenous Mps1, HeLa cells were fixed with methanol at -20°C and immunostained with affinity-purified anti-Mps1 antibody. Cells were costained with CREST serum, which serves as a marker for kinetochores. Mps1 colocalized with CREST in prometaphase cells whereas interphase cells exhibited a diffuse nuclear staining (fig 1). This indicates that Mps1 localizes to kinetochores in a cell cycle specific manner. Mps1 has been implicated in centrosomal duplication and Fisk et al have reported that Mps1 localizes to centrosomes in NIH3T3 cells {Fisk, 2001 #34}. To examine this possibility in HeLa cells, we tried different fixation protocols prior to immunostaining. Centrosomal staining was observed for Mps1 when cells were fixed with 4% paraformaldehyde and stained with anti- Mps1 antibody produced from rabbit #1 (fig1).

*Depletion of Mps1 results in the abrogation of spindle assembly checkpoint-* To understand the physiological role of Mps1, we turned to RNAi mediated depletion of endogenous Mps1. After 48 hours of transfection with Mps1 siRNA oligonucleotides HeLa cells were treated with Nocodazole for 18 hours. 90-95% of mock transfected cells were arrested in mitosis as indicated by cell and DNA morphology. In contrast approximately 50% of Mps1 siRNA treated cells were found to be in interphase (fig 2B). Immunoblotting of these samples indicated that the level of Mps1 was reduced by approximately 80% (fig 2A). To examine the DNA content of these cells

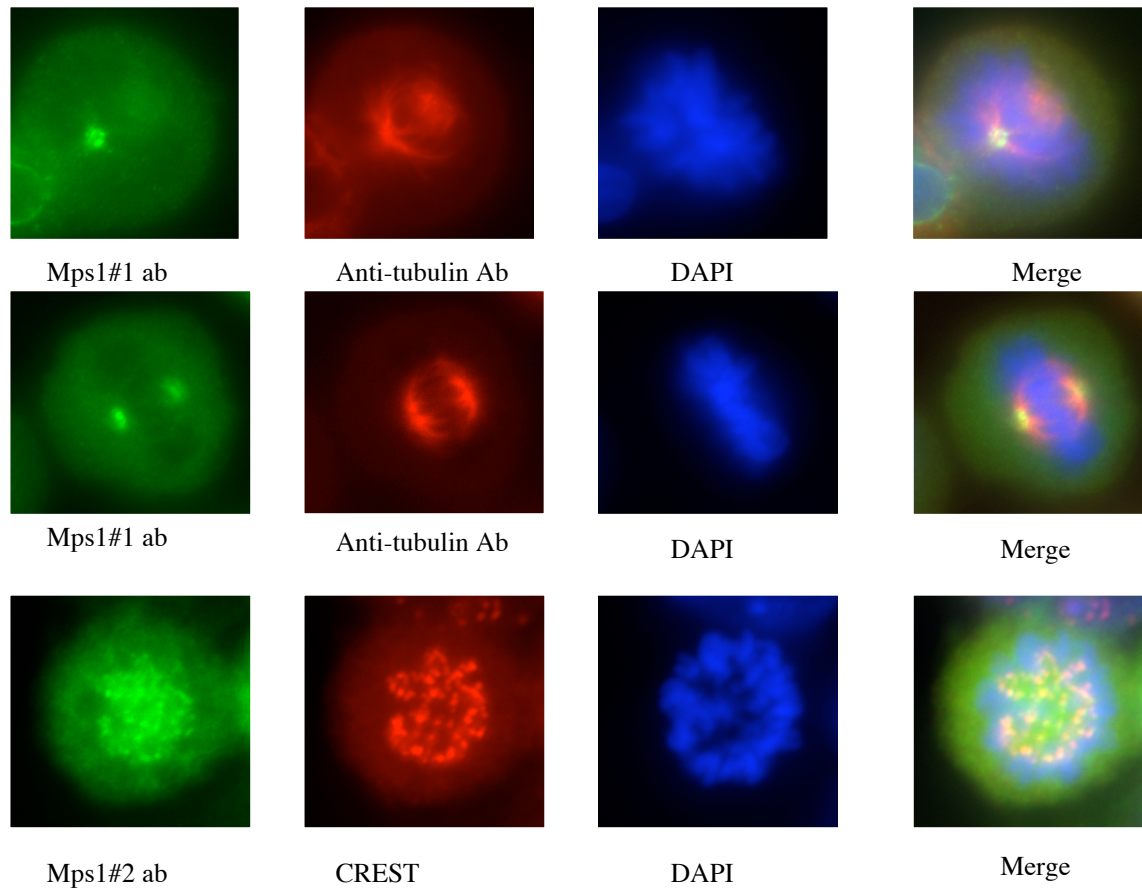


**Fig. 1. Mps1 localizes to kinetochores and centrosomes in mitosis.** HeLa cells were immunostained with anti-Mps1 antibody produced by two different rabbits (#1 and #2). DNA, kinetochores and microtubules were counterstained with DAPI, CREST and anti-tubulin antibody respectively. Mps1 staining is pseudocolored in green, DAPI in blue and CREST and tubulin in red.

we resorted to FACS analysis. Approximately 90% of mock transfected cells and 85% of Mps1 siRNA treated cells had a 4N DNA content suggesting that the interphase cells observed in response to Mps1 depletion and nocodazole treatment were not due to a G1 arrest. The interphase cells with 4N DNA content could represent either G2 arrested cells or cells escaped from mitosis without undergoing any chromosome segregation. To distinguish between these

two possibilities FACS analysis was performed on Mps1 depleted HeLa cells without synchronization with Nocodazole. No significant difference was observed in the FACS profiles of Mps1 depleted and control cells in the absence of nocodazole treatment indicating that 4n population observed in nocodazole treated Mps1 deficient cells represented cells escaped from mitosis and not G2-arrested cells (fig3). This suggests that Mps1 is required for the maintenance of mitotic arrest in response to spindle poisons.

*Mps1 is phosphorylated in mitosis-* To understand the regulation of Mps1 function, we compared the phosphorylation status of endogenous Mps1 at different stages of cell cycle. Western blotting of HeLa cell lysates prepared from asynchronous and nocodazole treated cells revealed that Mps1 migrated as a slower band in mitotic lysates. This was confirmed by comparing cells released from nocodazole arrest for different amounts of time. The Mps1 band progressively downshifted after release from nocodazole arrest (fig 2).

*Elucidating the biochemical function of Mps1-* To understand the exact function of Mps1 we examined its ability to interact or phosphorylate other known checkpoint proteins. His-tagged Mps1 WT or a kinase-dead mutant were expressed and purified from SF9 cells. The protein preparation, when resolved on SDS polyacrylamide gel stained with comassie blue, showed only one predominant band corresponding to the estimated size of His-Mps1, indicating that the recombinant protein was relatively pure. In vitro kinase assays were established by adding radio-labeled  $P^{32}$  and recombinant substrate purified from SF9 cells. The reaction mixture was resolved by SDS-PAGE and analyzed for  $P^{32}$  incorporation of substrates by autoradiography. As expected WT Mps1 could readily autophosphorylate itself whereas the kinase-dead mutant was

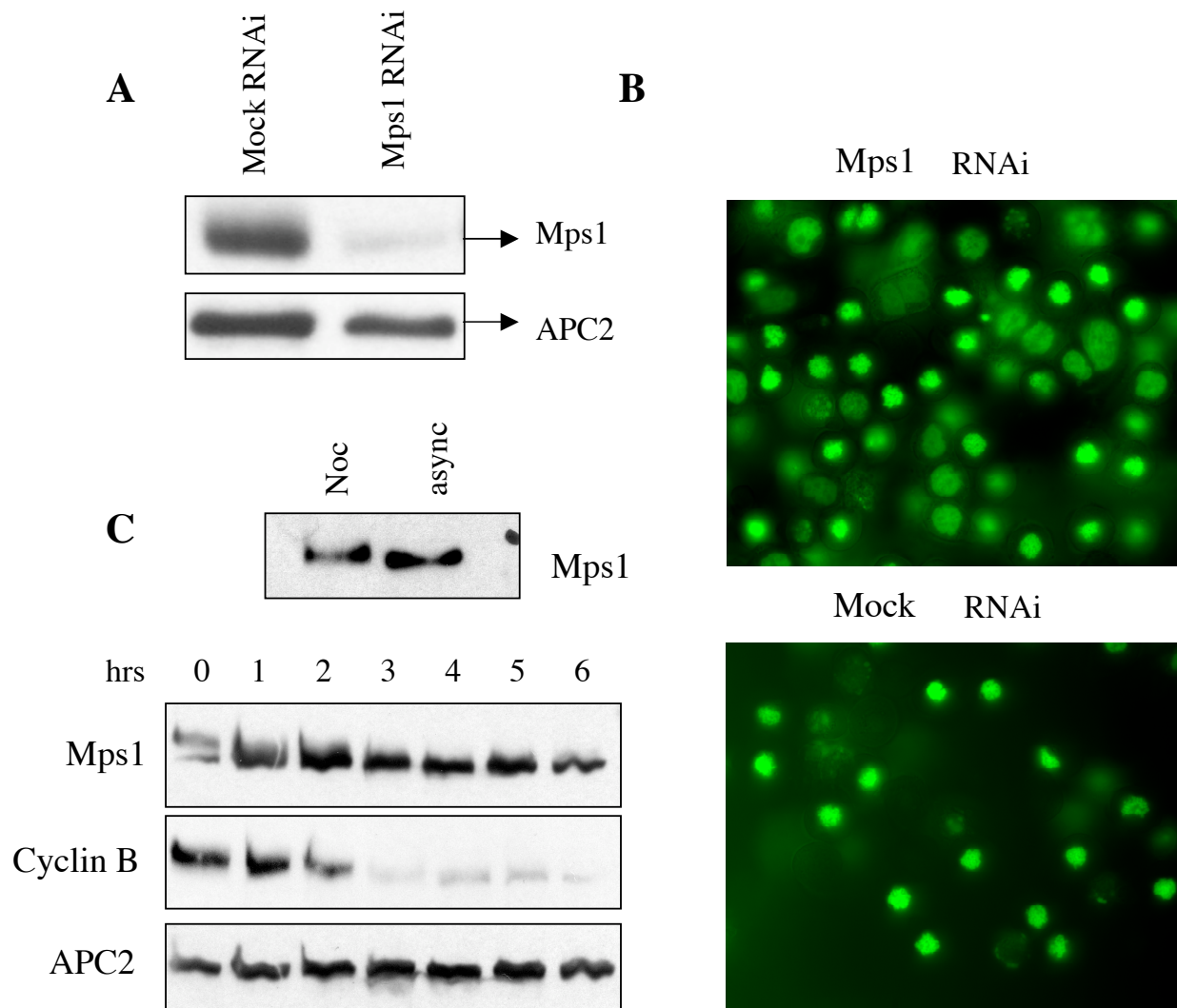
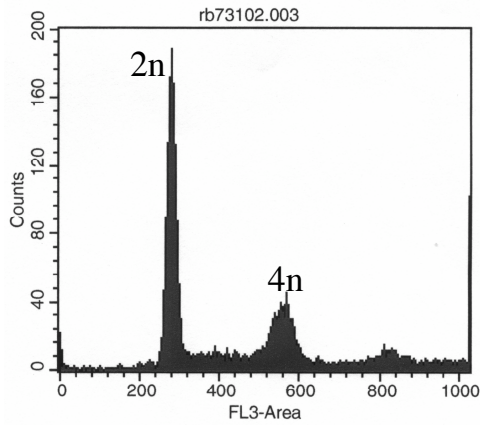
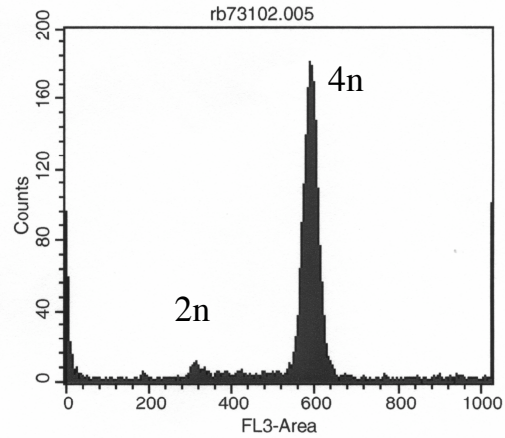


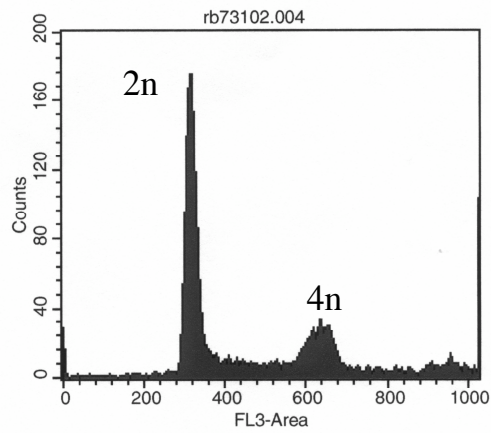
**Fig. 2. Mps1 is phosphorylated in mitosis and is required for mitotic arrest in the presence of Nocodazole.** HeLa cells transfected with Mps1 siRNA oligonucleotides were treated with Nocodazole 48 hours post-transfection. A, Protein levels were compared by immunoblotting cell lysates with the indicated antibody B, Mock and Mps1 RNAi cells were stained with Hoechst stain to examine the DNA morphology C, HeLa cells released from 18 hours nocodazole arrest were blotted with anti-Mps1, Cyclin B and APC2 antibody



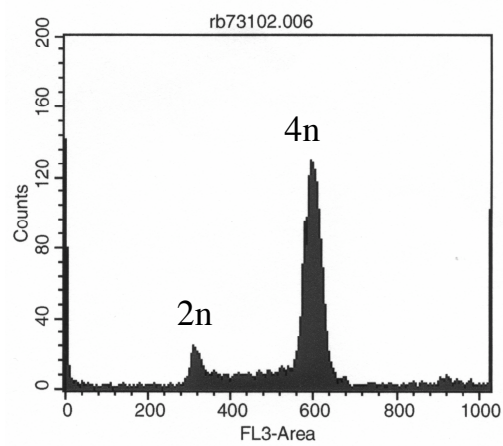
Mock RNAi Asynchronous



Mock RNAi Noc treated



Mps1 RNAi Asynchronous



Mps1 RNAi Noc treated

**Fig. 3.** FACS analysis of mock and Mps1 RNAi treated cells with or without Nocodazole treatment after 48 hours of transfection. The peaks corresponding to 4N and 2N DNA content are labeled.

**Fig. 4. Mps1 does not phosphorylate Cdc20, Cdh1, Bub1, BubR1 or Bub3 and does not inhibit APC** A, commassie stained gel showing WT and KD Mps1 purified from SF9 cells. B, in vitro APC ubiquitination assay with varying dosages of Mps1 added to Cdc20 or Cdh1. C, In vitro kinase assay examining Mps1 autophosphorylation by radiolabeled p<sup>32</sup> incorporation D, in vitro kinase assay using Mps1 WT or KD as kinase and other checkpoint proteins as substrate.

incapable of doing so. Recombinant Cdc20, Cdh1, Bub1 KD/Bub3 complex and BubR1/Bub3 complex were used as substrates in the in vitro kinase assay. None of these substrates could be phosphorylated by Mps1. Furthermore, we could not detect any interaction between Mps1 and any of the spindle checkpoint genes either in vivo or in vitro. We also checked if Mps1 could inhibit APC activity in vitro. Unlike Mad2 and BubR1, Mps1 could not inhibit APC activity at the concentrations tested.

*Mad 2B can inhibit APC in vitro-* The high sequence similarity between Mad2 and Mad2B prompted us to believe that like Mad2, Mad2B might also serve as an APC inhibitor. His-tagged Mad2 and Mad2B were purified from bacteria using Ni-NTA beads. As mentioned before, APC ubiquitination activity was reconstituted in vitro by adding recombinant E1, Ubc<sub>x</sub>, Ub, Cdc20 and Cyclin B N-terminus proteins to APC immunoprecipitated from xenopus oocyte lysate. Addition of recombinant Mad2B to the ubiquitination assay inhibited APC<sup>Cdc20</sup> activity. To compare the potency of Mad2B and Mad2 in inhibiting APC, a dose-response experiment was performed for both the proteins. Serial dilutions of Mad2 and Mad2B proteins resulting in a final concentration of 0.5-8  $\mu$ M, were added to ubiquitination assay. Though Mad2B can inhibit APC activity, its potency is approximately four fold less than Mad2.

*Overexpression of Mad2B does not cause a mitotic arrest-* To explore the physiological significance of Mad2B inhibition of APC in vitro, Mad2B was overexpressed in HeLa cells by transiently transfecting pCS2-Mad2B vector. Cells transfected parallelly with pCS2 Mad2 served as positive control. Both these constructs were cotransfected with pCS2-GFP, which served as a marker for positively transfected cells. Mitotic cells were identified on the basis of round shape and condensed DNA. As expected, after 48 hours of transfection 60-70% of Mad2 transfected



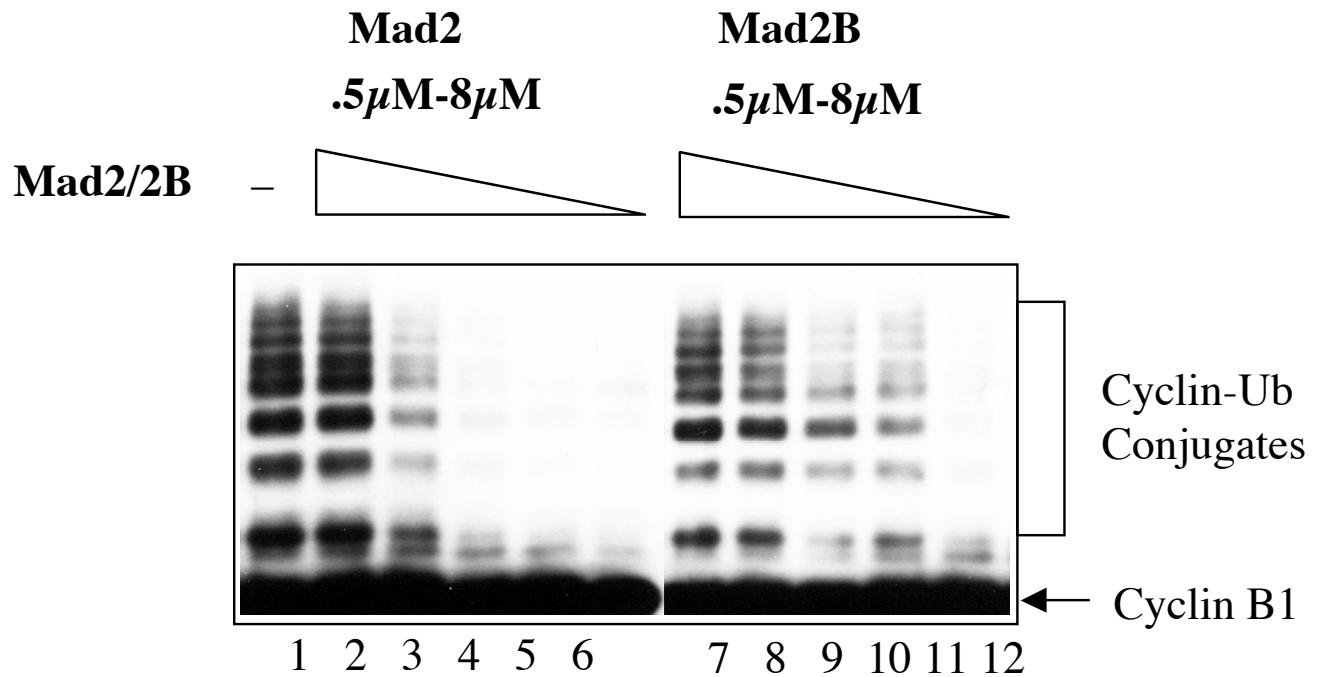


**Fig.5. Mad2B can inhibit APC activity in vitro.** A, I- APC was immunoprecipitated from *Xenopus* oocyte lysate and activated by incubation with recombinant Cdc20 preotein. Increasing concentrations of Mad2 or Mad2B (as indicated in the figure) were added to the reaction. The ubiquitination activity of APC was assayed with a Myc-tagged N-terminal fragment of human cyclin B1. The reaction mixtures were separated on SDS-PAGE and blotted with the anti-Myc antibody. The positions of the cyclin B1 substrate and the cyclin B1-ubiquitin conjugates are labeled.

cells were arrested in mitosis, whereas only 10% of Mad2B arrested cells were mitotic. Similar results were obtained upon overexpression of GFP-Mad2B and GFP-Mad2 fusion constructs.

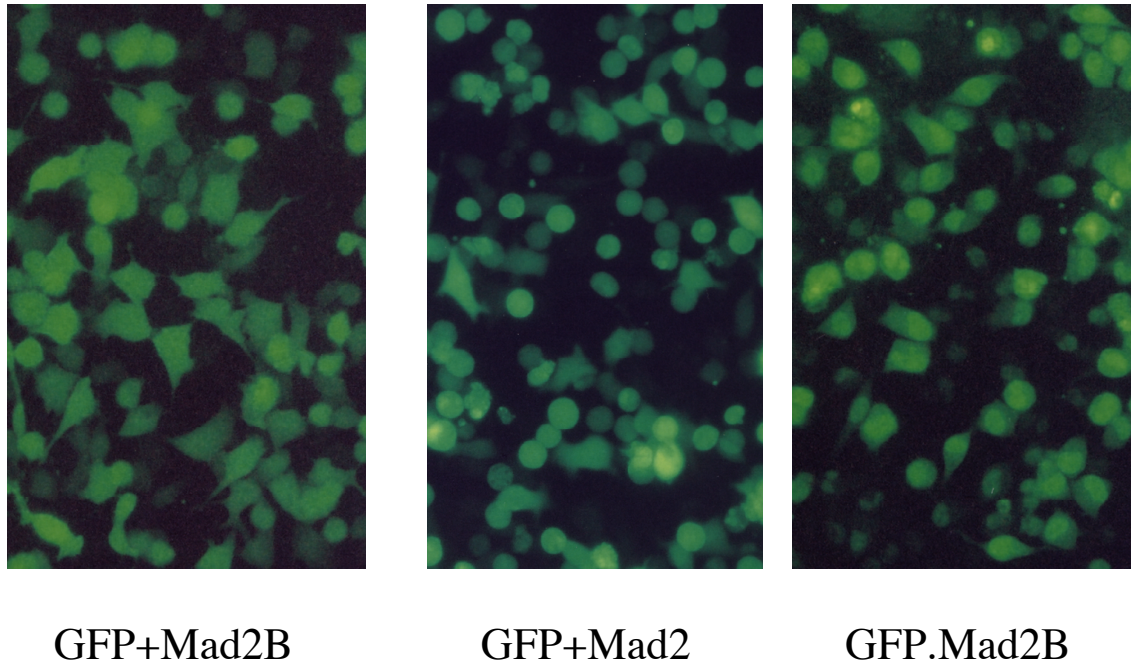


**Fig.6. Mad2B overexpression does not lead to mitotic arrest.** pCS2 constructs encoding Mad2b, Mad2 or GFP.Mad2B ORFs were transfected into HeLa cells. Cells were cotransfected with pCS2.GFP vector to mark the transfected cells. Mitotic cells were identified by characteristic round morphology.

## DISCUSSION:

*The role of Mad2B in cell cycle regulation-* Due to the high sequence similarity between Mad2B and Mad2, we hypothesized that Mad2B might be an APC inhibitor and might play some role in the spindle checkpoint. It should be noted however, that the concentration of Mad2B that can efficiently inhibit APC in vitro is far above its physiological concentration. Though Mad2B can inhibit APC in vitro, overexpression of Mad2B in HeLa cells did not produce any mitotic arrest. Furthermore, siRNA mediated depletion of Mad2 did not abolish mitotic arrest in HeLa cells upon Nocodazole treatment. This is in contrast with Mad2, a bonafide checkpoint protein, which blocks cells in mitosis when overexpressed and conversely, allows cells to escape mitosis in the presence of Nocodazole, when inhibited. We could not detect any binding between Cdc20 and Mad2B either in vitro or in vivo. These findings suggest that in most likelihood, Mad2B is not a spindle checkpoint protein. However, it is possible that Mad2B inhibits APC in response to stimuli other than lack of kinetochore attachment. Mad2B and its yeast homolog in ScRev7 have been implicated in DNA damage tolerance (24). Rev7/Mad2B forms a complex with Rev1 and Rev3 and is required for translesion DNA synthesis after DNA damage (18). Thus, Mad2B might serve as a link between DNA damage response and cell cycle control.

*Mps1 is a spindle assembly checkpoint gene-* Depletion of Mps1 allows cells to escape mitosis in the presence of Nocodazole. Like other checkpoint genes Mps1 also localizes to kinetochores during mitosis. Furthermore Mps1 is phosphorylated during mitosis. These findings suggest that like its yeast and xenopus counterpart, human Mps1 is also involved in spindle assembly checkpoint. Unlike yeast, however Mps1 overexpression does not cause a mitotic arrest. It is possible that higher organisms have acquired additional requirements for mitotic arrest. The evidence is further supported by findings from Zebrafish. A temperature

sensitive mutation in zebrafish Mps1 has been identified which is essential for fin regeneration at the restrictive temperature (11). Detailed analysis has revealed that these mutants exhibit a high frequency of aneuploidy in both somatic and germline cells (14). So far, efforts to characterize the exact biochemical function of Mps1 have not met any success. Mps1 does not phosphorylate any of the known Mad or Bub checkpoint proteins in vitro. However it is possible that Mps1 requires certain modifications to be activated that are missing in the recombinant Mps1 protein. We also performed binding assays between Mps1 and other known checkpoint proteins by cotransfecting them pairwise in HeLa cells, followed by immunoprecipitation of tagged Mps1 and immunoblotting for the other protein. We could not detect any significant interaction between Mps1 and any of these proteins. We also immunoprecipitated endogenous Mps1 and sequenced all the coprecipitating proteins by mass spectrometry. A few proteins like the components of Dynactin complex could be identified reproducibly in the Mps1 immunoprecipitates but further characterization revealed that these proteins were cross reacting with Mps1 antibody. Further studies are needed to unravel the exact physiological function of Mps1. We have made a small contribution in that direction by at least ruling out some of the obvious possibilities.

## REFERENCES:

1. Winey, M., Goetsch, L., Baum, P., and Byers, B. (1991) *J Cell Biol* **114**, 745-754
2. Weiss, E., and Winey, M. (1996) *J Cell Biol* **132**, 111-123
3. Hardwick, K. G., Weiss, E., Luca, F. C., Winey, M., and Murray, A. W. (1996) *Science* **273**, 953-956
4. Poddar, A., Daniel, J. A., Daum, J. R., and Burke, D. J. (2004) *Cell Cycle* **3**, 197-204
5. Biggins, S., and Murray, A. W. (2001) *Genes Dev* **15**, 3118-3129
6. Abrieu, A., Magnaghi-Jaulin, L., Kahana, J. A., Peter, M., Castro, A., Vigneron, S., Lorca, T., Cleveland, D. W., and Labbe, J. C. (2001) *Cell* **106**, 83-93
7. Fisk, H. A., and Winey, M. (2001) *Cell* **106**, 95-104
8. Mills, G. B., Schmandt, R., McGill, M., Amendola, A., Hill, M., Jacobs, K., May, C., Rodricks, A. M., Campbell, S., and Hogg, D. (1992) *J Biol Chem* **267**, 16000-16006
9. Douville, E. M., Afar, D. E., Howell, B. W., Letwin, K., Tannock, L., Ben-David, Y., Pawson, T., and Bell, J. C. (1992) *Mol Cell Biol* **12**, 2681-2689
10. He, X., Jones, M. H., Winey, M., and Sazer, S. (1998) *J Cell Sci* **111** ( Pt 12), 1635-1647
11. Poss, K. D., Nechiporuk, A., Hillam, A. M., Johnson, S. L., and Keating, M. T. (2002) *Development* **129**, 5141-5149
12. Millband, D. N., and Hardwick, K. G. (2002) *Mol Cell Biol* **22**, 2728-2742
13. Stucke, V. M., Sillje, H. H., Arnaud, L., and Nigg, E. A. (2002) *Embo J* **21**, 1723-1732

14. Poss, K. D., Nechiporuk, A., Stringer, K. F., Lee, C., and Keating, M. T. (2004) *Genes Dev* **18**, 1527-1532
15. Cahill, D. P., da Costa, L. T., Carson-Walter, E. B., Kinzler, K. W., Vogelstein, B., and Lengauer, C. (1999) *Genomics* **58**, 181-187
16. Lawrence, C. W., Das, G., and Christensen, R. B. (1985) *Mol Gen Genet* **200**, 80-85
17. Torpey, L. E., Gibbs, P. E., Nelson, J., and Lawrence, C. W. (1994) *Yeast* **10**, 1503-1509
18. Nelson, J. R., Lawrence, C. W., and Hinkle, D. C. (1996) *Science* **272**, 1646-1649
19. Nelson, J. R., Lawrence, C. W., and Hinkle, D. C. (1996) *Nature* **382**, 729-731
20. Murakumo, Y. (2002) *Mutat Res* **510**, 37-44
21. Esposito, G., Godindagger, I., Klein, U., Yaspo, M. L., Cumano, A., and Rajewsky, K. (2000) *Curr Biol* **10**, 1221-1224
22. Bemark, M., Khamlichi, A. A., Davies, S. L., and Neuberger, M. S. (2000) *Curr Biol* **10**, 1213-1216
23. Elbashir, S. M., Harborth, J., Lendeckel, W., Yalcin, A., Weber, K., and Tuschl, T. (2001) *Nature* **411**, 494-498
24. Lawrence, C. W., Nisson, P. E., and Christensen, R. B. (1985) *Mol Gen Genet* **200**, 86-91

## **CHAPTER FOUR**

# **Identification of Two Novel Components of the Human Ndc80 Kinetochore Complex**

## **INTRODUCTION**

The genetic stability of an organism depends on accurate segregation of sister-chromatids during mitosis (1,2). Macromolecular structures termed kinetochores that assemble on the centromeric regions of chromosomes are essential for various aspects of this process (3). Kinetochores form attachment sites for spindle microtubules, recruit microtubule motors and other nonmotor proteins that regulate spindle dynamics, and are indispensable for the subsequent alignment of chromosomes at the metaphase plate (3).

Kinetochores also play important roles in the spindle checkpoint (3). Premature separation of sister-chromatids prior to their proper attachment to the mitotic spindle results in chromosome mis-segregation and aneuploidy, which contributes to tumorigenesis or birth defects (4,5). To avoid these dire consequences, cells employ a surveillance mechanism called the spindle checkpoint to monitor the status of microtubule-attachment and tension at the kinetochores of sister-chromatids (6-11). The spindle checkpoint ensures that chromosome segregation ensues only after all the chromosomes have congressed to the metaphase plate.

Unattached kinetochores generate a diffusible signal that inhibits an E3 ubiquitin ligase called the anaphase-promoting complex or cyclosome (APC/C)<sup>1</sup>, and in turn prevents sister chromatid separation (6-13). It has been postulated that the APC/C-inhibitory signal generated by unattached kinetochores consists of a complex of Mad2, Cdc20, BubR1 and Bub3, known as the mitotic checkpoint complex (MCC) (11). Many checkpoint proteins exhibit dynamic kinetochore localization in mitosis (14,15). For example, Mad2 only localizes to unattached kinetochores and the kinetochore-bound pool of Mad2 exchanges rapidly ( $t_{1/2}$  = 24-28 s) with the cytoplasmic pools (14). Mad2 recruitment to kinetochores depends upon another checkpoint protein, called Mad1, which is constitutively bound to Mad2 and shows the same kinetochore localization pattern as Mad2 (16-18). An attractive model for spindle checkpoint signaling is that Mad2 is recruited to kinetochores by Mad1 (11,19). Through a poorly understood mechanism, possibly mediated by other checkpoint proteins, Mad2 dissociates from Mad1 and acquires a conformation that is compatible with its incorporation into the MCC (11,19).

Little is known about the mechanisms by which the spindle checkpoint proteins are recruited to kinetochores during mitosis. Detailed immunofluorescence analysis revealed that these proteins are recruited to the kinetochores with slightly different timing (20). Moreover, their kinetochore localization patterns vary in response to different spindle damaging agents (21-23). This suggests that the spindle checkpoint proteins might be recruited to the kinetochores through different mechanisms and via interactions with specific kinetochore proteins. Identification of the kinetochore protein interface to which Mad1–Mad2 associates might provide insights into the mechanism of the generation of MCC.

Genetic and biochemical studies in different organisms have led to the identification of a large number of kinetochore proteins, many of which are conserved during evolution (3). A

---



physical association map for the kinetochore proteins is beginning to emerge through biochemical purification of kinetochore sub-complexes and through analysis of the interdependencies of various proteins for kinetochore localization (3,24,25). Despite the vast divergence of the centromeric sequences among organisms and the limited sequence similarities among kinetochore proteins of different species, the basic architecture of kinetochores appears to be conserved (3). Kinetochore proteins can be divided into three groups: the inner kinetochore proteins that associate with the centromeric DNA, the outer kinetochore proteins that interact with the microtubules, and the central kinetochore proteins that lie in between (3). The inner kinetochore is formed in part by a histone H3 variant, CENP-A/Cse4, and a coiled-coil protein, CENP-C/Mif2 (3). The central kinetochore consists of at least three sub-complexes in yeast: the Ndc80 complex, the Mtw1 complex, and the Ctf19 complex (3,26). The central kinetochore proteins are responsible for the recruitment of the outer kinetochore proteins that, among other functions, regulate microtubule dynamics (3). These include microtubule motors such as dynein, CENP-E, and nonmotor proteins, such as CLIP-170 and the Dam1 complex (3,27). Nearly all of the spindle checkpoint proteins localize to the outer kinetochore (3). Many central kinetochore proteins, including components of the Ndc80, Mis12/Mtw1, and Ctf19 complexes, remain to be identified in mammals. Identification of these components will shed light on the structure, assembly, and function of mammalian kinetochores.

The yeast Ndc80 complex consists of four coiled-coil proteins: Ndc80, Nuf2, Spc25, and Spc24 (28). Homologs of Ndc80 and Nuf2 have been identified in various organisms and shown to perform important functions in processes ranging from kinetochore assembly, microtubule attachment, chromosome congression, and the spindle checkpoint (29-32). This suggests that the Ndc80 complex is an evolutionarily conserved kinetochore component. Several observations

support a role of the Ndc80 complex in the spindle checkpoint. In budding yeast, temperature-sensitive Spc25 and Spc24 mutants are checkpoint-deficient (31). Simultaneous disruption of both Ndc80 and Nuf2 genes also abrogates the spindle checkpoint (31). Recently, human Mad1 has been shown to interact with Hec1 in a yeast two-hybrid screen (29). Mad1 and Mad2 fail to localize to kinetochores in mitotic HeLa cells depleted for Hec1 by RNAi, suggesting that Hec1 is required for the kinetochore recruitment of Mad1 and Mad2 (29). However, direct binding between Hec1 and Mad1 cannot be detected *in vitro*.

Given the importance of the Ndc80 complex in both chromosome congression and the spindle checkpoint, we sought to characterize the composition and function of the human Ndc80 complex. In particular, despite their likely existence, the mammalian functional homologs of Spc25 and Spc24 have not been identified due to the lack of clear sequence homologs in the databases. We have now purified the human Ndc80 complex using an immuno-affinity approach, and identified the Spc25 and Spc24 components of the human Ndc80 complex. Human Spc25 interacts with Hec1 *in vitro* and *in vivo*. It localizes to the kinetochores during mitosis. RNAi-mediated depletion of hSpc25 in HeLa cells causes a plethora of mitotic defects and the loss of kinetochore localization of Mad1 and Hec1 in the absence of spindle damaging agents. Therefore, despite the lack of significant sequence similarity, hSpc25 is a functional homolog of yeast Spc25 and a component of the conserved Ndc80 complex. Interestingly, the Ndc80 complex is not required for the kinetochore localization of Mad1 in nocodazole-arrested mitotic cells. This suggests that the Ndc80 complex is not absolutely required for the recruitment of Mad1 to kinetochores upon checkpoint activation.

## EXPERIMENTAL PROCEDURES

*Expression and Purification of Recombinant Hec1 Proteins and Antibody Production*—The coding region of hHec1 was amplified from a human fetal thymus cDNA library (Clontech) using PCR. Two cDNA fragments of hHec1 containing either nucleotides 1-663 (Hec1N) or nucleotides 1285-1929 (Hec1C) of the Hec1 coding region were cloned into the pGEX4T-1 vector. The resulting plasmids were transformed into Rosetta DE3 bacteria cells. Expression of the GST-Hec1N and GST-Hec1C fusion proteins was induced by the addition of IPTG (250  $\mu$ M final concentration) to the bacterial culture at an OD<sub>600</sub> of 0.6. The cells were allowed to grow for another 3 hrs at room temperature. Soluble GST-Hec1 fusion proteins were isolated on glutathione-agarose beads (Amersham), eluted with 10 mM glutathione (Sigma), and exchanged into PBS using PD-10 columns (Amersham). The two GST-Hec1 fusion proteins were mixed and injected into rabbits for antibody production (Zymed). Crude antibody sera were first pre-cleared with GST-coupled Affi-gel beads to remove the  $\alpha$ -GST antibody, and subsequently affinity-purified using either GST-Hec1N or GST-Hec1C fusion proteins coupled to Affi-gel beads (Bio-Rad). For immunoblotting, the affinity-purified  $\alpha$ -Hec1 antibodies were used at a final concentration of 1  $\mu$ g/ml. For immunoprecipitation, the affinity-purified  $\alpha$ -Hec1 antibodies were coupled to Affi-prep protein A beads (Bio-Rad) at a concentration of 1 mg antibody/ml of protein A beads.

*Immunopurification of the Human Ndc80 Complex*—HeLa Tet-on cells (Clontech) were grown in Dulbecco's modified Eagle's medium (DMEM; Invitrogen) supplemented with 10% fetal bovine serum, 2 mM L-glutamine, and 100  $\mu$ g/ml penicillin and streptomycin. At 80% confluency, the cells were treated with nocodazole at a final concentration of 100 ng/ml for 18 hrs. For each immunoprecipitation experiment, 20 plates (150 mm) of nocodazole-arrested HeLa

cells were used. The cell pellet was resuspended in 12 ml of NP-40 lysis buffer (50 mM Tris, 150 mM KCl, 0.5% NP-40, 1 mM DTT, 1  $\mu$ M okadaic acid, 10  $\mu$ g/ml cytochalasin B, 10  $\mu$ g/ml each of leupeptin, pepstatin, and chymostatin). The suspension was kept on ice for 20 minutes, followed by brief sonication. The lysate was cleared by centrifugation at top speed in a microcentrifuge for 1.5 hrs. The supernatant was filtered with 0.4  $\mu$ m filters and pre-cleared using 200  $\mu$ l of protein A beads coupled with anti-GST antibody. The Ndc80 complex was immunoprecipitated by incubating the lysate with 200  $\mu$ l of either the anti-Hec1N or anti-Hec1C antibodies at 4°C for 2 hrs. The antibody beads were washed 4 times with the lysis buffer plus 400 mM KCl and once with the lysis buffer. Immunoprecipitated proteins were then eluted with 1 ml of 100 mM glycine-HCl (pH 2.5) and concentrated using microcon centrifugation filter devices (Millipore). The concentrated proteins were resolved by SDS-PAGE and detected by silver staining. The protein bands were excised and subjected to trypsin digestion followed by mass spectrometry analysis.

*Cloning, Expression, and Purification of Recombinant hSpc25 and Antibody Production*— The coding region of hSpc25 was amplified from a human fetal thymus cDNA library (Clontech) by PCR and cloned into pCS2-Myc and pCS2-HA vectors. The clones were sequenced to verify the identity of hSpc25. A cDNA fragment of hSpc25 containing nucleotides 1-450 (hSpc25N) of the hSpc25 coding region was cloned into the pGEX4T-1 vector. The GST-hSpc25N protein was expressed and purified essentially as described above for the purification of GST-Hec1 fusion proteins, except that expression of GST-hSpc25N was induced by the addition of IPTG (250  $\mu$ M final concentration) to the bacterial culture at an OD<sub>600</sub> of 0.9. The purified GST-hSpc25N fusion protein was injected into rabbits for antibody production (Zymed). Crude antibody sera were first pre-cleared with GST-coupled Affi-gel beads to

remove the  $\gamma$ -GST antibody, and subsequently affinity-purified using GST-hSpc25N-coupled Affi-gel beads (Bio-Rad).

*Tissue Culture and Transfection*—HeLa Tet-on cells (Clontech) were grown to 40-50% confluency and transfected with the pCS2-Myc or pCS2-HA plasmids containing the hHec1 or hSpc25 coding regions using the Effectene reagent (Qiagen) according to manufacturer's protocol. After 24 hrs, cells were treated with 100 ng/ml nocodazole for 16 hrs, harvested by trypsinization, and pelleted by centrifugation at 500 g for 5 minutes. After washing with PBS, the cells were lysed and subjected to immunoprecipitation and immunoblotting experiments.

For RNAi experiments, the siRNA oligonucleotides specific for human Hec1, hSpc25, and human Mad2 were chemically synthesized. They contained sequences corresponding to nucleotides 344-366 and 1517-1539 of the coding region of human Hec1, nucleotides 161-183 of the coding region of hSpc25, and nucleotides 143-165 of the Mad2 coding region, respectively. The annealing of the siRNAs and subsequent transfection of the RNA duplexes into HeLa cells were performed exactly as described (33). In the case of hSpc25, at 48 hrs after the first round of RNAi transfection, cells were re-plated to 30% confluency. At 12 hours after re-plating, the cells were transfected again with either Spc25 siRNA oligonucleotides alone or with both Spc25 and Mad2 siRNA duplexes. The time points mentioned in the paper for these RNAi experiments were referring to the time after the second round of RNAi transfection. Cells transfected with oligofectamine alone were used as controls. To determine the cell cycle status, the transfected cells were fixed with 70% ethanol, stained with propidium iodide (PI), and analyzed by flow cytometry (FACS). The phenotypes of these cells were also analyzed by indirect immunofluorescence.

*Immunoprecipitation, Immunoblotting, and Protein Binding Assays*—Lysates of HeLa tet-on cells transfected with Hec1 and hSp25 plasmids were prepared and immunoprecipitated as described for the immuno-purification of the Ndc80 complex. Myc-Hec1 or Myc-hSp25 was immunoprecipitated from lysates with a mouse monoclonal  $\alpha$ -Myc antibody (Roche) coupled to protein A beads. After washing, samples were resolved by SDS-PAGE and analyzed by immunoblotting with  $\alpha$ -HA at a final concentration of 1  $\mu$ g/ml. For the analysis of the interactions between endogenous Hec1 and hSp25 proteins, the  $\alpha$ -Hec1 immunoprecipitates were blotted with  $\alpha$ -hSp25 antibody at 1  $\mu$ g/ml final concentration. Horseradish peroxidase conjugated goat  $\alpha$ -rabbit or goat  $\alpha$ -mouse IgG (Amersham) were used as secondary antibodies and the immunoblots were developed using the ECL reagent per manufacturer's protocols (Amersham).

Plasmids encoding Myc-Hec1, Nuf2, and Sp25 were co-translated in rabbit reticulocyte lysate in the presence of  $^{35}$ S-methionine. The lysate was immunoprecipitated using either  $\alpha$ -Myc or  $\alpha$ -GST (as a negative control) antibodies. The beads were washed four times with NP-40 lysis buffer. The immunoprecipitated proteins were dissolved in SDS sample buffer, separated on SDS-PAGE, and analyzed by autoradiography.

*Immunofluorescence*—For the immunostaining of endogenous Hec1, hSp25, Mad1, Bub1, and BubR1, HeLa cells were grown to 40% confluency and transfected with different plasmids or siRNA duplexes in chambered coverslips. Cells were washed with PBS and extracted with 0.5% Triton X-100 in PHEM buffer (60 mM PIPES, 25 mM HEPES, 10 mM EGTA and 4mM MgSO<sub>4</sub>) for 5 minutes at 37°C. Cells were then fixed with 4% paraformaldehyde in PHEM buffer for 20 minutes at 37°C, washed three times with 0.2 %Triton X-100 in PBS, and incubated with blocking solution containing 3% BSA in PHEM for 1 hr.

Cells were incubated with primary antibodies in 3% BSA in PHEM for 1 hr, washed three times with PBS plus 0.2% Triton X-100, and further incubated with fluorescent secondary antibodies at 1:500 dilution (Molecular Probes). DNA was stained with DAPI. Cells were washed three times with PBS, mounted, and viewed with a 63 $\times$  objective on a Zeiss Axiovert 200M fluorescence microscope. The images were acquired with a CCD camera using the Intelligent Imaging software and further processed with Adobe Photoshop. The staining protocol for cyclin A1, cyclin B1, securin, and Myc-Spc25 was essentially the same as described above, except that cells were not detergent extracted prior to fixation. The immunostaining of tubulin and PARP1 of the hSpc25/Hec1 RNAi cells was performed as described above, except that the cells were fixed with methanol at -20°C. Antibodies used were mouse monoclonal  $\alpha$ -Myc antibody at 1  $\mu$ g/ml (Roche), CREST serum at 1:1000 dilution (Immunovision), rabbit  $\alpha$ -cyclin A1 antibody at 1  $\mu$ g/ml (Santa Cruz), rabbit  $\alpha$ -cyclin B1 antibody at 1  $\mu$ g/ml (Santa Cruz), rabbit  $\alpha$ -securin antibody at 1  $\mu$ g/ml (a gift from Hui Zou), mouse monoclonal  $\alpha$ -PARP1 antibody at 1:1000 dilution (Cell Signaling), rabbit  $\alpha$ -Mad1 antibody at 4  $\mu$ g/ml, rabbit  $\alpha$ -Hec1 antibody at 2  $\mu$ g/ml, rabbit  $\alpha$ -Bub1 antibody at 1  $\mu$ g/ml, rabbit  $\alpha$ -BubR1 antibody at 1  $\mu$ g/ml, and mouse  $\alpha$ -tubulin antibody at 1:1000 dilution. Annexin V staining was performed on Hec1 RNAi HeLa cells that were released from a thymidine arrest for 16 hours, using the Annexin V-FITC apoptosis detection kit (BD Pharmingen), according to manufacturer's protocols. Briefly, cells were washed twice with Annexin V binding buffer and incubated with Annexin V-FITC and PI for 15 minutes. Apoptotic cells were scored by positive Annexin V staining and negative PI staining.

*Cold-sensitive or Calcium-sensitive Microtubule Staining*—For cold-sensitive microtubule staining, at 48 hours after hSpc25 siRNA treatment, cells were incubated with ice cold media for 10 minutes, followed by extraction with 0.5% Triton X-100 in PHEM buffer for 5

minutes. For calcium treatment, samples were permeabilized with 100 mM PIPES, 1 mM MgCl<sub>2</sub>, 0.1 mM CaCl<sub>2</sub> and 0.1% Triton X-100 (pH 6.9). Cells were subsequently fixed with methanol and immunostained with  $\alpha$ -tubulin antibody and CREST as described above.

*Cell Synchronization Experiments*—At 24 hours after transfection of HeLa cells with Hec1 siRNA oligonucleotides, the mitotic cells were removed by mitotic shake-off and thymidine (2 mM final concentration) was added to the remaining cells. Another 18 hours later, the mitotic and dead cells were again washed off and the remaining cells were released into fresh media. Samples were taken at 2 hr intervals for 16 hours and stained with Annexin V or  $\gamma$ -PARP1 antibody to determine the percentage of apoptotic cells. To determine the timing of the appearance of spindle defects, samples were taken at 1 hr intervals starting from 9 hours after the release from thymidine arrest. These cells were fixed and stained with tubulin and DAPI. The effect of microtubule depolymerization on Mad1 staining and apoptosis in Hec1 RNAi cells was examined by adding nocodazole to these cells at 7 hrs after thymidine release. Immunostaining was performed at 7 hrs after nocodazole addition.



## RESULTS

*Identification of human Spc25 by immunopurification of the Ndc80 complex*—To characterize the human Ndc80 complex, we raised antibodies against human Hec1. In immunoblotting, the affinity-purified Hec1 antibody detected a 70 kD band in HeLa lysates that was identical in size to the untagged Hec1 protein in vitro translated in rabbit reticulocyte lysate (Figure 1A). The intensity of this band decreased significantly in lysates of HeLa cells transfected with Hec1-specific siRNA, indicating this band belonged to Hec1 (see Figure 4A). The affinity-purified Hec1 antibody was coupled to protein A beads and used to immuno-purify the human Ndc80 complex from HeLa cell lysates (Figure 1B). There were four proteins present in stoichiometric amounts in the anti-Hec1 immunoprecipitates. These proteins were absent in immunoprecipitates of antibody against GST (Figure 1A). To facilitate discussion, they were named p70, p50, p25, and p24 on the basis of their molecular weights.

Mass spectrometry analysis of these proteins revealed that p70 and p50 were human Hec1 (the homolog of yeast Ndc80) and human Nuf2, respectively (data not shown). Analysis of the p25 band yielded three peptides belonging to a novel coiled-coil protein (called AD024, NP\_065726) with unknown function and a predicted molecular weight of 26.2 kD (Figure 1C). The p24 protein was identified as another novel coiled-coil protein with a predicted molecular weight of 22.4 kD (NP\_872319). Neither of these proteins shares any significant sequence similarity with the *S. cerevisiae* Spc25 or Spc24 proteins. However, database searches did allow us to identify homologs of p25 in mouse and *S. pombe* (NP\_588208) (Figure 1C) and p24 homologs in mouse (NP\_080558). We chose to further characterize p25 (see below) and confirmed that it is a component of the human Ndc80 complex and a functional homolog of the yeast Spc25 protein. Thus, we will henceforth refer to p25 as hSpc25.

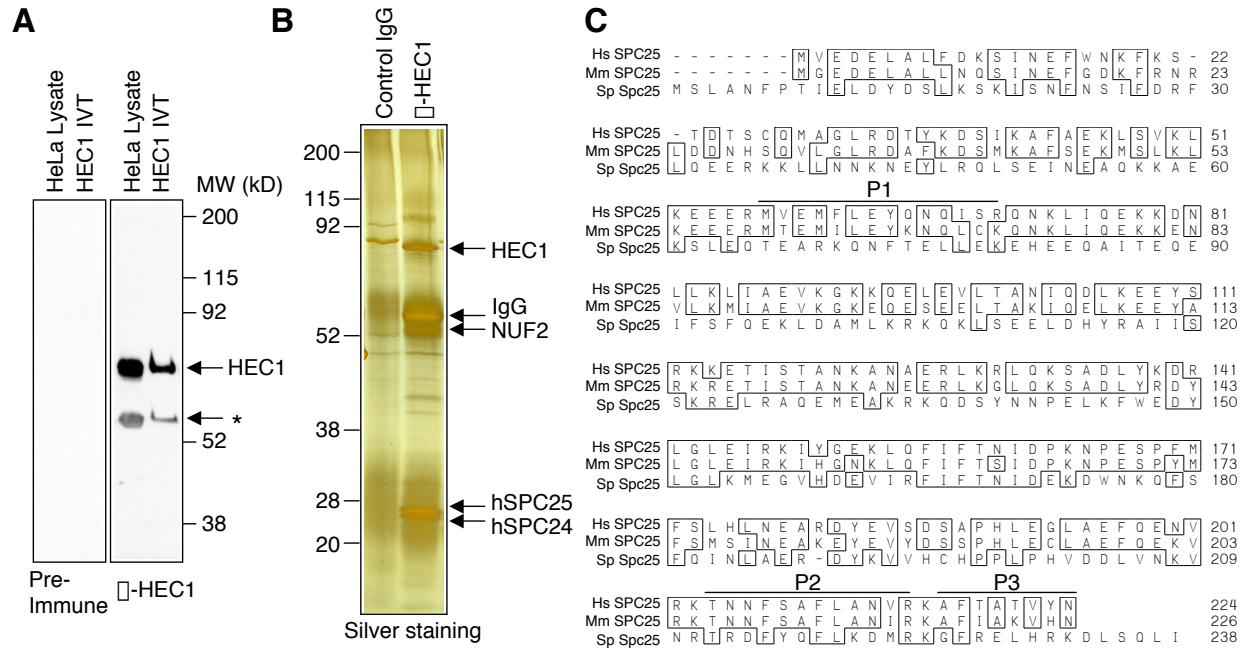


**Fig. 1. Identification of hSpC25.** *A*, characterization of the antibody against Hec1. HeLa cell lysate and Hec1 protein *in vitro* translated in rabbit reticulocyte lysate were blotted with the pre-immune serum or affinity-purified □-Hec1 antibody. A weak contaminating band is indicated by an asterisk. *B*, purification of Hec1-containing human Ndc80 complex. The Ndc80 complex was immuno-precipitated from lysates of nocodazole-arrested HeLa cells using □-Hec1 antibody covalently coupled to Protein A beads and analyzed by SDS-PAGE followed by silver staining. The □-GST antibody beads were used as a control. The bands corresponding to Hec1, hNuf2, hSpC25, and hSpC24 are labeled. *C*, sequence alignment of human (Hs), mouse (Mm), and fission yeast (Sp) homologs of SpC25. Identical residues are boxed. These proteins do not share significant sequence similarity with the budding yeast SpC25. The hSpC25 sequences corresponding to the three peptides (P1, P2, and P3) identified by mass spectrometry are indicated.

*Human Spc25 binds to Hec1 in vitro and interacts with Hec1 throughout the cell cycle in vivo*—To confirm the interaction between Hec1 and hSpc25, we transfected HeLa cells with plasmids encoding Myc-tagged Hec1 and HA-tagged hSpc25. The lysates of the transfected cells were then immunoprecipitated using an anti-Myc antibody and blotted with an anti-HA antibody (Figure 2A). The HA-hSpc25 protein was present in the anti-Myc immunoprecipitates, indicating that HA-hSpc25 interacted with Myc-Hec1 in these cells (Figure 2A). In a complementary experiment, plasmids encoding Myc-hSpc25 and HA-Hec1 were co-transfected into HeLa cells. The cell lysates were again immunoprecipitated with an anti-Myc antibody and blotted with an anti-HA antibody. HA-Hec1 was again found to interact with Myc-hSpc25 (Figure 2B). These results demonstrated that, when overexpressed, Hec1 and hSpc25 formed a complex in living cells. In another experiment, we co-translated plasmids encoding HA-Hec1 and Myc-hSpc25 in rabbit reticulocyte lysate *in vitro* in the presence of <sup>35</sup>S-methionine. HA-Hec1 and Myc-hSpc25 were co-immunoprecipitated in these lysates, indicating that Hec1 and hSpc25 also interacted with each other *in vitro* (Figure 2C).

To further characterize hSpc25, we raised an antibody against the N-terminal 150 residues of this protein. After purification with the corresponding antigen, the hSpc25 antibody recognized a 25 kD band in HeLa cell lysates, which disappeared in lysates of cells subjected to hSpc25 RNAi treatment (see Figure 4A). This indicated that this antibody selectively detected the hSpc25 protein at its endogenous levels. Immunoprecipitation with anti-Hec1 followed by immunoblotting with anti-hSpc25 showed that the endogenous Hec1 and hSpc25 proteins interacted with each other (Figure 2D). This interaction was also observed in log-phase cells, suggesting that the Ndc80 complex exists throughout the cell cycle (Figure 2D).

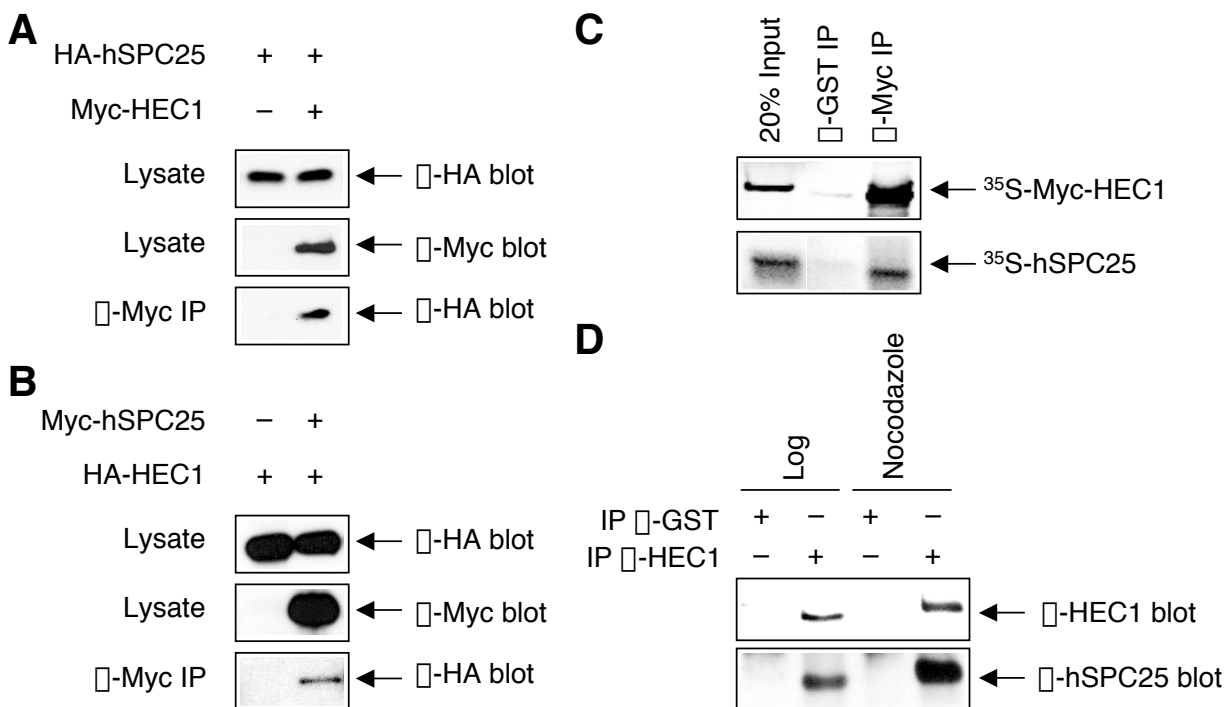


**Fig. 2. Binding between hSpc25 and Hec1.** *A&B*, HeLa-Tet-on cells were transfected with the indicated plasmids and lysed. The resulting lysates were immunoprecipitated with anti-Myc beads, and the immunoprecipitates were then blotted with anti-HA. *C*, Myc-Hec1, hNuf2, and hSpc25 were co-translated *in vitro* in rabbit reticulocyte lysate in the presence of  $^{35}\text{S}$ -methionine and subjected to immunoprecipitation with  $\square$ -Myc. The immunoprecipitates were analyzed by SDS-PAGE followed by autoradiography. Twenty percent of the input proteins were included for comparison. *D*, lysates of log phase or nocodazole-arrested HeLa cells were subjected to immunoprecipitation with  $\square$ -GST or  $\square$ -Hec1 antibodies. The immunoprecipitates were then resolved by SDS-PAGE and blotted with  $\square$ -hSpc25.

*Human Spc25 localizes to kinetochores during mitosis*—Hec1 and hNuf2, two known components of the human Ndc80 complex localize to kinetochores during mitosis (29,30). We next examined whether hSpc25 exhibited a similar localization pattern. To determine the cellular localization of hSpc25, we transfected HeLa cells with plasmids encoding Myc-tagged hSpc25 and stained the transfected cells with an anti-Myc antibody and a human autoimmune serum (CREST) that labeled the kinetochores (Figure 3A-C). Myc-hSpc25 exhibited a punctate staining pattern that matched well with that of CREST during all stages of mitosis, including prometaphase, metaphase, and anaphase (Figure 3A-C). This indicated that Myc-hSpc25 localized to kinetochores in mitosis. We next determined the cellular localization of the endogenous hSpc25 protein during mitosis. As shown in Figure 3D, the endogenous hSpc25 protein also showed a punctate staining pattern that was similar to that of CREST, indicating that the endogenous hSpc25 also localizes to kinetochores during mitosis.

*Human Spc25 is required for proper progression through mitosis*—To further demonstrate that hSpc25 is a functional homolog of yeast Spc25, we depleted hSpc25 from HeLa cells using RNAi and compared the phenotypes of the hSpc25 RNAi cells with those of the Hec1 RNAi cells (Figure 4). The protein levels of hSpc25 and Hec1 were significantly reduced in HeLa cells transfected with the corresponding siRNA oligonucleotides (Figure 4A). We first examined the cell cycle status of the hSpc25 RNAi cells by FACS. At 48 hrs after RNAi treatment, about 30% of these cells possessed 4N DNA contents whereas only 15% of the control cells had 4N DNA contents (Figure 4B). About 30% of the hSpc25 RNAi cells possessed less than 2N DNA contents, suggesting that they had undergone cell death (Figure 4B). Thus, depletion of hSpc25 from HeLa cells caused an accumulation of cells in G2/M and cell death. To determine whether the hSpc25 RNAi cells accumulated in G2 or mitosis, we examined the

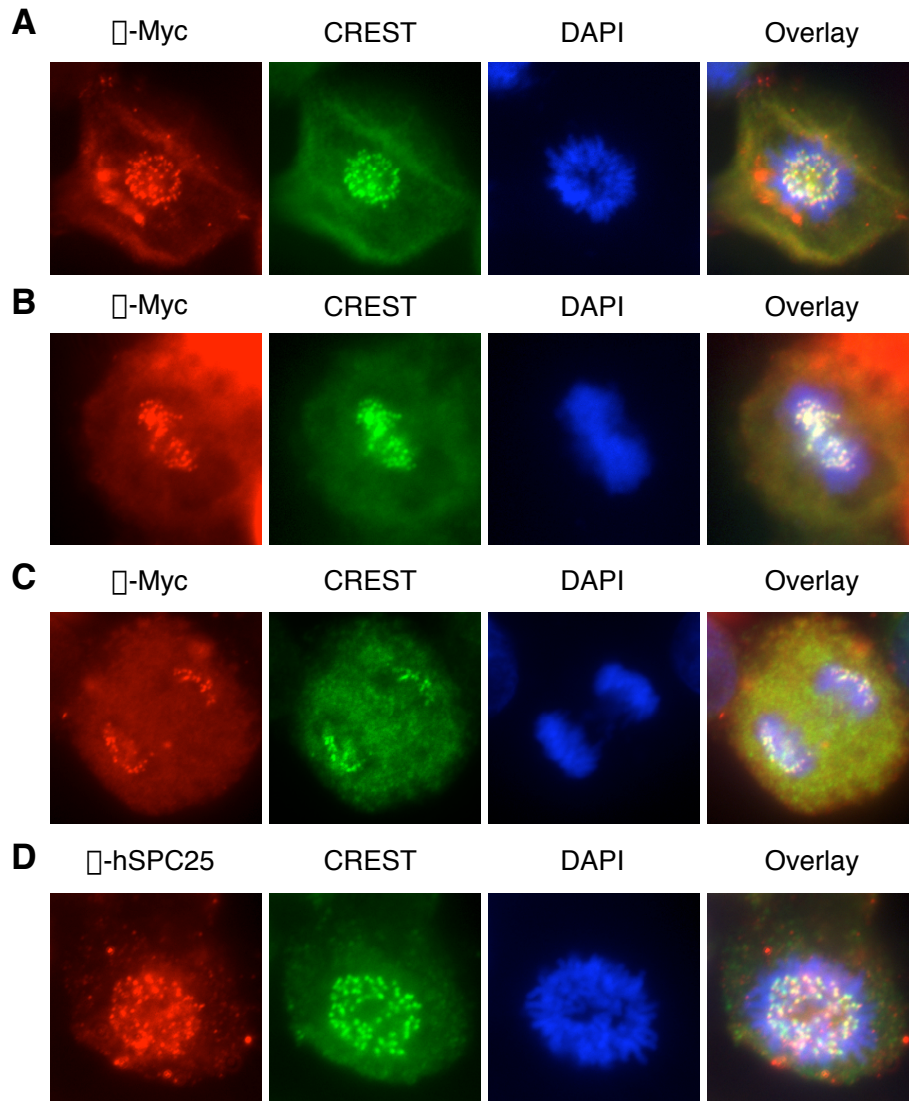


**Fig. 3. Kinetochore localization of hSpc25 during mitosis.** *A-C*, HeLa cells transfected with pCS2-Myc-hSpc25 in prometaphase (*A*), metaphase (*B*), and anaphase (*C*) were immunostained with  $\square$ -Myc. DNA and kinetochores were counterstained with DAPI and CREST serum, respectively. The Myc-staining, CREST-staining, and DNA-staining are pseudo-colored red, green, and blue, respectively. *D*, immunostaining of a HeLa cell in prometaphase with the purified  $\square$ -hSpc25 antibody. DNA and kinetochores were counterstained with DAPI and CREST serum, respectively. The endogenous hSpc25-staining, CREST-staining, and DNA-staining are pseudo-colored red, green, and blue, respectively.

cell and DNA morphology of these cells using a fluorescence microscope. Cells in mitosis were typically round with condensed DNA. At 24 hours after RNAi, we noticed an accumulation of hSpc25 RNAi cells in mitosis. The mitotic index of the hSpc25 RNAi cells was 32%, as compared to a mitotic index of 10% in control cells (Figure 4C). At 48 hours after RNAi treatment, the mitotic index was about 28% (Figure 4C). This indicated that the hSpc25 RNAi cells accumulated in mitosis and the majority of the 4N cells as determined by FACS represented cells in mitosis, rather than G2 (Figure 4B & 4C). While the mitotic index of the hSpc25 RNAi cells did not increase at later time points, there was a dramatic increase of cell death (Figure 4C). For example, at 72 hrs after transfection, about 75% of the hSpc25 RNAi cells had undergone cell death while less than 10% of the control cells had died (Figure 4C). Therefore, our results are consistent with the notion that inactivation of hSpc25 causes a delay or arrest in mitosis followed by cell death. Very similar phenotypes were observed with cells depleted for Hec1 by RNAi (Figure 4C) (29). This indicates that inactivation of either hSpc25 or Hec1 has similar effects on the cell cycle, further supporting that hSpc25 is a component of the Ndc80 complex.

*Mitotic arrest in hSpc25-depleted cells depends upon a functional spindle checkpoint*—The mitotic arrest of hSpc25 cells can be explained by two equally plausible scenarios. First, inactivation of hSpc25 causes a defect in kinetochore function and arrests cells in prometaphase. Second, the hSpc25 RNAi cells undergo a mitotic arrest mediated by an active spindle checkpoint. One way to distinguish these two possibilities is to determine the protein level of cyclin A1 in these cells. As shown previously, the level of cyclin A1 is high in prometaphase cells and it is already degraded by the metaphase-anaphase transition.

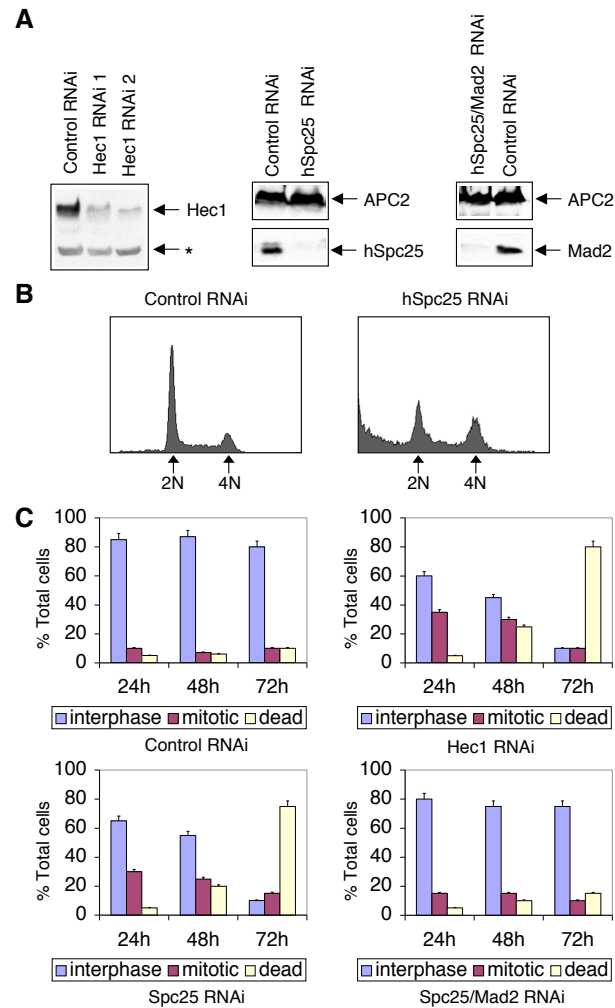


**Fig. 4. Phenotypes of HeLa cells depleted for hSpc25.** *A*, HeLa cells were transfected with Hec1, hSpc25, or hSpc25/Mad2 siRNA duplexes or mock transfected with oligofectamine alone and harvested at 48 hrs after transfection. Protein levels were compared by immunoblotting with the indicated antibodies. In the case of hSpc25 and Mad2 RNAi, samples were also blotted with  $\alpha$ -APC2 to demonstrate uniform sample loading. For Hec1 RNAi, the nonspecific band detected by  $\alpha$ -Hec1 serves as a loading control. *B*, FACS analysis of HeLa cells mock transfected or transfected with siRNA specific for hSpc25 at 48 hrs after transfection. The peaks corresponding to 2N and 4N DNA contents are labeled. *C*, quantitation of the percentage of interphase, mitotic, and dead cells of HeLa cells subjected to mock, Hec1, hSpc25 and hSpc25/Mad2 RNAi at 24 hrs, 48 hrs, and 72hrs post-transfection. For each quantitation, three fields of more than 100 cells were counted and averaged.



Interestingly, though an active spindle checkpoint blocks the APC/C-mediated degradation of cyclin B1 and securin, it does not prevent cyclin A1 degradation (34). Therefore, mitotic cells arrested with an active spindle checkpoint are expected to contain low levels of cyclin A1 and high levels of cyclin B1 and securin. On the other hand, cells in prometaphase are expected to contain high levels of all three proteins. To determine the status of spindle checkpoint and the stage of mitotic arrest of mitotic hSpc25 RNAi cells, we examined the protein levels of cyclin A1, cyclin B1, and securin in these cells by immunostaining with the corresponding antibodies. As shown in Figure 5, the levels of cyclin B1 and securin were high in mitotic hSpc25 RNAi cells while the levels of cyclin A was low. This suggests that these cells might be arrested in mitosis by an active spindle checkpoint, instead of a mechanical slowdown in prometaphase.

Martin-Lluesma *et al.* (29) had shown that the mitotic delay observed in Hec1 RNAi cells was dependent on the spindle checkpoint, as simultaneous depletion of Hec1 and Mad2 by RNAi allowed cells to escape from this mitotic arrest. To examine whether the mitotic arrest observed in the hSpc25 RNAi cells also depended on the spindle checkpoint, we depleted both hSpc25 and Mad2 simultaneously in HeLa cells by RNAi. Both the mitotic arrest and cell death phenotypes observed in the cells subjected to hSpc25 siRNA alone were mostly reversed in cells that received both hSpc25 and Mad2 siRNA. For example, at 24 and 48 hrs after RNAi treatment, only 15% of the double RNAi cells were arrested in mitosis while about 30% of the hSpc25 RNAi cells were mitotic (Figure 4C). At 72 hrs after RNAi treatment, the majority of the hSpc25 RNAi cells had undergone cell death while more than 70% of the hSpc25/Mad2 double RNAi cells were viable (Figure 4C). It is worth noting that many of the hSpc25/Mad2 double

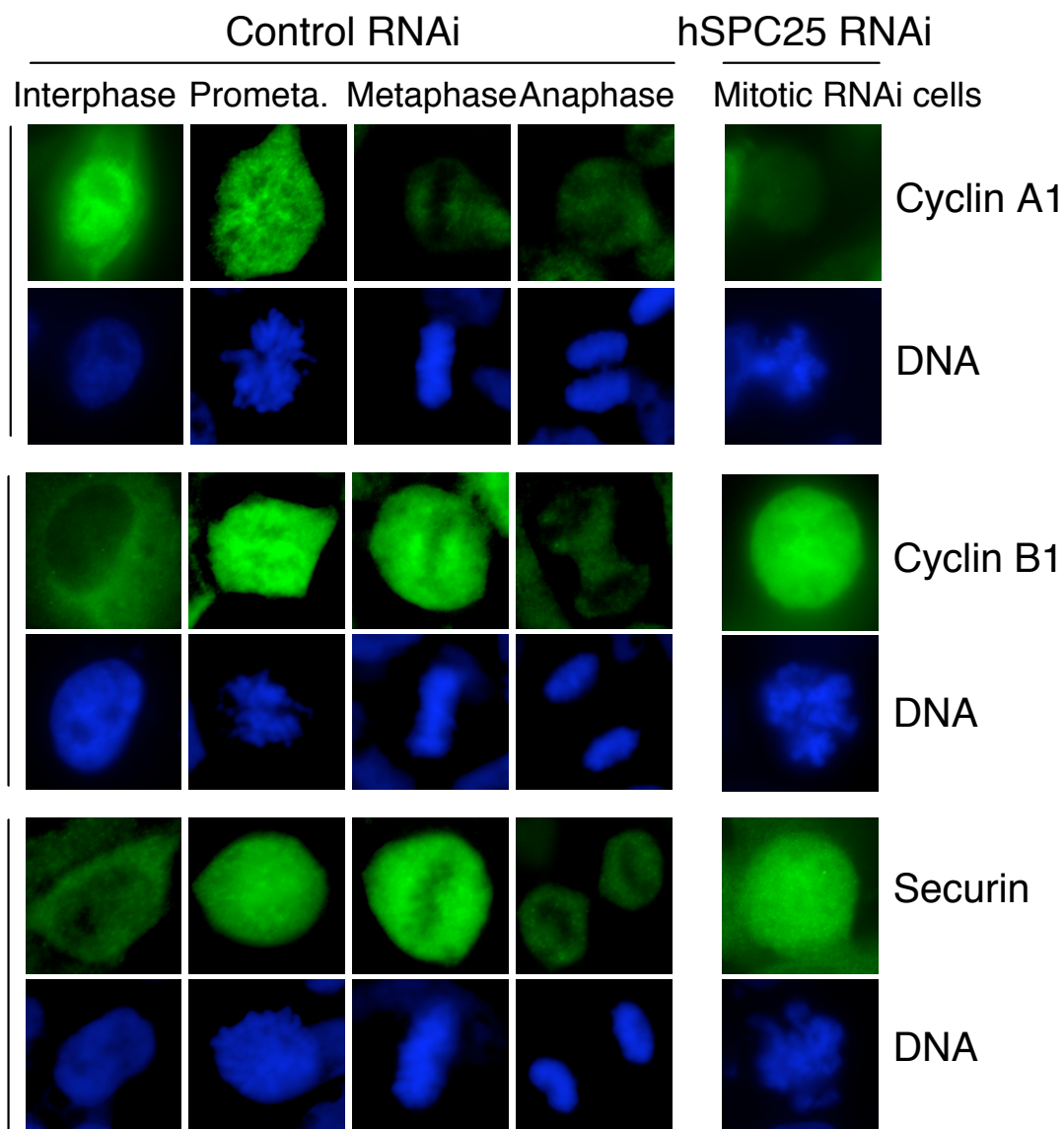


**Fig. 5. Cells depleted for hSpc25 arrest in mitosis with low levels of cyclin A1 and high levels of cyclin B1 and securin.** At 48 hours after hSpc25 siRNA treatment, HeLa cells were immunostained with  $\alpha$ -cyclin A1 (top two panels),  $\alpha$ -cyclin B1 (middle two panels), or  $\alpha$ -Securin antibody (bottom two panels). DNA was counterstained with DAPI. Mock-transfected cells at different mitotic stages were also stained and served as standards for comparison of protein levels.

RNAi cells escaped from mitosis abnormally, as a vast majority of the hSpc25/Mad2-depleted interphase cells contained multiple or aberrant multi-lobed nuclei (data not shown). Therefore, similar to Hec1-depleted cells (29), the mitotic delay or arrest caused by the inactivation of hSpc25 also requires a functional spindle checkpoint.

*Inactivation of the hNdc80 complex causes apoptosis after a transient mitotic arrest*—To determine the timing of cell death in response to the loss of Ndc80 function, we followed Hec1 siRNA transfected cells after synchronization at G1/S boundary by thymidine treatment. The percentage of cell death was significantly lower in thymidine-treated Hec1 RNAi cells (12%), as compared to untreated RNAi samples (28%), suggesting that blocking cells at G1/S reduces cell death in Hec1-depleted cells. We next washed off the mitotic and dead cells that had accumulated during the 18-hour thymidine treatment and examined Hec1-depleted cells and mock transfected cells for 16 hours after release from the thymidine arrest (Figure 6). As expected, a major increase in the mitotic index was observed 9-10 hours after thymidine release in both samples (Figure 6A). Comparison of the mitotic index at later time points revealed that mitotic progression was much slower in the Hec1-depleted cells as compared to the mock-transfected cells (Figure 6A). After 14 hours of thymidine release, only 10-15% control cells were in mitosis whereas approximately 30-35% of Hec1 depleted cells were mitotic (Figure 6A). There was no significant cell death in the Hec1 siRNA treated cells until 14 hours after thymidine release, at which time a sharp increase in cell death was observed (Figure 6B). By 16 hours, around 50% of Hec1-depleted cells were dead (Figure 6B). This indicates that Hec1-depleted cells die following a transient arrest in mitosis. During the same period, no significant

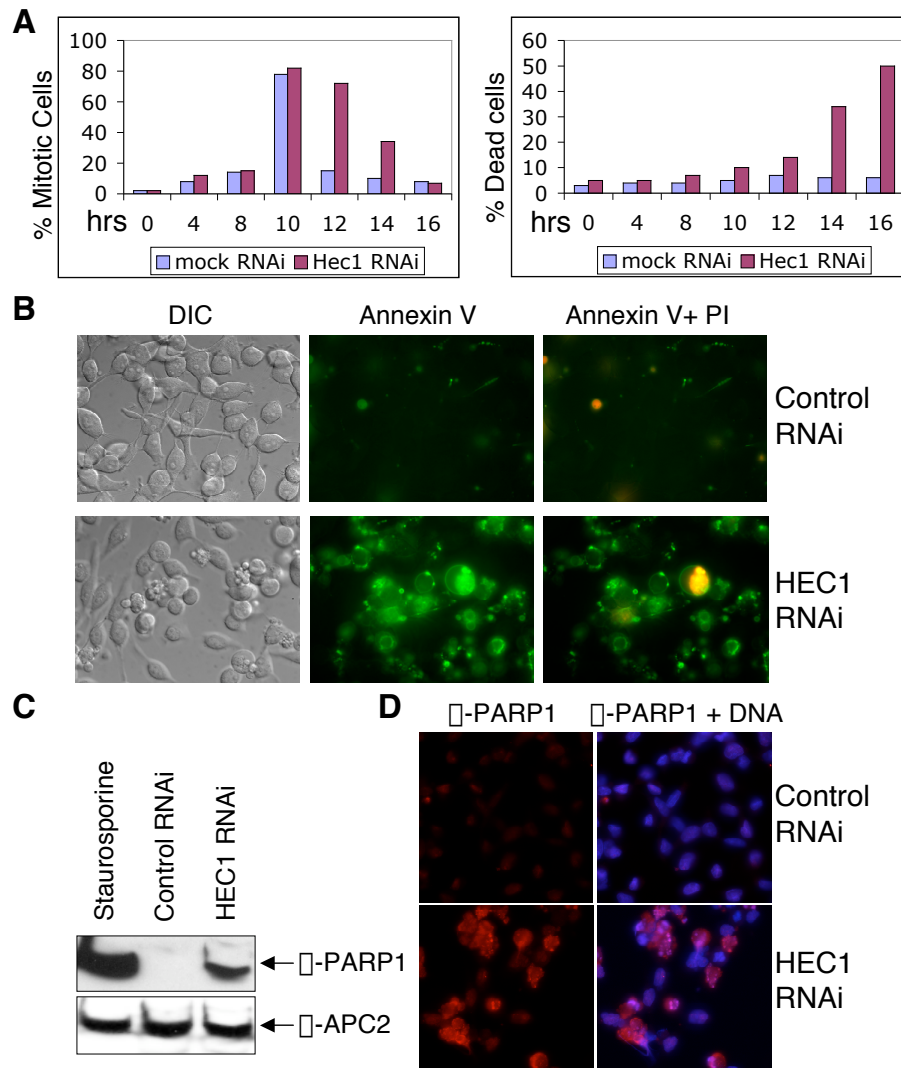


**Fig. 6. Hec1 RNAi cells undergo a transient mitotic arrest followed by apoptosis.** *A*, the mitotic index (left panel) and percentage of dead cells (right panel) for mock or Hec1 siRNA transfected HeLa cells at 0, 4, 8, 10, 12, 14, and 16hrs after release from a thymidine arrest. *B*, HeLa cells subjected to mock (upper panel) or Hec1 siRNA (lower panel) were stained with Annexin V-FITC and Propidium iodide (PI). Apoptotic cells are positive for Annexin V-FITC staining and negative for PI staining. *C*, cell lysates of staurosporine, mock RNAi, and Hec1 RNAi treated cells were blotted with an antibody specific for the cleaved form of PARP1. *D*, Mock (upper panel) or Hec1 (lower panel) siRNA transfected HeLa cells were fixed and stained with the same  $\square$ -cleaved-PARP1 antibody.

cell death was observed for the control cells. These results are consistent with time lapse video microscopy by us (data not shown) and DeLuca *et al.* (30). A large percentage of the cells with a compromised Ndc80 function die following a 5-8 hr arrest in mitosis.

To determine whether cell death observed in cells without proper Ndc80 function is due to apoptosis or necrosis, we stained the dead Hec1 RNAi cells with the commonly used apoptotic markers, Annexin V and PARP1. The Hec1 RNAi cells were first synchronized at G1/S with thymidine and released for 18 hrs. Most of the dead Hec1 RNAi cells stained positive for Annexin V and negative for PI, indicating that the Hec1-depleted cells underwent apoptosis (Figure 6B). This was further confirmed by the detection of cleaved PARP1 in immunoblots of Hec1 RNAi samples (Figure 6C) and positive immunostaining of these dead cells with an antibody specific for the cleaved form of PARP1 (Figure 6D). Staurosporine was known to trigger apoptosis in HeLa cells and staurosporine-treated cell lysate was used as a positive control in the anti-PARP1 immunoblot (Figure 6C). Interestingly, we found that treatment of Hec1 RNAi cells with nocodazole did not prevent cell death (data not shown). This suggests that apoptosis of the Hec1 RNAi cells is not a secondary consequence of cells attempting to undergo mitosis in the presence of a functional spindle, but dysfunctional kinetochores. It is possible that kinetochores with a compromised Ndc80 function trigger an apoptotic pathway directly only following a 5-8 hr mitotic arrest. Cell death can be avoided if cells do not undergo this mitotic arrest due to the inactivation of the spindle checkpoint (as in Hec1/Mad2 RNAi cells). To examine whether the cell death in response to Hec1/hSpc25 RNAi is specific to HeLa cells and other cell lines with defective p53/Rb pathways, we depleted hSpc25 from HCT116 cells, which contained wild-type p53. About 20% of HCT116 cells underwent apoptosis after 48 hours of hSpc25 siRNA transfection, as compared to 5% in mock-transfected cells. This clearly indicates

that hSpc25 RNAi also induces cell death of a cell line with wild-type p53, albeit to a lesser extent.

*Inactivation of hSpc25 leads to multiple spindle abnormalities*—Several groups had observed various mitotic defects in vertebrate cells depleted of Hec1 or Nuf2 (29-32). We also analyzed the DNA and spindle morphology of the hSpc25 RNAi cells. As shown in Figure 7, the hSpc25 RNAi cells also exhibited defects in spindle morphology and chromosome congression. First, about 18% of the mitotic hSpc25 RNAi cells contained multipolar spindles (Figure 7A). In the mitotic cells with bipolar spindles, there were also clear defects: these spindles were more elongated and often distorted (Figure 7A). Second, despite the presence of bipolar spindles, the chromosomes in most mitotic hSpc25-depleted cells were scattered throughout the cell, indicating a failure for the chromosomes to align at the metaphase plate. In a few cells, while most of the chromosomes were aligned at the metaphase plate, some chromosomes were still lagging behind (Figure 7A). These results indicate that hSpc25 is required for the proper execution of many mitotic processes, again consistent with it being a subunit of the Ndc80 complex.

To examine whether the spindle defects in cells lacking proper Ndc80 function are an indirect consequence of prolonged mitotic arrest, Hec1 RNAi cells were synchronized by thymidine treatment for 18 hours. Cells were then allowed to enter mitosis 9-10 hours after thymidine release. The morphology of the mitotic spindle was monitored by immunostaining cells for tubulin and DNA at 1 hr intervals after 9 hours of thymidine release. Surprisingly, even at 9 hours after thymidine release, most mitotic cells exhibited an elongated spindle and around 25% of these mitotic cells contained multipolar spindles (Figure S2). There was no significant

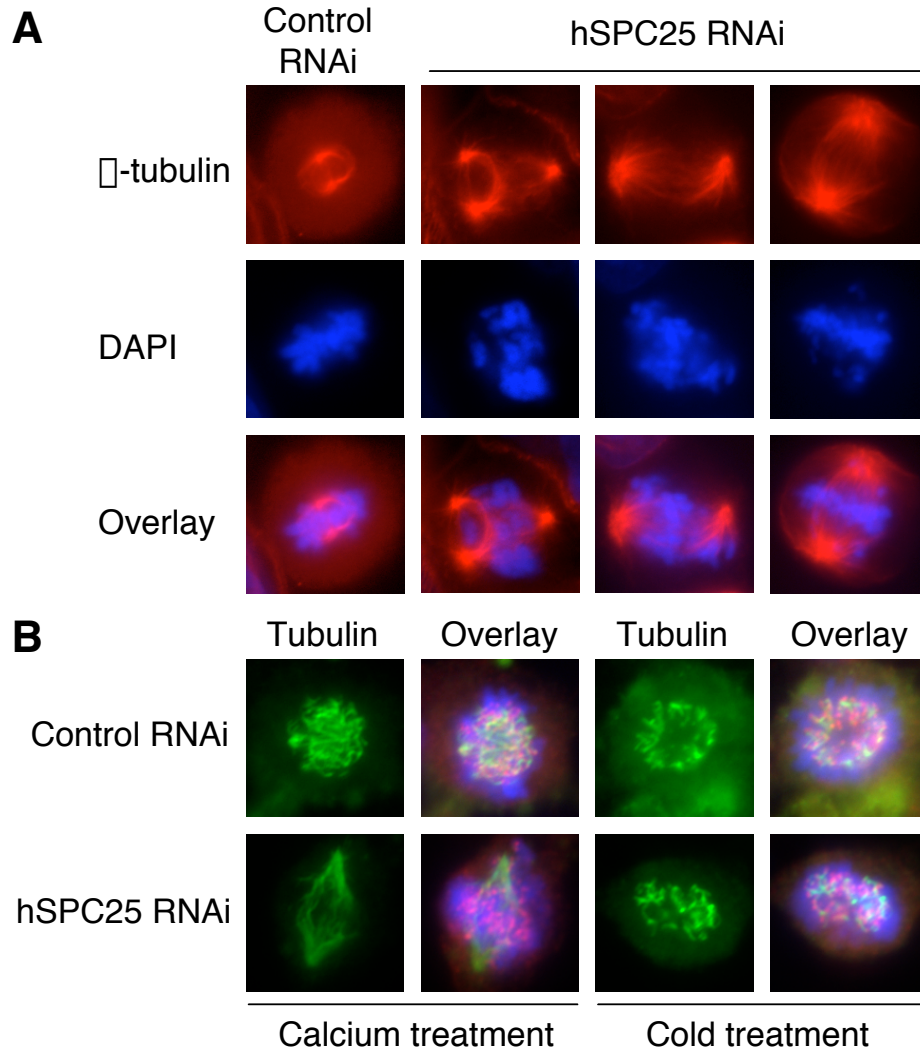


**Fig. 7. Aberrant DNA and spindle morphology of mitotic hSpc25 RNAi cells.** *A*, At 48 hrs after transfection, the hSpc25 RNAi cells were stained with  $\alpha$ -tubulin antibody and DAPI. As compared to the normal metaphase (leftmost panel), there are multiple spindle defects, including multipolar spindles (2<sup>nd</sup> panel from left), distorted/misaligned spindles (3<sup>rd</sup> panel from left), and elongated spindles (rightmost panel). *B*, hSpc25-depleted cells were subjected to calcium (left panels) or cold (right panels) treatment to destabilize nonkinetochore microtubules and the remaining kinetochore-bound microtubules were visualized by immunostaining with anti-tubulin antibody (green). The overlay panel shows DNA (blue) and CREST staining (purple), along with tubulin staining (green).

increase in the number of cells with multipolar spindle at later time points (Figure S2). This indicates that these spindle defects occur shortly after the entry into mitosis and are unlikely to be a nonspecific consequence of prolonged mitotic arrest. However, we did observe an increase in the number of cells with fractured spindles at later time points, suggesting that this defect might be an indirect consequence of a prolonged mitotic arrest (Figure S2).

*hSpc25 deficient kinetochores retain the ability to form microtubule attachments*—The chromosome congression defect observed in hSpc25 depleted cells might be due to their inability to form functional kinetochore-microtubule connections. The presence of kinetochore bound microtubules can be specifically detected by incubating cells for a short period with ice cold media or by permeabilizing them in the presence of high levels of calcium. Both these treatments destabilize nonkinetochore microtubules whereas kinetochore-bound microtubules are preserved. Microtubules appear to be stable under both these circumstances in hSpc25-deficient cells (Figure 7B), suggesting that the Ndc80 complex is not completely indispensable for the formation of kinetochore-microtubule attachments. However, we do not know whether these kinetochore-microtubule attachments formed in Spc25 RNAi cells are functional.

*Depletion of hSpc25 leads to the loss of kinetochore localization of Mad1 in a microtubule-dependent manner*—Martin-Lluesma *et al.* showed that Hec1 interacts with Mad1 in yeast two-hybrid assays and is essential for the localization of Mad1 to kinetochores during mitosis (29). We next tested whether hSpc25 was also required for the kinetochore recruitment of Mad1. We examined the kinetochore localization of three spindle checkpoint proteins (Mad1,



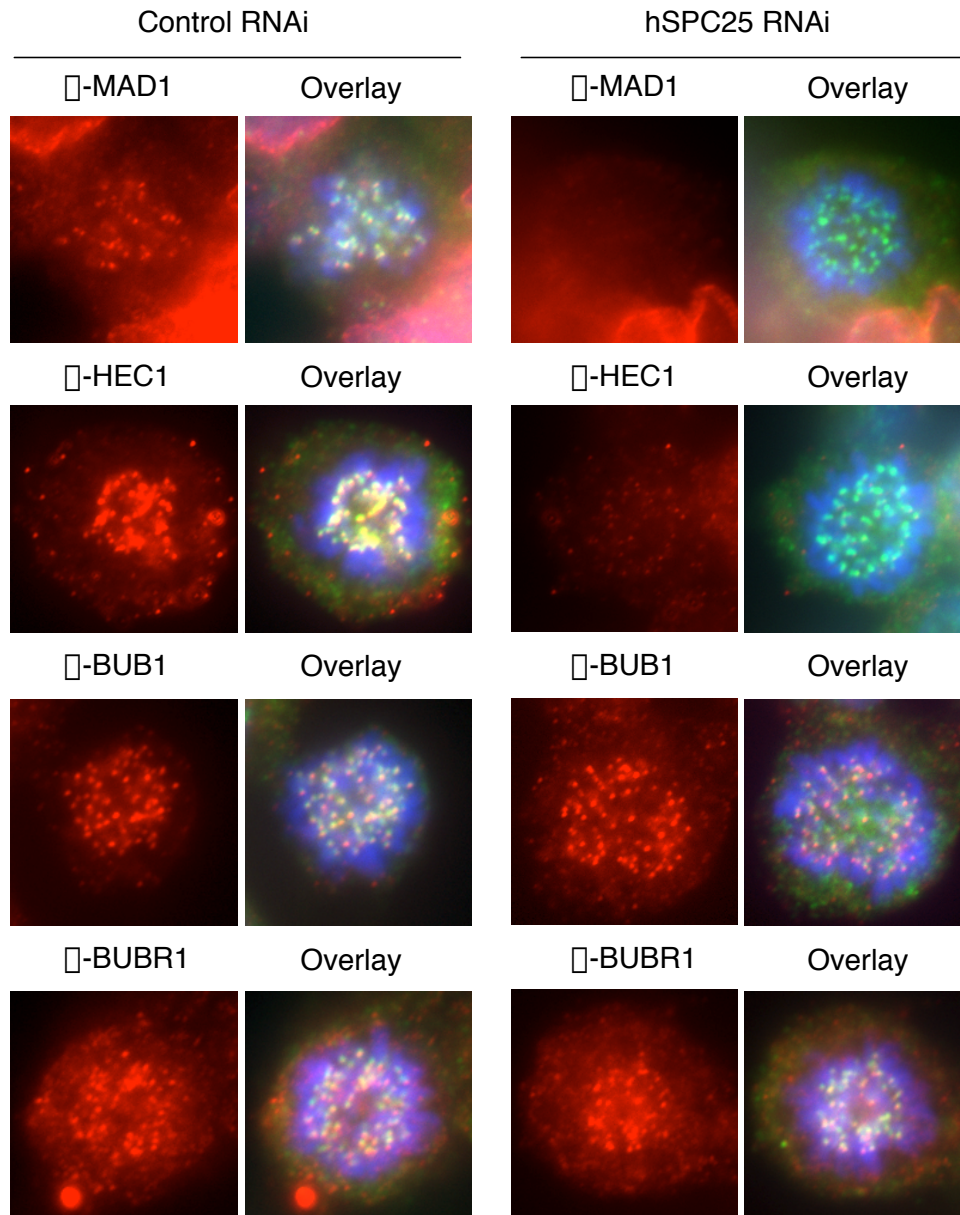


**Fig. 8. Human Spc25 is required for the kinetochore localization of Mad1 and Hec1 during mitosis.** At 48 hrs after transfection, the hSpc25 RNAi cells were stained with  $\alpha$ -Mad1,  $\alpha$ -Hec1,  $\alpha$ -Bub1, and  $\alpha$ -BubR1 antibodies (pseudo-colored red). DNA and kinetochores were counterstained with DAPI and CREST serum and pseudo-colored blue and green, respectively. In hSpc25 RNAi cells, Mad1 is undetectable at kinetochores during mitosis. The intensity of Hec1 kinetochore staining is greatly reduced at the kinetochores. The staining of Bub1 and BubR1 remains unaffected.

Bub1, and BubR1) in the hSp25-depleted cells (Figure 8). In control cells, Mad1 was clearly observed at the kinetochores during prometaphase (Figure 8). However, the kinetochore staining of Mad1 was undetectable in prometaphase cells depleted of hSp25 (Figure 8). Depletion of hSp25 did not adversely affect the integrity of the kinetochores in a general way, as CREST-staining at the kinetochores was normal. The kinetochore staining of other checkpoint proteins, such as Bub1 and BubR1, were also largely unaffected by the RNAi-mediated depletion of hSp25 (Figure 8). This indicates that inactivation of hSp25 specifically abolishes the kinetochore localization of Mad1. Martin-Lluesma *et al.* showed that the intensity kinetochore staining of Bub1 is reduced by 50% in Hec1 RNAi cells (29). In our hands, the Bub1 and BubR1 kinetochore staining does not appear to be weaker in either Hec1 or hSp25 RNAi cells. We do not know the underlying reason for this discrepancy, though it may result from the use of different antibodies and different fixation protocols.

We also tested whether hSp25 is required for the kinetochore localization of Hec1 in mitosis. As shown in Figure 8, Hec1 localizes to the kinetochores in control mitotic cells. The intensity of the kinetochore staining of Hec1 was greatly diminished in mitotic hSp25-depleted cells. This indicates that the kinetochore localization of Hec1 depends on hSp25. This is again consistent with hSp25 being a component of the Ndc80 complex.

We next tested whether the Ndc80 complex is also required for the kinetochore localization of Mad1 in nocodazole-arrested mitotic cells. As shown in Figure 9, Mad1 localized to kinetochores in mock-transfected mitotic cells treated with nocodazole. As expected, the kinetochore localization of Mad1 was absent in mitotic Hec1 RNAi cells in the absence of nocodazole (Figure 9). Surprisingly, the kinetochore localization of Mad1 was restored in Hec1 RNAi cells upon nocodazole treatment (Figure 9). Though we cannot determine whether a

particular cell indeed received RNAi, we did analyze more than 100 mitotic cells and the vast majority of them exhibited positive Mad1 staining. Therefore, it appears that the Ndc80 complex is not absolutely required for Mad1 kinetochore localization in nocodazole-arrested mitotic cells that lack a functional spindle.

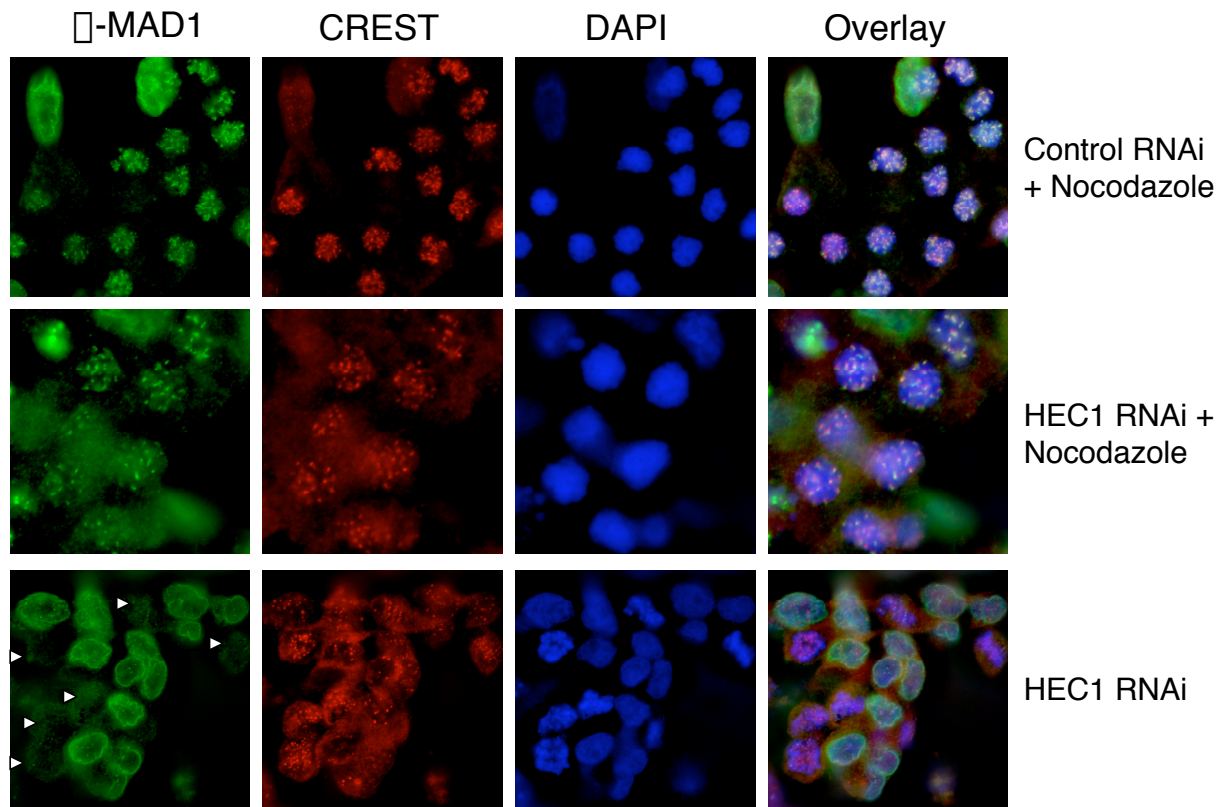


**Fig.9. Kinetochores localization of Mad1 is restored in Hec1-depleted cells upon microtubule depolymerization.** HeLa cells transfected with mock (upper panel) or Hec1 siRNA (middle panel) were treated with nocodazole and immunostained with  $\alpha$ -Mad1 antibody. Kinetochores and DNA were labeled with CREST and DAPI, respectively. Lower panel shows disappearance of Mad1 kinetochore staining in Hec1-depleted mitotic cells in the absence of nocodazole treatment. Mitotic cells are indicated by arrows.

## DISCUSSION

We have identified two novel components of the human Ndc80 complex through immuno-affinity purification. Despite the lack of significant sequence homology, hSpc25 is the functional homolog of the yeast Spc25 protein based on the following observations. First, hSpc25 is isolated based on its physical interaction with Hec1, a known component of human Ndc80 complex. It also interacts with Hec1 *in vitro*. Second, similar to Hec1 and hNuf2 (two known components of human Ndc80 complex), hSpc25 localizes to kinetochores during mitosis. Third, depletion of hSpc25 in HeLa cells by RNAi causes similar mitotic defects as does RNAi-mediated depletion of Hec1 or hNuf2. Though we have not performed a detailed characterization of the 24 kD protein identified from the Hec1 immunoprecipitates, it is very likely the human ortholog of the yeast Spc24 protein, because it is one of the most abundant proteins in the Ndc80 immunoprecipitate and because it is also a coiled-coil protein, similar to the yeast Spc24 protein.

*Roles of the Ndc80 complex in chromosome congression and spindle morphology*—The Ndc80 complex has now been characterized in several organisms, including *S. cerevisiae*, *Xenopus*, chicken, and mammals (28-32). In all the systems studied so far, the Ndc80 complex proteins localize to kinetochores in mitosis and their inactivation leads to a defect in chromosome congression. We have observed a similar phenotype for HeLa cells transfected with either hSpc25 or Hec1 siRNA. The exact function of the Ndc80 components in this process is not yet understood. The simplest explanation for the chromosome congression defect in these cells would be their inability to form functional kinetochore-microtubule attachments. But the resistance of

microtubules to cold or calcium-mediated destabilization in these cells indicates that these cells can achieve certain degree of kinetochore-microtubule attachment. Moreover, some degree of chromosomal alignment can be observed in many hSpc25/Hec1-depleted mitotic cells. The inability of these cells to align their chromosomes might then stem from their unstable or improper kinetochore-microtubule connections.

Apart from defects in chromosome alignment, cells with a compromised Ndc80 function exhibit multiple spindle aberrations, including abnormally elongated spindles, multipolar spindles, and misaligned bipolar spindles. These abnormalities might be an indirect consequence of a prolonged mitosis. Alternatively, certain kinetochore components, such as the Ndc80 complex, are essential to maintain the integrity of the spindle. Our experiments with synchronized cells treated with Hec1 RNAi support the second possibility. Elongated and multipolar spindles can be observed at early stages of mitosis in Hec1-depleted cells and no significant increase in the frequency of these abnormal spindles is observed at later time points. In addition, functional disruption of other kinetochore components, such as Mis12, Mis6, CENP-A and CENP-C also leads to abnormally elongated spindles (35). Multipolar and fractured spindles are also observed in response to inactivation of other kinetochore proteins. For example, disruption of the dynactin complex by overexpressing p50 dynamitin leads to fractured spindles (36). Similarly, depletion of human CENP-I/Mis6 results in multipolar spindles (35). The underlying mechanism for these spindle aberrations in cells with defective kinetochores is not known. However, it is conceivable that a functional kinetochore might regulate spindle length by counteracting the forces that tend to extend the spindle. It is also

possible that kinetochores might have checkpoint functions that prevent precocious elongation of spindles and the formation of additional spindle poles.

*Loss of Ndc80 function and apoptosis*—Another important phenotype of cells depleted for components of the Ndc80 complex is that these cells die after a mitotic arrest of about 5-8 hours. The majority of these dead cells show a cellular and nuclear morphology characteristic of apoptosis, including membrane blebbing and fragmented nuclei. Furthermore, these cells are positively stained with Annexin V and an antibody against cleaved PARP1, indicating that the Ndc80-deficient cells die by apoptosis. Thus, the mitotic arrest observed in these Ndc80-depleted cells differs from that caused by CENP-E depletion or by microtubule poisons, such as nocodazole. In the latter cases, cells can stay arrested in mitosis for as long as 18 hours without undergoing apoptosis. In addition, Hec1 RNAi cells die with the same kinetics in the presence of nocodazole. Therefore, it appears that apoptosis of Hec1 RNAi cells is not a secondary consequence of cells attempting to divide in the presence of a defective kinetochore, but functional spindle. In the future, it will be interesting to determine whether and how the Ndc80-deficient kinetochores actively trigger apoptosis.

*Role of Ndc80 in the spindle checkpoint*—Martin-Lluesma *et al.* have reported that Hec1 interacts with Mad1 in yeast two-hybrid assays and is required for the localization of Mad1 to kinetochores during mitosis (29). These observations have been confirmed by our findings in this study and by Hori *et al.* using Nuf2-deleted chicken DT40 cell lines (32). There are two possible explanations for the lack of Mad1

kinetochore localization in Ndc80-deficient cells. The Ndc80 complex might form the docking surface through which Mad1 latches onto the kinetochores. Alternatively, it could be a secondary consequence of an aberrant mitosis with a defective kinetochore, but functional spindle. For example, Hec1-deficient kinetochores might be able to attach to microtubules to some extent, but cannot undergo chromosome congression due to the lack of tension.

The existence of kinetochore-microtubule attachment in these cells, as detected by cold-sensitive or calcium-sensitive staining prompted us to examine Mad1 localization in hSpc25/Hec1 depleted cells after treatment with microtubule depolymerizing agent, such as nocodazole. Surprisingly, Mad1 localization to kinetochores remains unaffected in Hec1-depleted cells treated with nocodazole. Our findings are consistent with those of DeLuca *et al.* (30,37). This suggests that Hec1-deficient kinetochores might still retain the ability to recruit Mad1. As mentioned above, Hec1-depleted cells can achieve a certain degree of kinetochore-microtubule attachment. This attachment might be sufficient for the dissociation of Mad1 from kinetochores. A similar situation is observed in Ptk1 cells treated with hypothermia or HeLa cells treated with microtubule stabilizing agents, such as Taxol (38,39). In all these situations, kinetochores are attached to microtubules, but lack tension. These kinetochores also lack Mad1 and Mad2 staining, suggesting that microtubule attachment to kinetochores is sufficient to trigger the dissociation of Mad1 from the kinetochores, even in the absence of tension. Despite the lack of Mad1 and Mad2 localization to kinetochores, these cells maintain a mitotic arrest in a spindle checkpoint-dependent manner. Though the kinetochore localization of Mad1 and Mad2 appears to be dispensable for mitotic arrest in these cells, the cytoplasmic pool

of Mad2 is absolutely necessary for the checkpoint activity. Microinjection of anti-Mad2 antibodies results in escape from mitotic arrest in all these circumstances. Similarly, the spindle checkpoint is active in Ndc80-deficient cells, as indicated by low levels of cyclin A1 and high levels of cyclin B1 and securin, and this checkpoint activity is dependent upon proper Mad2 function. Simultaneous depletion of hSpc25/Hec1 and Mad2 from HeLa cells abolishes the mitotic arrest observed with the depletion of hSpc25/Hec1 alone.

Studies on the Ndc80 complex and all of the above-mentioned scenarios, where kinetochore attachment is established without tension, pose an important question: how do these cells maintain a mitotic arrest despite a lack of Mad1 and Mad2 localization to the kinetochores. We suggest two possible explanations. First, it is possible that small amounts of Mad1, undetectable by our microscopy techniques, are still present on the kinetochores in the Ndc80-deficient cells and is responsible for an active checkpoint. Alternatively, it is possible that Mad1 recruitment to kinetochores is required for the initial generation of the APC/C-inhibitory checkpoint complexes and the establishment of the spindle checkpoint, but not for its maintenance. Other checkpoint proteins are then responsible for the maintenance of these APC/C-inhibitory signals through mechanisms that do not require the kinetochore localization of Mad1 and Mad2. Clearly, more studies are needed to clarify these issues.

In conclusion, we have identified two novel components of the human Ndc80 complex. Detailed characterization of hSpc25 reveals that it plays a pivotal role in chromosome congression and the maintenance of spindle integrity. Our studies also suggest that loss



of Ndc80 function in cells might serve as a direct signal to trigger apoptosis. Finally, we also demonstrate that Hec1-depletion results in microtubule-dependent dissociation of Mad1 from kinetochores, reinforcing the notion that kinetochore localization of Mad1 and Mad2 is dependent primarily upon the microtubule occupancy status of kinetochores.

## REFERENCES

1. Nasmyth, K., Peters, J. M., and Uhlmann, F. (2000) *Science* **288**, 1379-1385
2. Nasmyth, K. (2002) *Science* **297**, 559-565
3. Cleveland, D. W., Mao, Y., and Sullivan, K. F. (2003) *Cell* **112**, 407-421
4. Jallepalli, P. V., and Lengauer, C. (2001) *Nat. Rev. Cancer* **1**, 109-117
5. Hunt, P. A., and Hassold, T. J. (2002) *Science* **296**, 2181-2183
6. Nicklas, R. B. (1997) *Science* **275**, 632-637
7. Wassmann, K., and Benezra, R. (2001) *Curr. Opin. Genet. Dev.* **11**, 83-90
8. Gorbsky, G. J. (2001) *Curr. Biol.* **11**, R1001-1004
9. Musacchio, A., and Hardwick, K. G. (2002) *Nat. Rev. Mol. Cell Biol.* **3**, 731-741
10. Millband, D. N., Campbell, L., and Hardwick, K. G. (2002) *Trends Cell Biol.* **12**, 205-209
11. Yu, H. (2002) *Curr. Opin. Cell Biol.* **14**, 706-714
12. Peters, J. M. (2002) *Mol. Cell* **9**, 931-943
13. Harper, J. W., Burton, J. L., and Solomon, M. J. (2002) *Genes Dev.* **16**, 2179-2206
14. Howell, B. J., Hoffman, D. B., Fang, G., Murray, A. W., and Salmon, E. D. (2000) *J. Cell Biol.* **150**, 1233-1250
15. Kallio, M. J., Beardmore, V. A., Weinstein, J., and Gorbsky, G. J. (2002) *J. Cell Biol.* **158**, 841-847
16. Jin, D. Y., Spencer, F., and Jeang, K. T. (1998) *Cell* **93**, 81-91
17. Chen, R. H., Shevchenko, A., Mann, M., and Murray, A. W. (1998) *J. Cell Biol.* **143**, 283-295

18. Campbell, M. S., Chan, G. K., and Yen, T. J. (2001) *J. Cell Sci.* **114**, 953-963
19. Luo, X., Tang, Z., Rizo, J., and Yu, H. (2002) *Mol. Cell* **9**, 59-71
20. Jablonski, S. A., Chan, G. K., Cooke, C. A., Earnshaw, W. C., and Yen, T. J. (1998) *Chromosoma* **107**, 386-396
21. Skoufias, D. A., Andreassen, P. R., Lacroix, F. B., Wilson, L., and Margolis, R. L. (2001) *Proc. Natl. Acad. Sci. U. S. A.* **98**, 4492-4497
22. Taylor, S. S., Hussein, D., Wang, Y., Elderkin, S., and Morrow, C. J. (2001) *J. Cell Sci.* **114**, 4385-4395
23. Zhou, J., Panda, D., Landen, J. W., Wilson, L., and Joshi, H. C. (2002) *J. Biol. Chem.* **277**, 17200-17208
24. Cheeseman, I. M., Anderson, S., Jwa, M., Green, E. M., Kang, J., Yates, J. R., 3rd, Chan, C. S., Drubin, D. G., and Barnes, G. (2002) *Cell* **111**, 163-172
25. Westermann, S., Cheeseman, I. M., Anderson, S., Yates, J. R., 3rd, Drubin, D. G., and Barnes, G. (2003) *J. Cell Biol.* **163**, 215-222
26. Pinsky, B. A., Tatsutani, S. Y., Collins, K. A., and Biggins, S. (2003) *Dev. Cell* **5**, 735-745
27. Cheeseman, I. M., Drubin, D. G., and Barnes, G. (2002) *J. Cell Biol.* **157**, 199-203
28. Wigge, P. A., and Kilmartin, J. V. (2001) *J. Cell Biol.* **152**, 349-360
29. Martin-Lluesma, S., Stucke, V. M., and Nigg, E. A. (2002) *Science* **297**, 2267-2270
30. DeLuca, J. G., Moree, B., Hickey, J. M., Kilmartin, J. V., and Salmon, E. D. (2002) *J. Cell Biol.* **159**, 549-555

31. McClelland, M. L., Gardner, R. D., Kallio, M. J., Daum, J. R., Gorbsky, G. J., Burke, D. J., and Stukenberg, P. T. (2003) *Genes Dev.* **17**, 101-114
32. Hori, T., Haraguchi, T., Hiraoka, Y., Kimura, H., and Fukagawa, T. (2003) *J. Cell Sci.* **116**, 3347-3362
33. Elbashir, S. M., Harborth, J., Lendeckel, W., Yalcin, A., Weber, K., and Tuschl, T. (2001) *Nature* **411**, 494-498
34. Geley, S., Kramer, E., Gieffers, C., Gannon, J., Peters, J. M., and Hunt, T. (2001) *J. Cell Biol.* **153**, 137-148
35. Goshima, G., Kiyomitsu, T., Yoda, K., and Yanagida, M. (2003) *J Cell Biol* **160**, 25-39
36. Echeverri, C. J., Paschal, B. M., Vaughan, K. T., and Vallee, R. B. (1996) *J. Cell Biol.* **132**, 617-633
37. DeLuca, J. G., Howell, B. J., Canman, J. C., Hickey, J. M., Fang, G., and Salmon, E. D. (2003) *Curr Biol* **13**, 2103-2109
38. Waters, J. C., Chen, R. H., Murray, A. W., and Salmon, E. D. (1998) *J. Cell Biol.* **141**, 1181-1191
39. Shannon, K. B., Canman, J. C., and Salmon, E. D. (2002) *Mol. Biol. Cell* **13**, 3706-3719

# CHAPTER FIVE

## CONCLUSIONS AND FUTURE DIRECTIONS

How chromosomes are properly segregated in mitosis is not only a fundamental biological question that tickles our intellectual curiosity but also might have significant relevance to the understanding and cure of cancers. Analogous to the DNA damage checkpoint that helps guard the integrity of the genome by blocking cell cycle progression in response to DNA damage, spindle assembly checkpoint blocks anaphase onset until all the chromosomes are aligned on the metaphase plate. It has been about a decade since the major molecular players in this pathway- the Mad and Bub genes were identified. The recent years (including the six years of my graduate school) have witnessed significant advances in the understanding of the exact biochemical function of the spindle checkpoint proteins. Genetic studies in yeast and later biochemical studies using recombinant proteins had pointed out that Mad2 binds to Cdc20 - the activator and possibly the substrate recruiting subunit of Anaphase-promoting complex and inhibits its activity. Xuelian Luo et al have solved the structure of Mad2 alone or in complex with a peptide resembling the Mad2 binding motif in Cdc20. These structural studies have indicated that Mad2 can exist in two conformations- an active state and an inactive state. It is this conformational transition that is most probably being triggered by an unattached kinetochore.

A smaller addition to this whole picture comes from the finding that the full length Cdc20 binds to Mad2 with much lower affinity as compared to a fragment just containing the N-terminus of Cdc20 as indicated by yeast hybrid or in vitro binding assays using recombinant proteins. How is then Mad2 able to inhibit APC activity in vivo? There are two possible answers – either

binding of Cdc20 to APC or the other spindle checkpoint proteins might open up Cdc20 in such a way that the N-terminus is now exposed to bind to Mad2. I am more inclined towards the first possibility because Mad2 can inhibit APC in vitro without the aid of other checkpoint proteins. Furthermore, Mad2 can inhibit APC in the in vitro ubiquitination assay even when it is added and washed off prior to the addition of Cdc20. I believe that APC can bind to Mad2 independent of Cdc20, though this binding might not be sufficient for APC inhibition, because Cdc20 mutants that do not bind Mad2 can not be inhibited by Mad2. In the APC-Mad2-Cdc20 ternary complex Mad2 might interact with APC and Cdc20 through different surfaces and both these interactions might be necessary for APC inhibition. This might explain the puzzling observation that a Mad2 mutant with a C-terminal 10 amino acid deletion (Mad2  $\Delta$ C) serves as a dominant negative mutant in vivo and when overexpressed disrupts endogenous Mad2's ability to inhibit APC despite the fact that it does not bind to any of the known Mad2 interactors including Cdc20 or Mad1. It is possible that this mutant retains its ability to bind to APC, but not Cdc20 and thus acts as a dominant negative preventing endogenous Mad2 from forming a functional inhibitory complex with APC and Cdc20. This hypothesis can be tested by examining APC –Mad2 interaction in cells depleted of Cdc20 by RNAi and in vitro binding assays between recombinant Mad2, Mad2  $\Delta$ C and APC immunopurified from xenopus lysate.

A significant contribution to the understanding of spindle assembly checkpoint was made by Zhanyun Tang who demonstrated that the checkpoint protein BubR1 can inhibit APC activity in vitro much more effectively than Mad2. This inhibition is stoichiometric in nature because it does not depend upon BubR1's kinase activity and is possibly mediated by its ability to bind Cdc20 directly. Bub3, which binds to BubR1 does not contribute to the inhibitory potency of BubR1. Despite their ability to inhibit APC independently both these proteins are essential for a

robust spindle checkpoint activity in vivo. The exact contribution of both these protein to spindle checkpoint inside the cell needs to be understood at both qualitative and quantitative levels in future. Another unresolved question is the role of BubR1 kinase activity. Recently it has been shown that the motor protein CENP-E can activate BubR1 kinase activity. This might prove to be an important step towards the identification of BubR1 substrates and understanding the physiological relevance of these phosphorylation events.

Apart from the Mad and Bub proteins, a dual specificity kinase termed Mps1 has been shown to play a pivotal role in the establishment and maintenance of spindle checkpoint in many different systems. Through RNAi mediated depletion of Mps1 in HeLa cells I have shown that the human Mps1 is also an essential component of the spindle assembly checkpoint. While there is a general agreement over the role of Mps1 in spindle assembly checkpoint, there is some controversy regarding the role of Mps1 in centrosomal duplication. Mps1 was initially described in yeast as a protein required for spindle pole body duplication. Fisk et al have shown that mouse Mps1 is involved in centrosomal duplication in NIH3T3 cells through overexpression of WT or dominant negative Mps1. However, we and others could not observe any defects in centrosome duplication by either RNAi or overexpression studies in HeLa cells or U2OS cells. Furthermore the *S. pombe* or zebrafish mutants are fine with regards to centrosomal duplication. Further studies in different mammalian cell lines would be needed to resolve these issues. The exact biochemical function of Mps1 is not yet clear. Efforts to identify Mps1 interactors through immunopurification of Mps1 complex has not yielded any physiologically significant results. Neither could we detect any physical or biochemical interaction between Mps1 and any other known checkpoint proteins. Identification of the substrates and upstream regulators of Mps1 are some of the key questions that need to be addressed in future. Mps1 is phosphorylated in

mitosis. Mapping the Mps1 phosphorylation sites and identification of the kinase responsible for these phosphorylations appears to be the next reasonable step in that direction.

One of the fundamental questions in the understanding of spindle checkpoint is that how an unattached kinetochore generates the wait anaphase signal. All the known checkpoint proteins including Mad1, Mad2, Bub1, BubR1 and Bub3 are recruited to kinetochores in mitosis. However, nothing is known about the kinetochore components that recruit these proteins. These kinetochore components might not only provide a passive interface for the kinetochore localization of Spindle assembly checkpoint proteins but might also be involved in the sensing of kinetochore microtubule attachment and subsequent generation of wait anaphase signal. The first step in that direction is the identification of various kinetochore subcomplexes. In future we hope to purify these kinetochore subcomplexes and study their interaction with the known checkpoint proteins, using various biochemical and biophysical assays including conformational changes in the Mad2 protein or the ability to potentiate the APC-inhibitory activity of BubR1 or Mad2.

With this long term goal in mind we set out to purify the human Ndc80 kinetochore complex. We were specifically interested in this complex because Ndc80 was reported to bind to Mad1 in yeast two hybrid assays and Ndc80 deficient cells were unable to recruit Mad1 to kinetochores. We identified two novel components of the human Ndc80 complex. Functional characterization of these proteins suggests that they are orthologs of the yeast Spc25 and Spc24 proteins. Like Ndc80 inactivation of these proteins leads to defects in chromosome congression accompanied by a mitotic arrest that is dependent upon a functional spindle checkpoint. These cells undergo apoptosis after staying arrested in mitosis for 5-8 hours. It will be interesting to know how the absence of these proteins on the kinetochore triggers apoptosis. A final interesting note is that



the depletion of Ndc80 complex proteins results in multiple spindle aberrations including multipolar, fractured and elongated spindles.

Apart from Spc25 and Spc24, we also found a known kinetochore protein- Mis12 in the Ndc80 immunoprecipitates. Mis12 fails to localize to kinetochores in Ndc80 deficient cells, providing a physiological significance for the Ndc80-Mis12 interaction. The yeast Mis12 complex is composed of four proteins- Dsn1, Mis12, Nsn1 and Nfn1. It is possible that like the Ndc80 complex, Mis12 complex is also conserved throughout evolution. Homologs of other Mis12 components could not be identified on the basis of sequence data base searches. It is of interest to purify the endogenous Mis12 complex from mammalian cells and identify the other components. Apart from advancing our understanding of spindle assembly checkpoint these studies would provide valuable mechanistic insights into another vaguely understood problem i.e. how chromosomes are aligned on the metaphase plate in mitosis. Analyzing the pattern of chromosome movement by live imaging and examining the architecture of kinetochores through electron microscopy in cells depleted of different kinetochore proteins, would go a long way in answering this question. The advent of RNAi, powerful proteomic tools and imaging techniques brings the promise of an exciting scientific journey for the kinetochore biologist.

## **VITAE**

Rajnish Bharadwaj was born in Madubani, India on December 14, 1974, the first of two sons to Parma Nand and Veena Mishra. He received his earlier education at two boarding schools- Ram Krishna Mission Vidyapith, Deoghar and Delhi Public School, RK Puram. He joined All India Institute of Medical Sciences in 1992 and received his M.B.B.S. (MD) degree in 1998. In August 1998, he entered the Division of cellular and Molecular Biology at UT Southwestern Medical Center as a graduate student. He did his thesis work under the supervision of Dr. Hongtao Yu.

Permanent Address:

C/o Parma Nand Mishra

House # 140

Suratgunj, Madhubani

Bihar-847211 (India)